12-2011

Optimization of Dissolved Air Flotation for Algal Harvesting at the Logan, Utah Wastewater Treatment Plant

Andrew R. Elder
Utah State University

OPTIMIZATION OF DISSOLVED AIR FLOTATION FOR ALGAL HARVESTING AT THE LOGAN, UTAH WASTEWATER TREATMENT PLANT

by

Andrew R. Elder

A thesis submitted in partial fulfillment
of the requirements for the degree

of

MASTER OF SCIENCE

in

Biological Engineering

Approved:

_____	_____
Dr. Ronald Sims Major Professor	Dr. Byard Wood Committee Member
_____	_____
Mr. Issa Hamud Committee Member	Dr. Mark R. McLellan Vice President for Research and Dean of the School of Graduate Studies

UTAH STATE UNIVERSITY
Logan, Utah

2011

ABSTRACT

Optimization of Dissolved Air Flotation for Algal Harvesting at the

Logan, Utah Wastewater Treatment Plant

by

Andrew R. Elder, Master of Science

Utah State University, 2011

Major Professor: Dr. Ronald Sims
Department: Biological Engineering

This research evaluated dissolved air flotation (DAF) as a separation method for algae and phosphorus from municipal wastewater at the City of Logan, Utah Wastewater Reclamation Facility. DAF uses the supersaturation of air to raise suspended algae and other particles to the surface, where they can be easily removed. DAF, in conjunction with chemical coagulants and flocculants, can approach 95% algae and phosphorus removal. The algae removed using the DAF process will be used in the production of biofuels and bioplastics.

A pilot DAF unit was used to determine the optimum alum dose for total phosphorus (TP) and algae removal. In addition, a bench-scale jar test unit was used to study the effects of various alum and polymer doses on removal efficiencies at different times of the day. An optimal alum dose was found to be 30 mg/L based on results from both the pilot and bench-scale units. No advantage to adding polymer was found.

Algae removal efficiencies on the pilot DAF ranged from 68-70%, and the effluent algae concentration was reduced to 10 mg/L. Approximately 65% of the total phosphorus was removed, from 1.1 to 0.4 mg/L, which is low enough to meet regulations anticipated to be

promulgated by the state of Utah. Using the assumption that the molar weight of algae is 3,550 g/mole, the molar ratio of Al/TSS was found to be 30.1 and the molar ratio of Al/TP was found to be 7.5.

Extracellular polymeric substances (EPS) excreted by algal cells act as a natural flocculant and may allow for chemical usage to be minimized. Autoflocculation and bioflocculation, natural processes caused by EPS production and an increased pH level, were not observed to be a significant factor.

The chemical dosing rates provide the City of Logan with basic operational parameters for a full-scale (15 million gallons per day) DAF plant, providing an effluent phosphorus level below 0.5 mg/L. The alum will cost $1,118 per day, with a daily electrical cost of approximately $149. This full-scale DAF plant would harvest 1,563 kg of algal biomass per day, with a cost per kilogram of algae at $0.81.

(161 pages)

PUBLIC ABSTRACT

Optimization of Dissolved Air Flotation for Algal Harvesting at the Logan, Utah Wastewater Treatment Plant

Research being completed at the Logan, UT wastewater treatment plant could provide a locally-sourced gasoline replacement by collecting algae that grows naturally. This process would also provide the City of Logan with a method to meet certain standards set by the state of Utah.

Problem and proposed solution:

The water leaving Logan's wastewater treatment plant has high levels of phosphorus and nitrogen, two elements that are found in all wastewater treatment plants. These two substances need to be controlled, because they kill fish and cause pond scum to grow in recreational reservoirs downstream. A unique method has been found to remove these elements.

The wastewater treatment plant is a lagoons design, consisting of a series of large, open-air ponds. Algae naturally grow in these ponds, and consume the phosphorus and nitrogen found inside. If the algae can be harvested from the ponds, the phosphorus and nitrogen can be removed as well. As an added benefit, the algae can be used to create a gasoline replacement, known as biodiesel.

Current research:

One research project completed at the Logan wastewater treatment plant was the optimization of a method to harvest this algae. Andrew Elder worked with a device called a Dissolved Air Flotation, or DAF, unit. This machine uses microscopic bubbles to lift the algae to the surface of the water, where it can be easily removed. (Removing the algae removes much of

the phosphorus). The phosphorus not in the algae cells is removed by the small amount of chemical additives required for the DAF process to work.

The goal of this research project was to determine the optimum amount of chemicals required for proper algae harvesting. Additionally, there is a possibility that chemicals naturally secreted by the algae could help eliminate some additional chemical addition.

Two different methods were used to determine the proper chemical addition. First, a large DAF unit was used to determine the proper chemical dose. Next, a miniature DAF unit was used to study different chemical doses at different times of day. There is evidence that different amounts of sunlight could increase the quantity of these natural chemicals being produced.

Results:

The optimum amount of chemicals needed was determined to be 30 mg of aluminum sulfate per liter. The naturally-produced chemicals were found to have no significant effect on algae harvesting, at any time of day.

Conclusion:

This project demonstrated the ability for a DAF system to successfully harvest algae from the Logan wastewater treatment plant, with only minimal chemical addition. Along with meeting state of Utah requirements, this process could allow the Logan wastewater treatment plant to collect enough algae to create a significant amount of a locally-based, sustainable automobile fuel. Enough algae could be grown to fuel all of the City trucks with biodiesel. This process would save the City money and be beneficial to the environment at the same time.

ACKNOWLEDGMENTS

I am very grateful for all of the support provided throughout the course of my research. This includes USTAR (the Utah Science Technology and Research initiative) and the U.S. Department of Energy for funding my studies, as well as the Biological Engineering Department, the Sustainable Waste-to-Bioproducts Engineering Center, and the City of Logan Environmental Department. I would also like to thank my thesis committee, Dr. Ronald Sims, Dr. Byard Wood, and Mr. Issa Hamud, for their advice and support during the last two years. Other colleagues have been very helpful, including Dr. Daniel Dye, Reese Thompson, Erick Griffiths, Nathan Israelsen, Katie Glaittli, Alexa Lunt, Brian Smith, and Zak Dymock.

I would finally like to thank my wife, Caitlin, for her love and support over the last two years.

Andrew R. Elder

CONTENTS

Page

LIST OF TABLES

LIST OF FIGURES

Figure Page

LIST OF SYMBOLS, NOTATION, AND DEFINITIONS

Al	aluminum
$Al_2(SO_4)_3$ - $18H_2O$	aluminum sulfate
Al_2O_3	aluminum oxide
alum	another term for aluminum sulfate
BOD	biological oxygen demand (mg/L)
^oC	degrees Celsius
CO_2	carbon dioxide
DAF	dissolved air flotation
DI water	deionized water
DO	dissolved oxygen concentration (mg/L)
effluent	treated wastewater
EPS	extracellular polymeric substance
^oF	degrees Fahrenheit
gpm	gallons per minute
HCO_3^-	bicarbonate
in Hg	inches of mercury
influent	untreated wastewater
K_2HPO_4	dipotassium phosphate
KH_2PO_4	monopotassium phosphate
L	liter
mg/L	milligrams per liter
MGD	million gallons per day
mL	milliliters (one thousandth of a liter)
mL/L	milliliters per liter
N	nitrogen
$NaNO_3$	sodium nitrate
NaOH	sodium hydroxide
nm	nanometer (one billionth of a meter)
OH^-	hydroxide
P	phosphorus
PhosVer 3	a reagent used in the Hach “Test 'N Tube” Total P kit
PPFD	photosynthetic photon flux density (µmoles photons/m^2/sec)
psi	pounds per square foot
r	a distance unit
R^2	correlation coefficient

rpm	revolutions per minute
scfh	standard cubic feet per hour
T-Floc AE-204	synthetic anionic polymer, manufactured by Thatcher Chemical
TP	total phosphorus concentration (mg/L)
TSS	total suspended solids (mg/L)
UDEQ	Utah Department of Environmental Quality
µL	microliter (one millionth of a liter)
µm	micrometer (one millionth of a meter)
VOC	volatile organic compounds
VS	volatile solids (g/L)
W/m^2	watts per square meter
% wt/wt	percentage a substance is of the solute, on a weight basis

CHAPTER 1

INTRODUCTION

Our current dependence on petroleum-based fuels is not sustainable (Chisti, 2007; Demirbas, 2009; Hill et al., 2006; Pimentel and Patzek, 2005). There is only a finite quantity of oil present, and it will eventually be depleted (Adelman, 1990; Chisti, 2007; Demirbas, 2009; Pimentel and Patzek, 2005). As supplies start to dwindle, prices will drastically increase, causing serious economic damage (Demirbas, 2009; Hirsch, 2008; Kilian, 2008; Ragauskas et al., 2006). Additionally, fossil fuels contribute to the increasing levels of greenhouse gases in our atmosphere (Chisti, 2007; Brandt and Farrell, 2007; DeLuchi, 1991; Demirbas, 2009). A viable option to fossil fuels is needed for both economic and environmental stability. Biofuels, derived from oil crops, is one such option.

Biofuels have the potential to replace fossil fuels for many uses, and have a number of advantages. They are renewable; it is common for microalgae to double their biomass in 24 hours (Chisti, 2007). They are also carbon-neutral (Chisti, 2008; Fargione et al., 2008; Ragauskas et al., 2006; Tilman et al., 2006). Any carbon dioxide released from the burning of biofuels will be reabsorbed in the creation of more fuel. This energy source would also decrease our dependence on foreign sources of oil, as well as providing additional domestic jobs. Finally, the creation of these biofuels could have advantageous side effects, including the treatment of wastewater.

However, the dominant biofuel in the United States is corn ethanol (Demirbas, 2009; Kim and Dale, 2005). This poses a number of problems, the first being the relatively low energy density of corn per acre. In order for 50% of the current domestic transport needs to be offset by corn ethanol, 846% of the existing US cropland would have to be used for this purpose (Chisti, 2007). Additionally, the use of corn as a fuel source competes with its use as a food

source. For these and other reasons, there is an interest in finding alternative, more sustainable biofuel sources.

Table 1
Comparison of biodiesel yields of various crops (Chisti, 2007)

Crop	Oil yield (L/ha)	Land area needed (M ha)[a]	Percent of existing US cropping area[a]
Corn	172	1540	846
Soybean	446	594	326
Canola	1190	223	122
Jatropha	1892	140	77
Coconut	2689	99	54
Oil palm	5950	45	24
Microalgae[b]	136,900	2	1.1
Microalgae[c]	58,700	4.5	2.5

[a] For meeting 50% of all transport fuel needs of the United States.
[b] 70% oil (by wt) in biomass.
[c] 30% oil (by wt) in biomass.

Algae have the potential of replacing corn as an effective, renewable biofuel in the United States due to several reasons. Algae (along with cyanobacteria and diatoms) are inherently more efficient solar energy collectors. They have a 6-12 fold energy yield advantage compared to terrestrial plants, due to increased solar energy conversion efficiency, the ability to live in a greater range of photon flux, and are more efficient capturing light along their entire growth cycle. Additionally, algae do not have the structure required for higher plants, like cellulose, hemi-cellulose, and ligin. This eliminates the need for these polymers to be broken down during biofuel production. Finally, algae have a large ecological and metabolic diversity. With over 4,000 species of cyanobacteria alone, this variety allows for the selection of algal species that are properly adapted to local environments (Dismukes et al., 2008).

Other studies have observed that there is potential for an algal-biofuel economy to succeed, due to available land, water and CO_2 resources. Algae can be incorporated into

wastewater treatment processes very easily. An algal culture can use the wastewater for nutrients, as well as absorb CO_2 from the air. The algae can be continuously harvested for oil due to its high growth rate, and any waste biomass can be reused as feed material for the algal culture (Behzadi and Farid, 2007).

However, this optimism must be tempered with a few facts. In order for algae-based fuels to become reality, their high cost must be surmounted (Sheehan et al., 1998). There is a lack of an efficient method to harvest this algal biomass, because of the small size of the individual cells, the large quantities of water that must be treated to collect this biomass, and the algal culture's similar density to water (Zhang et al., 2010). There is no harvesting method that works perfectly in every case, so the selection of the right process and the optimization of this process is of upmost importance (Wang et al., 2008).

CHAPTER 2

LITERATURE REVIEW AND RESEARCH OBJECTIVES

2.1 Algal Characteristics

Algae are defined as any organisms with chlorophyll *a* and without roots, stems, or leaves. Cyanobacteria, formerly known as blue-green algae, are closely related to algae, even though they are prokaryotic organisms. Microalgae are primarily found in water, but are also found on the surface of soils all over the world (Richmond, 2004).

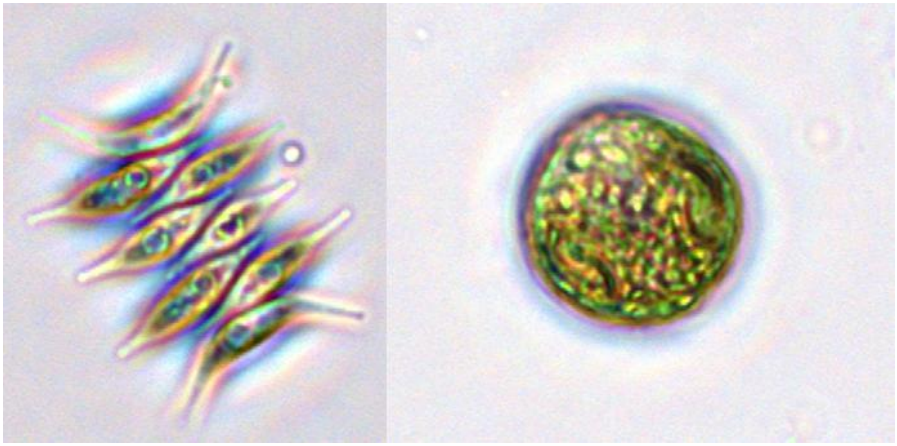

Fig. 1. *Scenedesmus* and *Chlorella*, two common algae species

As a whole, algal cells range in size from 3-15 µm (Bare et al., 1975), and have a wide range of cellular organization and structure. Microalgae can be unicellular, colonial, or filamentous. Most of the unicellular algae are nonmotile, but those species that move usually do so via flagella. The microalgae that form colonies can also be either motile or nonmotile. Many filamentous algal species have the ability to move under their own power, usually by rotation or creeping (Richmond, 2004).

It has been established that in general, algae grow faster in warm temperatures (Goldman and Carpenter, 1974). Increasing the algae population has a number of significant

effects on its growth solution. First, since gaseous oxygen is a product of photosynthesis, the dissolved oxygen (DO) concentration will increase. Also, since photosynthesis requires the uptake of carbon dioxide, an increased number of dissolved bicarbonates (HCO_3^-) will be split, releasing carbon dioxide (CO_2) and hydroxide ions (OH^-). The increased concentration of hydroxide ions causes the pH to increase (Larsdotter et al., 2007). A higher DO concentration and pH is evidence of increased algal growth (Griffiths et al., 2009; Sawyer et al., 2003). This higher pH level may help with the flocculation of an algae culture; this phenomenon, called "autoflocculation," will be discussed later.

2.2 Eutrophication and the Logan Lagoons

For rural and small communities in the United States, the most popular and cost effective process of wastewater treatment is the lagoon method. These lagoons usually cost less than half as much as other methods and require less maintenance (Wolverton and McDonald, 1979). This is the design of the treatment plant operating in Logan, UT. This facility serves Logan and the nearby cities of Nibley, Providence, River Heights, North Logan, Hyde Park, and Smithfield, all part of Cache Valley. This system consists of a series of seven facultative ponds, covering a total area of 460 acres. They are relatively shallow (around 5 feet deep), with an anaerobic zone near the bottom and an aerobic zone near the surface. The annual average flow is 15 million gallons per day (MGD) (City of Logan, UT, 2008), and a conservative estimate of the biomass production is 14 tons per day (Griffiths et al., 2009). This lagoons system is able to effectively remove the solids, biological oxygen demand (BOD), and pathogens from Cache Valley's wastewater (Griffiths et al., 2009). This treatment plant could provide a valuable source of algal biomass; however, there is a significant environmental impact that is caused by this algae which must be addressed first.

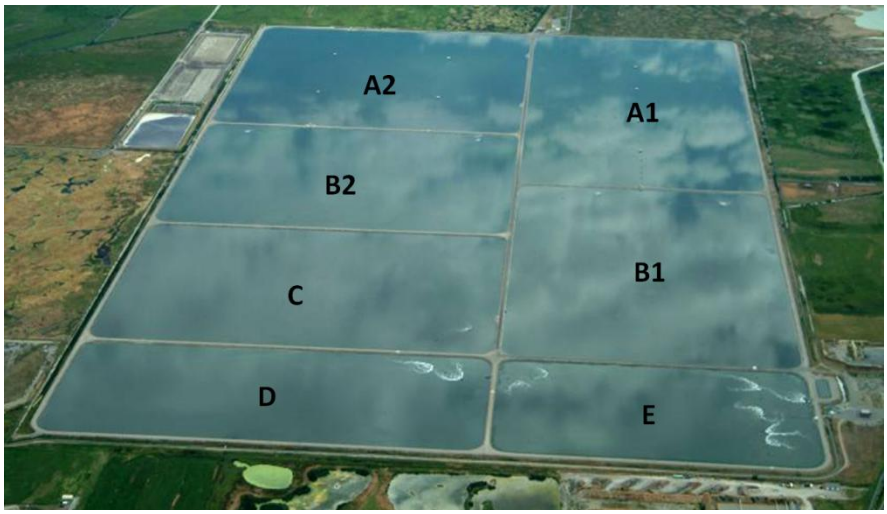

Fig. 2. The Logan Lagoons (the wastewater treatment facility for Logan, Utah)

The algae-inflicted changes in the DO concentration are serious because of eutrophication. This is the addition or recycling of nutrients (such as nitrogen and phosphorus) into bodies of water, and the effects of these nutrients. There are significant algal blooms (concentrations of 500 cells per milliliter or greater) in the Logan Lagoons, which aid in the treatment of the wastewater. However, they are also the primary cause of eutrophication (Moellmer, 1974). The nitrogen consumed by the algae is eventually volatilized as ammonia, and is therefore removed from the lagoon system. However, phosphorus is non-volatile, and will cycle in and out of the algae. Since algae are not being removed from the effluent currently, all of the phosphorus in the Logan Lagoons is being discharged into Cutler Reservoir (Griffiths et al., 2009). These algae will survive for a time downstream of the wastewater treatment plant but will eventually die, releasing phosphorus back into the watershed. The decomposition of the algal cells will also decrease the oxygen present in the water, which has a detrimental effect on the ecosystem as a whole (Moellmer, 1974).

Fig. 3. Algal bloom in the Logan Lagoons

Even though the wastewater is classified as "weak wastewater," and the City currently meets regulations on effluent phosphorus, this may not be the case in the near future. These limits will be lowered to counteract the eutrophication of Cutler Reservoir, the eventual destination of the Logan Lagoons effluent.

Fig. 4. Effluent from the Logan Lagoons

Recently determined UDEQ regulations will require a 61% reduction in total phosphorus (TP) in the summer months and a 45% reduction during the winter months (SWCA Environmental Consultants, 2010). The City of Logan has seven years to meet these

requirements, and must find a way to lower the amount of phosphorus and nitrogen leaving the Logan Lagoons.

Table 2
Required TMDL reduction for the Logan Lagoons (SWCA Environmental Consultants, 2010)

Table 7.4. Summary of Phosphorus LAs (kg TP/season) for Southern Reservoir TMDL

	Current Load (kgTP/season)		TMDL Allocated Load (kgTP/season)		Load Reduction (kgTP/season)	
	May - Oct	Nov - Apr	May - Oct	Nov - Apr	May - Oct	Nov - Apr
New Wasteload Allocations (WLAs)						
Logan City Wastewater Treatment Plant	11,236	21,597	4,405	11,831	6,831	9,766

2.3 Current plan by the City of Logan

The City of Logan has two possible solutions to this problem. The first is a traditional mechanical plant. This option would successfully remove the nitrogen and phosphorus from the effluent, meeting the UDEQ requirements. However, this would not come without a high cost. This plant would cost at least 180 million dollars, with a maximum price of 294 million dollars. Even the $180 million price tag would cause Logan's base utilities rate to jump from just over $16 a month to over $60 (Benson, 2007).

An alternative method to meeting these environmental requirements is made possible by the algae currently growing in the Logan Lagoons. This method would convert several of these ponds into a raceway system.

These shallow, winding ponds would be optimized for algae growth, and would increase the concentration already present in the Logan Lagoons. This increased concentration of algae, which would uptake phosphorus as it grows, could then be harvested from the Logan Lagoons. This would remove the phosphorus from the effluent, and would provide the City of Logan with a valuable source of biomass. This algae could be converted into biodiesel, or converted into biomethane with a digester. This system, properly optimized, could produce 35 tons of algae daily. Over the course of a year, this would be enough biodiesel to power 140 City trucks, or

enough methane to power 300 homes. All this could be done for a cost significantly less than the previous option. The primary technology being considered for the harvesting of the algae is dissolved air flotation (DAF).

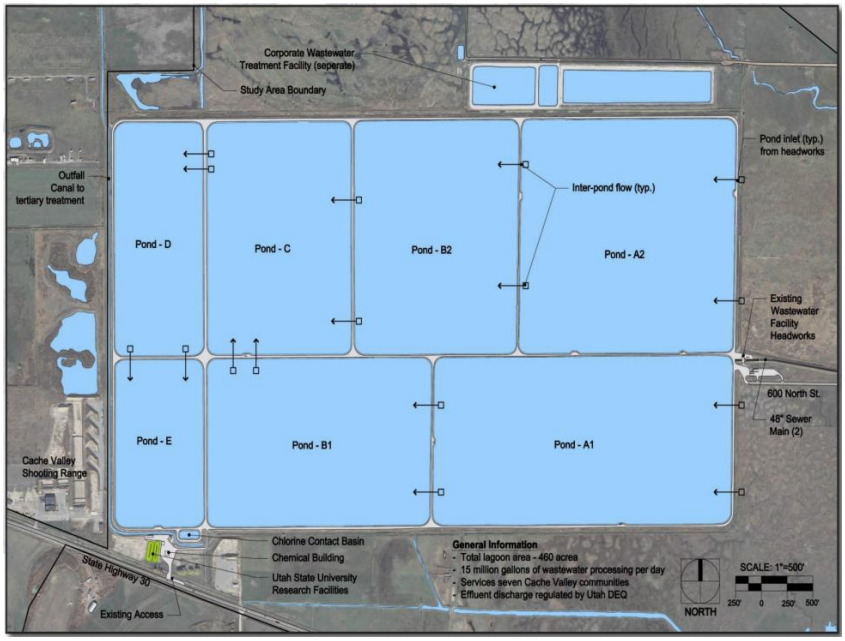

Fig. 5. Current Logan Lagoons flow diagram

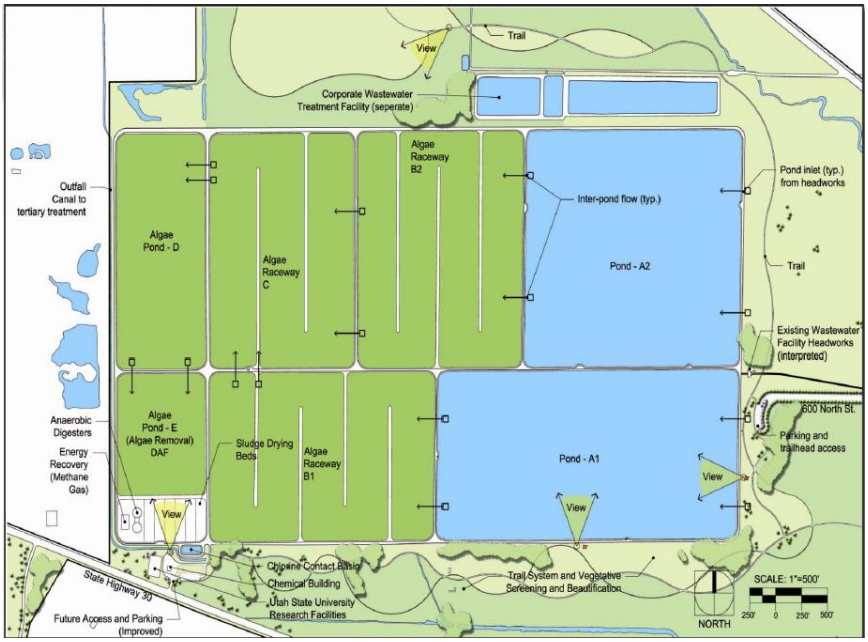

Fig. 6. Potential Logan Lagoons flow diagram

2.4 Dissolved Air Flotation (DAF)

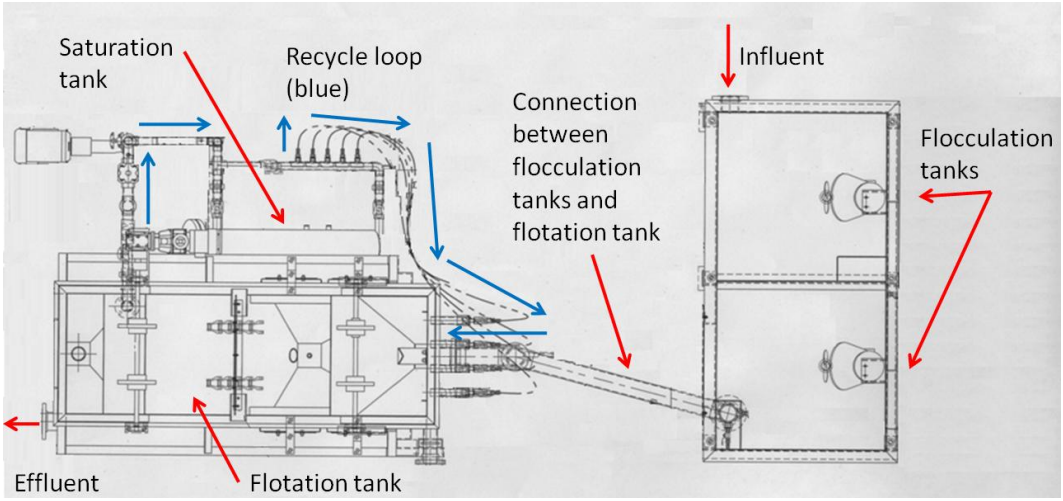

Fig. 7. Diagram of pilot DAF unit operating at the Logan Lagoons (top view)

The City of Logan is considering the use of dissolved air flotation (DAF) to remove the algae from the Logan Lagoons effluent. With this method, several mixing tanks allow the necessary contact time for the coagulants and flocculants to mix with the effluent from the Logan Lagoons. At the same time, a portion of the effluent from the DAF unit is saturated with compressed air in a saturation tank, which dissolves the air into the liquid. This part of the system is called the recycle loop. Once enough air has been dissolved in the saturation tank, the liquid is pumped to the bottom of a large flotation tank, where it mixes with the Logan Lagoons effluent that has had the contact with the chemicals. Bubbles are formed by the reduction in pressure when this supersaturated water encounters atmospheric pressure. This causes the dissolved air to leave solution, generating micro-bubbles (30-100 µm diameter), which carry the suspended matter to the surface. This matter is then gently skimmed off the surface and removed (Rubio et al., 2002).

Flotation had its beginnings in ore processing, where it was used to selectively separate different minerals. It has since been used in protein separation, analytical chemistry, the

clarification of fruit juices, and the harvesting and removal of algae. Despite the use of the same process, there are a number of differences between the use of flotation for ores and for wastewater treatment. One of the most important involves the bubble size. Medium to large bubble sizes (300-1500 µm in diameter) are optimal for the flotation of coarse particles found in mining operations. Flotation devices used in ore processing do not produce many bubbles smaller than 600 µm in diameter. For water treatment, however, micro bubbles (smaller than 100 µm) are required to float the extremely small particles present (Rubio et al., 2002).

Since the first generation of DAF technology was developed in the 1920s, it has been used in the clarification of wastewater, the separation of solids in drinking water treatment plants, the separation of biological flocs, sludge thickening, the removal of organic solids, dissolved oils, and VOCs, the treatment of ultra-fine minerals, and the removal of algae. DAF is the most widely used flotation method for the treatment of effluents from industrial sites, and it is projected that DAF applications will soon become even more prevalent in the waste treatment and mining fields (Rubio et al., 2002).

Coagulation and flocculation are a necessary part of algae removal from wastewater using dissolved air flotation. It is understood that algae cells are negatively charged, and because of this, will repel each other. Coagulation, or charge neutralization, is necessary for flocculation to proceed (Teixeira and Rosa, 2006). Flocculation is defined as the reversible increase of the size of particles to be separated. This occurs when the London forces (weak, intermolecular attractive forces) are not countered by the repulsive electrostatic forces (Harrison et al., 2003).

Traditionally, the DAF process uses two different types of destabilizing agents (an inclusive term for both coagulants and flocculants). The first category contains hydrolyzing metal coagulants. These are commonly aluminum or ferric salts (currently, aluminum sulfate in

the form $Al_2(SO_4)_3$-$18H_2O$ is being used at the Logan Lagoons). The trivalent metal ions hydrolyze water (split an H_2O molecule into H^+ and OH^-) because of their strong ionic strength. This happens when the Al^{3+} ion is surrounded by six water molecules, with the negatively-charged hydroxide molecules closest to the aluminum. Since the aluminum ion has such a high positive charge, electrons are drawn toward the metal from the water molecules. This causes an H^+ to break away from the water molecule, leaving the OH^- attached to the aluminum atom. These protons are then attracted to the negatively-charged particles, neutralizing their charge (Gregory, 2006).

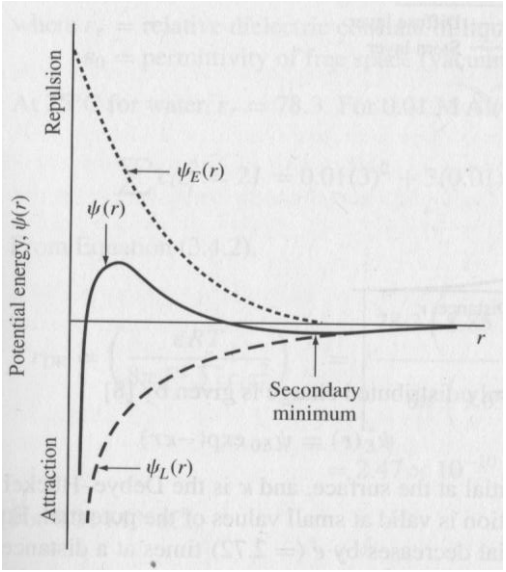

Fig. 8. Potential energy between two similarly-charged particles, as a function of distance (Harrison et al., 2003)

Fig. 9 graphically illustrates how coagulation works with different colloid concentrations. At the Logan Lagoons, the colloid concentration (the concentration of the algae) would be represented by either S_2 or S_3. (S_1 represents the turbidity in natural surface waters, which is too low for the Logan Lagoons effluent). As the coagulant dose increases, Zone 2 is approached, where there is a stoichiometric relationship between the algae and the alum. Further increasing

the dose would then stop removing algae, but would eventually cause a "sweep floc," where virtually all of the algae would be removed from the system (Faust and Aly, 1998).

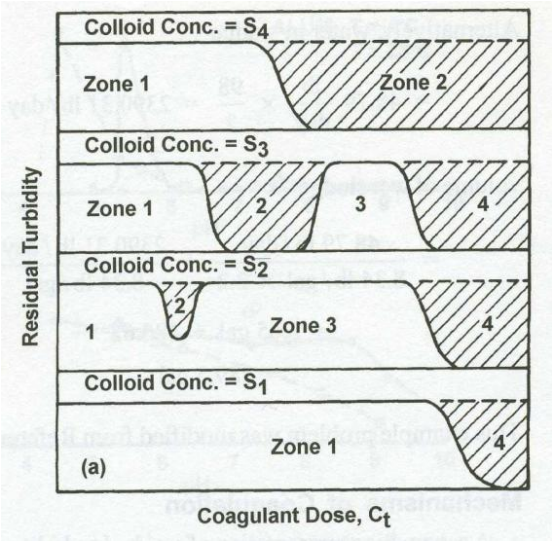

Fig. 9. Comparison of coagulation observed in jar tests using Al(III) at constant pH (Faust and Aly, 1998)

When phosphate is being precipitated in this fashion, the following equation governs the reaction (Hsu, 1975):

$$Al^{3+} + H_2PO_4^- = AlPO_4 + 2H^+ \quad (1)$$

DAF is considered an effective alternative to conventional sedimentation (Chung et al., 2000). However, algae still pose a problem for removal because of the small size of individual algal cells (3-15 μm), the dilute suspensions in which algae occur, and the low specific gravity of the individual cell (Bare et al., 1975). Bare et al. (1975) completed some of the original research on algae removal using dissolved air flotation in 1975, on algae growing in the Logan Lagoons at a concentration of 100-125 mg/L. These researchers compared flotation without coagulants, with ferric sulfate, and with aluminum sulfate. It was found that flotation without coagulant usage was not sufficient to remove a substantial amount of algae. A pressurized recycle system,

in conjunction with a small dose of ferric sulfate (85 mg/L) or aluminum sulfate (75 mg/L) was sufficient to obtain 90% removal in an algal suspension of 100 mg/L (Bare et al., 1975).

More recently, DAF was compared to the conventional sedimentation of the cyanobacteria *Microcystis aeruginosa* (Teixeira and Rosa, 2006). These researchers looked at DAF with and without a pressurized recycle system, and the addition of either alum or WAC (aluminum polyhydroxichlorosulphate). They discovered that DAF without coagulant addition provides low cell removal and virtually no removal of dissolved organic matter. The pressurized recycle system did not improve particle removal. This was explained by the lack of destabilized particles; in fact, particle destabilization is more important to DAF effectiveness than large floc size. The researchers found that a recycle system is vital, but increasing the percent recycle past 8% showed little improvement. They also found that sedimentation and DAF could both remove *M. aeruginosa*, but DAF performed better. It provided very high chlorophyll *a* removal, lower coagulant doses, slower coagulation speed, and stronger (but shorter) flocculation times than sedimentation (Teixeira and Rosa, 2006).

2.5 Bioflocculation and DAF

Some cellular excretions may help DAF removal efficiency, especially with low chemical dosage rates. Extracellular polymeric substances, also known as EPS, are excreted from algal cells and are a major component in biofilms. They fill the intracellular space and serve as a carbon and energy sink during stress situations, as well as environmental protection (against changes in pH, water content, and hydraulic pressure, for example). They have a unique composition, which makes them very effective in the settling, flocculation, dewatering, and metal-binding characteristics in an activated sludge system (Tian et al., 2006). A large variety of polymers have been found in EPS. Most of these are polysaccharides, but also include amino

acids, amino sugars, phosphates, pyruvate, and glycoproteins. These polymers serve several important functions that allow the cell to compete and survive in changing environments. Several of the more important roles of EPS include: buffering against minute environmental changes, the sequestration of nutrients, protection against toxins, attachment of the cell to surfaces, and movement, just to name a few (Decho, 1990).

Extracellular polymeric substances have a characteristic that is especially important to researchers working to harvest algae from the Logan Lagoons; their role in coagulation and flocculation. These interactions are based on the following types of intermolecular attractive forces: London forces, electrostatic interactions, and hydrogen bonds. London forces, also known as dispersion forces, are intermolecular forces due to random, temporary dipoles formed within a molecule. These momentary dipoles polarize nearby molecules, creating a temporary attractive force. These forces drop off very quickly with distance (at a rate of $1/r^6$), but are the main force between hydrocarbon chains. Electrostatic interactions are the attractive forces between ions and permanent dipoles. These interactions are relatively strong. Finally, hydrogen bonds primarily exist between the hydrogen and oxygen atoms between different water molecules, and are very common in polysaccharides (Tian et al., 2006).

Based on all three of these attractive forces, adhesion and cohesion occur between the biomass and the EPS. The result of these interactions is a three-dimensional network of EPS, providing a huge amount of surface area and structure. These structures (which are negatively charged) can be bridged by cations to bring multiple flocs (large groups of cells) together (Tian et al., 2006). This bioflocculation, the natural flocculation of algal cells due to EPS secretion (Lavoie and de la Noue, 1987), may be enough to cause mass flocculation to take place (Tian et al., 2006).

The cellular production of EPS is affected by environmental conditions, primarily irradiance and temperature. Wolfstein and Stal (2002) theorized that since photosynthesis is dependent on light and temperature, EPS production would also be dependent on these two conditions. A direct relationship was found between the amount of irradiance and the quantity of excreted material. Additionally, a clear effect was found of temperature on biomass and EPS production. The preferred temperature for growth was between 15-25^{o}C (Wolfstein and Stal, 2002).

Additionally, the growth stage of an algal culture will also affect EPS production. Smith and Underwood (2000) found that during logarithmic growth of five diatom species, the amount of extracellular carbohydrates that consisted of polymeric substances was around 20%. During the stationary growth phase, this percentage increased to 24-50%. In fact, the maximum EPS production always occurred in the stationary phase. The researchers suggested that this release during the stationary phase is a method of disposing of excess carbon from the cell. Also, in periods of darkness up to three days, the EPS content in extracellular carbohydrates increased to 85-99% (Smith and Underwood, 2000).

It appears that nutrient depletion can also have a positive effect on EPS production. Staats et al. (2000) discovered that the limitation of nitrogen in culture of diatoms slowed algal growth and increased EPS production. This was also found to be the case for phosphorus, but not for silicon or iron (Staats et al., 2000).

Researchers have found EPS to influence bioflocculation in several different ways. The first of these methods involves EPS interwinding, in which flocs are created due to the adhesive nature of the EPS itself. The second involves hydrogen bonding between the EPS molecules and the surrounding water. The final, and most significant, method may involve the bridging of multivalent cations, including (Al^{3+}) (Tian et al., 2006).

Another mechanism has been described that causes spontaneous flocculation of algae; autoflocculation. This phenomenon has been observed since the 1960s, and has been linked with an increased pH due to photosynthetic CO_2 consumption (Sukenik and Shelef, 1984). This phenomenon was first studied by William Moellmer (1974) at the University of California, Berkeley. When the pH in an algal culture increases (either as a natural consequence of photosynthesis or intentionally with chemical addition), the culture becomes supersaturated with respect to calcium and phosphate ions. This creates a calcium phosphate precipitate, which will be positively charged if excess calcium ions are present. This precipitate will then bind to the negatively-charged algae cells, causing mass flocculation (Lavoie and de la Noue, 1987).

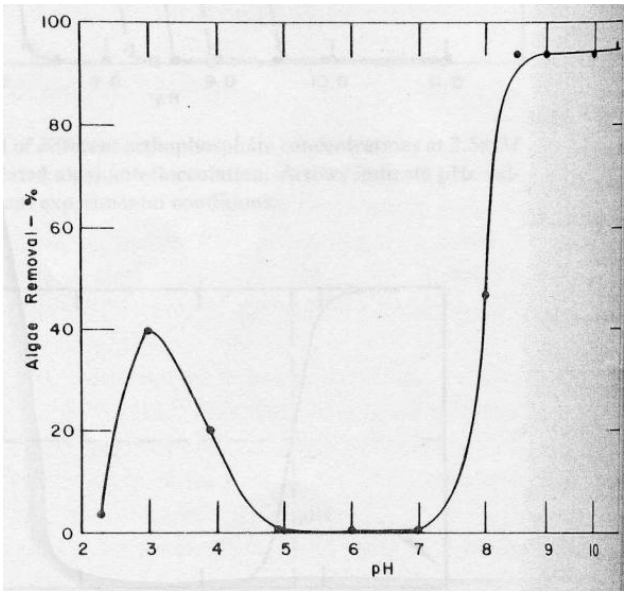

Fig. 10. Algal removal efficiency via autoflocculation vs. pH (Sukenik and Shelef, 1984)

A decade later, Sukenik and Shelef (1983) studied the correlation between autoflocculation and pH, and found that this phenomenon can be successful in certain pH ranges. A removal efficiency of 40% was achieved at pH 3.0, when the algae cells had a zero net

surface charge. Above pH 8.5, however, the efficiency for removal was over 95% (Sukenik and Shelef, 1984).

Autoflocculation and bioflocculation are considered to be very promising for the economical harvesting of algae. Chemical flocculation is also an effective method, but this is a very expensive step that could be eliminated with natural processes. Additionally, the physiological state of the algal culture influences both natural and chemical flocculation. Chemical flocculation is most efficient at the end of the exponential growth phase, and quickly looses efficiency as the culture enters endogenous growth. EPS growth, which is greatly increased during this phase, may be masking the surface charge on the individual algae cells, decreasing the chemical flocculation efficiency. If one can focus on the use of autoflocculation and bioflocculation, this interference can be avoided altogether (Lavoie and de la Noue, 1987).

The knowledge of autoflocculation and bioflocculation has been advanced with the goal of providing an inexpensive method of algal harvesting. Bioflocculation was shown to occur in specific environmental conditions as far back as the 1960's (Pavoni et al., 1974). In 1965, Golueke and Oswald demonstrated bioflocculation in an actively photosynthetic algal culture, on a relatively warm day with plenty of sunlight (Golueke and Oswald, 1965). At this point, however, the mechanism for bioflocculation was unknown. In 1967, Schuessler showed that bioflocculation was most efficient during the declining growth phase, when the EPS production and excretion was the highest. He hypothesized that the polysaccharide polymers would bridge between algal cells (Pavoni et al., 1974; Schuessler, 1967).

More recently, Pavoni et al. (1974) set out to determine the feasibility of algal harvesting from wastewater treatment plants using natural flocculation techniques. They studied the relationship between algal growth, turbidity, and EPS production. If EPS is the cause

of bioflocculation, they reasoned, then the turbidity of an algal culture should decrease as the EPS increases (Pavoni et al., 1974).

They discovered a number of interesting facts. It appeared that flocculation is controlled by the physiological state of the algal cells. Flocculation did not occur until the culture had entered endogenous growth. Additionally, a direct relationship was found between EPS production and flocculation. Finally, a reduction in the surface charge of the algal cells was not a necessary first step to algal bioflocculation (Pavoni et al., 1974). This means that a coagulant (such as aluminum sulfate) would not be required to cancel the surface charge, which is currently required for chemically-treated DAF operation.

Bioflocculation via EPS secretion is dependent on a number of variables, including temperature, irradiance, and growth stage of the algal culture. Autoflocculation is also dependent on environmental conditions, especially the pH. These are both phenomena that could be used with dissolved air flotation to minimize chemical usage required for efficient harvesting.

2.6 Research Objectives

Three objectives were identified for evaluation of dissolved air flotation for algae and phosphorus removal at the Logan, Utah wastewater treatment plant. First, determine the dosage rate of alum for optimal algae and phosphorus removal, and if organic polymer addition improves removal of algae and/or phosphorus. As part of this objective, determine if operating the DAF without chemical addition and evaluating autoflocculation and bioflocculation is a feasible and efficient method for algae removal. Second, determine if autoflocculation and bioflocculation can improve the efficiency of DAF operation when chemical coagulants are used.

Third, conduct an economic analysis for DAF operation for algae removal with and without chemical addition.

CHAPTER 3

PILOT DAF UNIT

3.1 Introduction

In order to determine the feasibility of a dissolved air flotation (DAF) unit to bring the City of Logan's total phosphorus discharge in compliance, WesTech Engineering loaned the City a pilot DAF unit. This unit is built to process up to 60 gallons per minute (gpm), and measures approximately 22 feet long by 12 feet wide. A diagram of the unit can be found below in Fig. 11, Fig. 12, and Fig. 13.

Fig. 11. Flocculation tanks on pilot DAF unit

Fig. 12. Compressor and flotation tank on pilot DAF Unit

In Fig. 11, the chemical mixing tanks are seen in the foreground. The white PVC piping leading into the mixing tanks is the influent of the pilot DAF unit, and pulls liquid from the Logan Lagoons effluent. In the background, the stainless steel flotation tank can be seen, which is illustrated more clearly in Fig. 12.

The large rectangular tank in the background of Fig. 12 is the flotation tank, where the micro-bubbles lift the algae flocs to the surface to be skimmed off. The cylindrical stainless steel tank on its side, just in front of the flotation tank, is the saturation tank, where the recycle stream is supersaturated with air. The five small hoses coming off of this tank bring the recycle stream back into the flotation tank.

Fig. 13 details the top of the flotation tank, where the skimmer harvests the algae raised to the surface by the dissolved air. The skimmer pulls the algae float toward the camera, where it falls into another container.

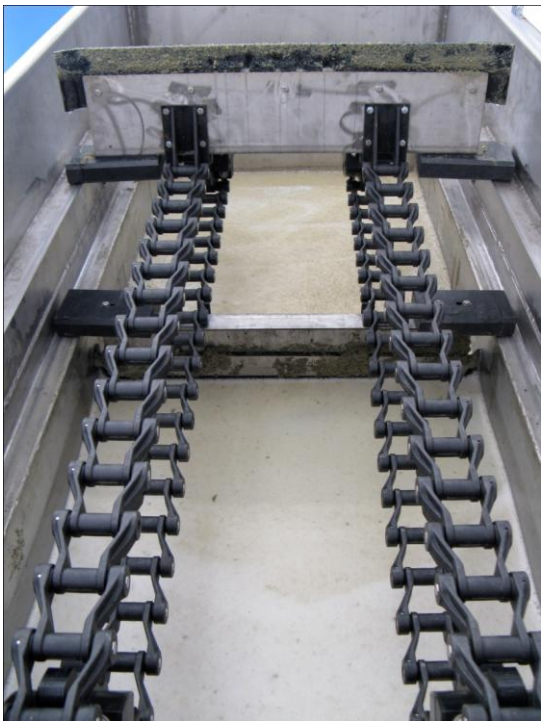

Fig. 13. Skimmer on top of flotation tank on pilot DAF unit

The goal of this phase of the research was to become familiar with the operation of the pilot DAF unit and gather initial data on removal rates of both TSS and TP using varying alum doses.

3.2 Materials and Methods

3.2.1 Overall sampling procedure

The general method for operating the sampling from the pilot DAF unit is as follows. After turning on the influent pump that supplies the wastewater to the pilot DAF unit, and making sure that it has filled the entire unit, turn on the recycle pump. A needle valve controls the flow from the flotation tank to the recycle pump. This valve should be closed until -10 in Hg backpressure is being exerted on the recycle pump. At that point, open the air control valve between the recycle pump and the needle valve to allow the air to enter the recycle system. Adjust the air control valve to the desired air flow rate in scfh (standard cubic feet per hour).

After the air is flowing, adjust the flow of water out of the recycle pump for the proper recycle rate, reading this value off of the flow meter. Once the proper recycle rate has been reached, double check the air control valve from the previous step to make sure the correct amount of air is still flowing.

At this point, the pressure in the saturation tank needs to be adjusted. The pressure in the tank needs to be at least 50 psi, but the common operating pressure is 60 psi. The primary method of adjusting the pressure is with the 4 ball valves at the end of the recycle system, immediately before the lines re-enter the flotation tank. Carefully closing these valves will increase the pressure in the saturation tank. Finally, open the saturation tank bleed valve slightly, in order to let a bubble out of the system every few seconds. Nitrogen does not saturate as well as oxygen, and this bleed valve helps prevent a buildup of nitrogen gas in the saturation tank.

The final check is to climb up the attached ladder and look down at the top of the flotation tank. The water should change to a milky color, indicating that the air is saturating in the recycle system. If there is a “boiling water” effect at end of the flotation tank where the recycle enters, there is an air buildup in the saturation tank. Crack the bleed valve open farther, in order to get rid of this extra air.

After adjusting all of the parameters to the desired settings, wait 5 minutes and check the parameters again. The pilot DAF unit reacts slowly, and sometimes it takes several minutes for changes to become visible.

Once it is time to sample, use three 250 mL bottles for both the influent and the effluent. The influent is collected as close to the influent pump as possible. Fill each of these bottles with an influent sample. The effluent sample is collected from the liquid that is flowing over the weirs in the flotation tank. Fill each of the three effluent bottles with a sample.

Following Standard Methods for the Examination of Water & Wastewater, a TSS test was performed on each of the three samples (Eaton et al. 2005a). Additionally, a total phosphorus test (using the acid persulfate digestion method) (Eaton et al. 2005b) was performed in triplicate on these samples. These tests were performed using Hach Test 'N Tube kits, which are based on the Standard Methods procedures. These tests allow the percent removal of both suspended solids and total phosphorus concentration to be determined. However, an assumption was made with respect to the TSS determination. When the aluminum sulfate is added to the wastewater, the aluminum can form a precipitate with the phosphate in the water (see equation 1 in section 2.4 DISSOLVED AIR FLOTATION (DAF)). This precipitate, if present in large enough quantities, could be adding to the TSS that was originally present in the wastewater. However, for the purposes of this report, it is assumed that this additional TSS is negligible. This same assumption was made in the important DAF research completed in 1975 at the Logan Lagoons by Bare et al. (1975).

3.2.2 Sampling plan

Before the optimum alum dose can be determined, the time for the pilot DAF unit to reach a steady-state condition must be determined. To accomplish this, influent and effluent samples will be taken immediately after the pilot DAF unit is operating, and every 15 minutes thereafter, for a total of 90 minutes. Total suspended solids testing will be used to determine algae removal efficiency.

After this steady-state time has been determined, the optimum alum dose will be determined by varying the alum dose from 0-100 mg/L, in increments of 10 mg/L.

3.2.3 Statistical Analysis

Statistical analysis for this section was completed in SAS, a software package commonly used in scientific applications. A generalized linear model was used to determine which values being observed are considered statistically equivalent at a 5% significance level ($\alpha = 0.05$). Tukey's Studentized Range (HSD) was used to determine the statistical groupings.

When data is presented, the same letter on two data points indicates that the two points are considered statistically equal, given the assumption described above. Additionally, when present, error bars are equal to the standard deviation.

Further testing was completed to ensure that our assumption of independent and identically distributed error terms was correct. The distribution of the error terms was checked, to ensure normality. Also, the data was checked for heteroscedasticity (a phenomenon where an error term trends larger or smaller as the factor levels change). If there was a normal distribution, and no heteroscedasticity, then the data could be used for analysis.

3.3 Results and Discussion

The first test to be completed was the determination of the steady-state time for the pilot DAF unit. In Fig. 14, the tests used to determine the steady-state time are displayed. These tests were all completed in November 2010.

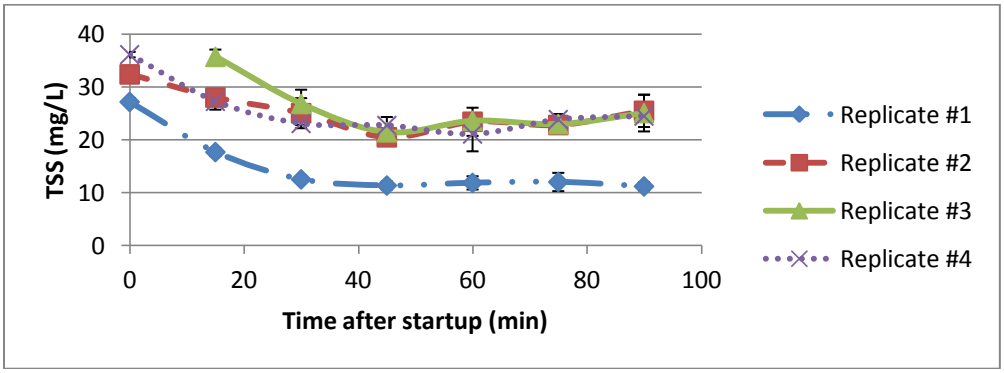

Fig. 14. Steady-state testing on pilot DAF unit

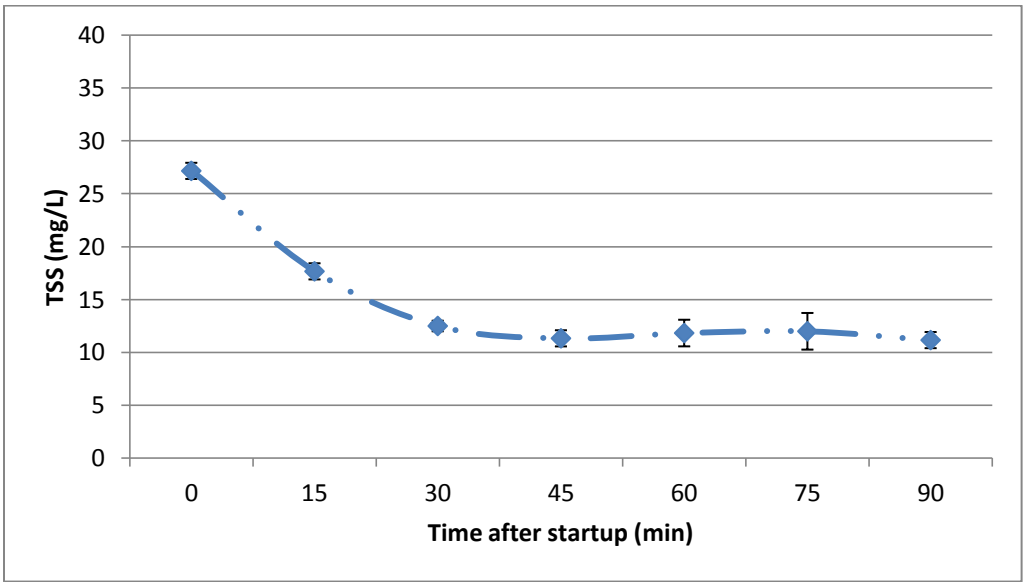

Fig. 15. Steady-state testing for pilot DAF unit (replicate #1)

Table 3
Statistical groupings for pilot DAF unit steady-state testing

Time after startup (min)	Tukey Grouping		
0	A		
15		B	
30			C
45			C
60			C
75			C
90			C

In Fig. 15, we can see a single test in more detail. Since the error bars are equal to the standard deviation, the 30 minute sample is almost equal to the 45 minute sample. This is confirmed by a statistical analysis by SAS in Table 3: since the TSS values from 30-90 minutes have the same letter, they are statistically the same.

Now that the steady-state time was known, the testing of the range of alum doses on TSS and TP removal could start. This testing took place over the course of several days, and produced the following result.

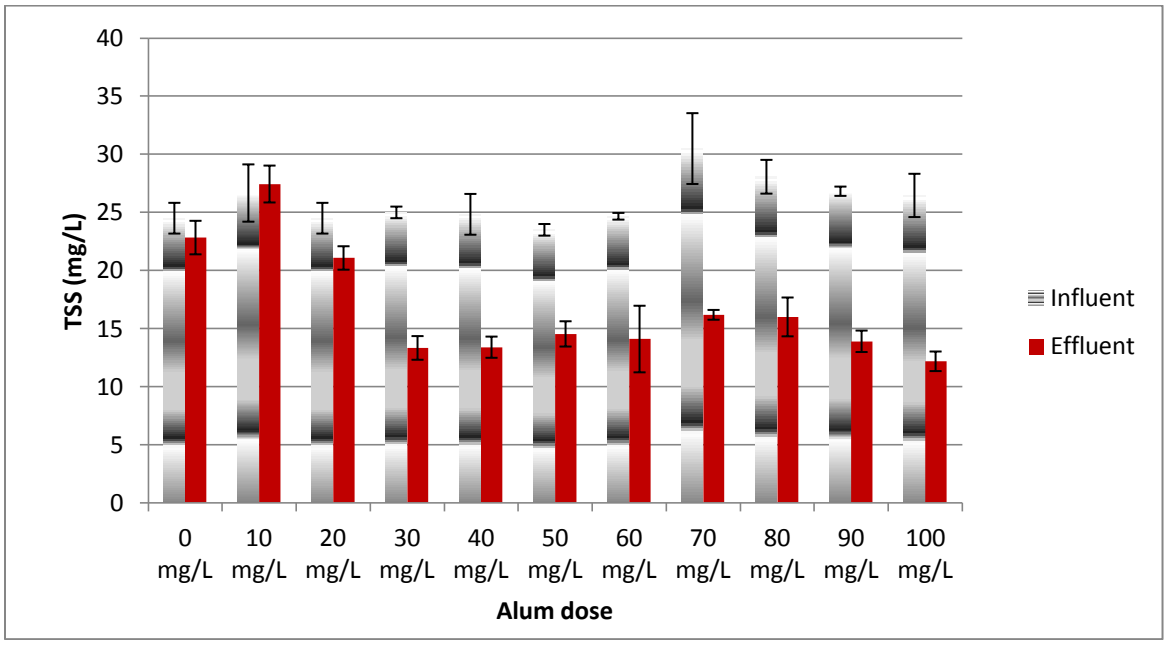

Fig. 16. TSS vs. alum dose, pilot DAF unit

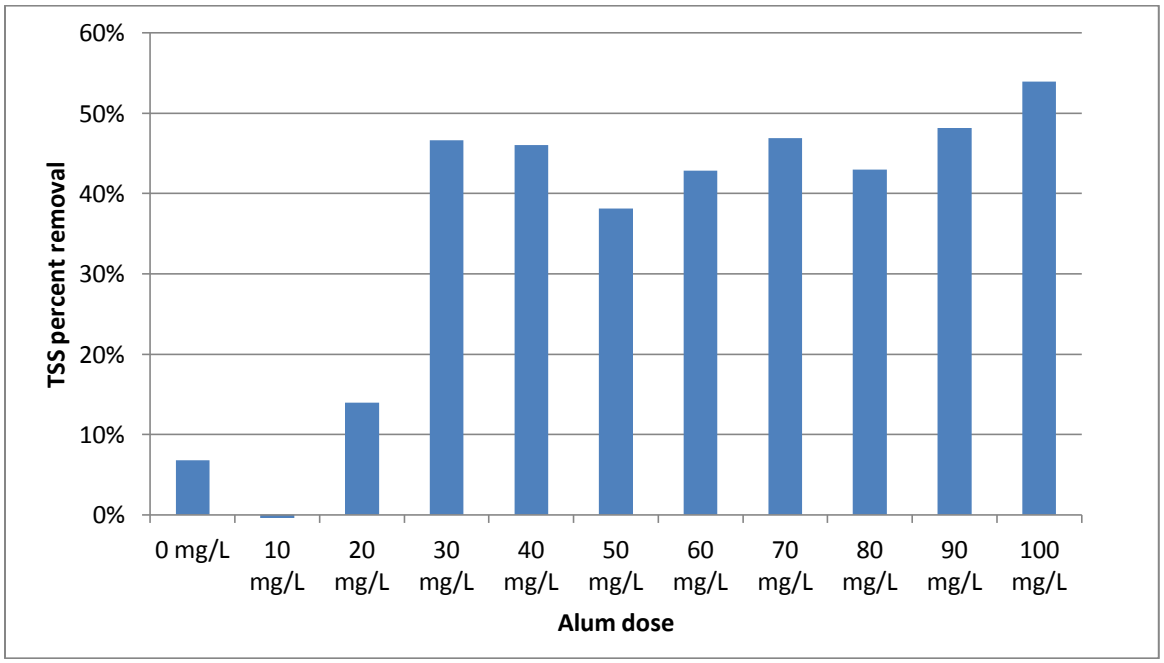

Fig. 17. TSS percent removal vs. alum dose, pilot DAF unit

In order to tell which of these dosing rates produced a statistically different result, the influent and effluent TSS values need to be compared.

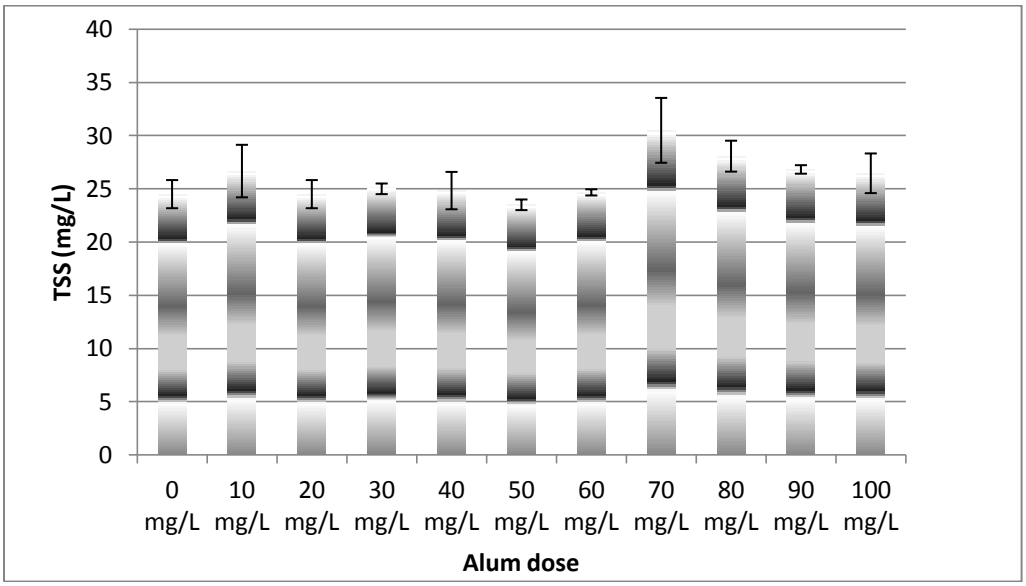

Fig. 18. TSS in pilot DAF unit influent

Table 4
Statistical groupings for TSS in pilot DAF unit influent

Alum dose (mg/L)	Tukey Grouping		
0		B	
10		B	
20		B	
30		B	
40		B	
50		B	
60		B	
70	A		
80	A	B	
90	A	B	
100	A	B	

Fig. 18 contains the comparison of the TSS in the influent. All of the values are statistically the same, except for the run that used a dose of 70 mg/L (see Table 4). This dose, however, had the same TSS dose as the 80-100 mg/L runs, so those four runs can be compared

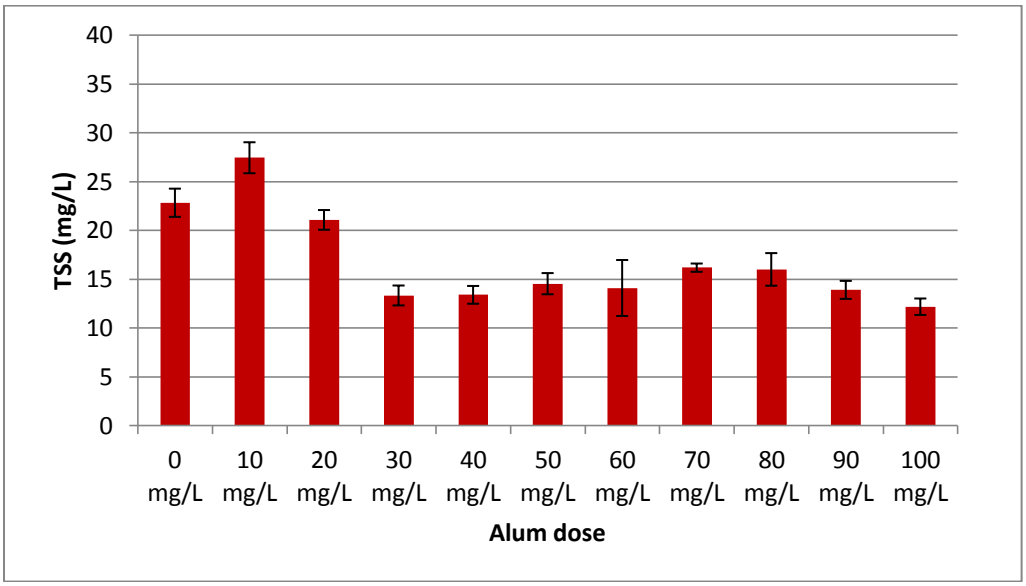

Fig. 19. TSS in pilot DAF unit effluent

Table 5
Statistical groupings for TSS in pilot DAF unit effluent

Alum dose (mg/L)	Tukey Grouping		
0		B	
10	A		
20		B	
30			C
40			C
50			C
60			C
70			C
80			C
90			C
100			C

together. Additionally, 70 mg/L is much higher than the optimum alum dose should be; after talking to other engineers in the field, the researcher determined that the optimum value should be below 50 mg/L. Because of this, the uniqueness of the 70 mg/L test was ignored.

Fig. 19 shows the TSS concentration is the pilot DAF unit effluent, and we can see a statistically significant difference. There is no difference between 30 mg/L and any other higher dose. This is our optimum dose, at least with respect to TSS removal.

According to the TSS removal data, with any dose higher than 30 mg/L, no more algae is harvested. Approximately the same results can be seen with the total phosphorus removal data.

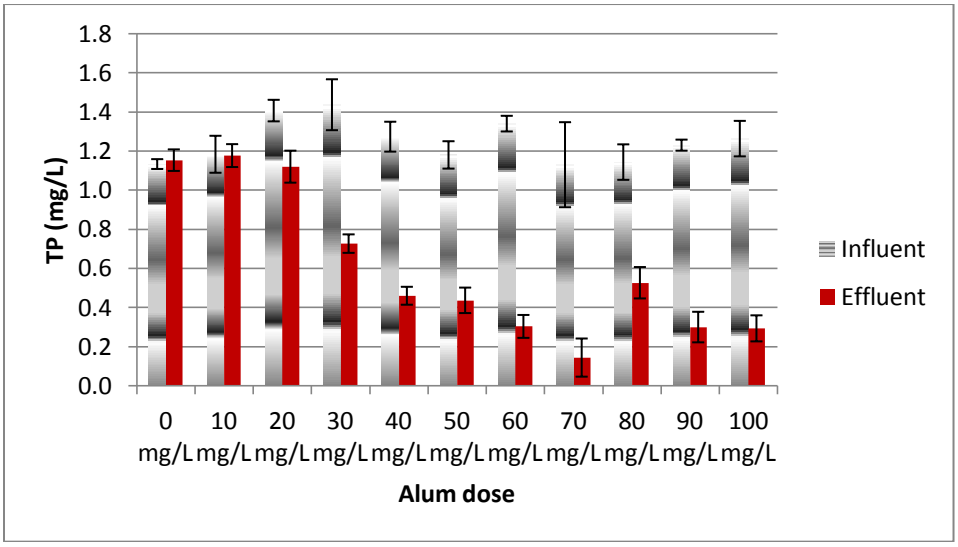

Fig. 20. TP vs. alum dose, pilot DAF unit

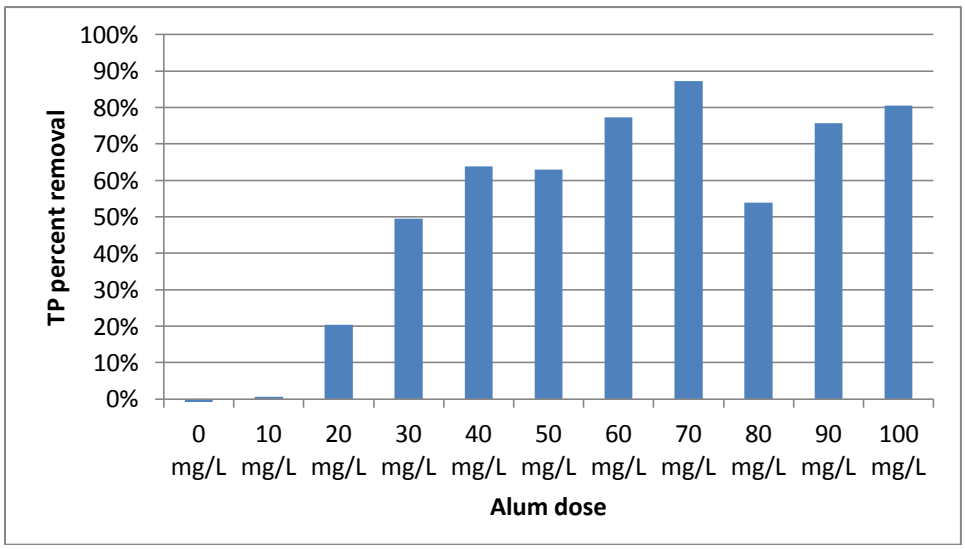

Fig. 21. TP percent removal vs. alum dose, pilot DAF unit

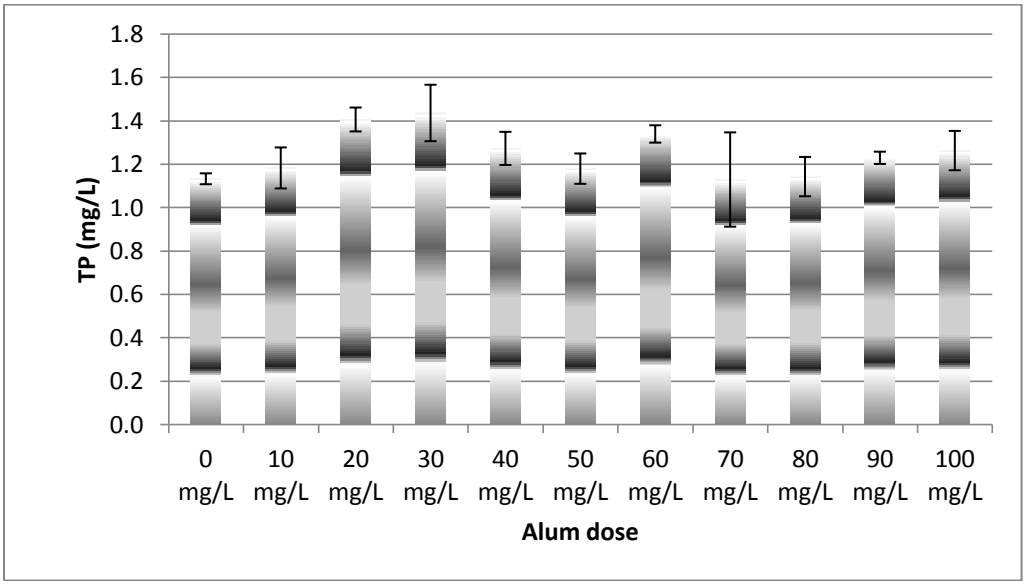

Fig. 22. TP in pilot DAF unit influent

Table 6
Statistical groupings for TP in pilot DAF unit influent

Alum dose (mg/L)	Tukey Grouping		
0	A		
10	A		
20	A		
30	A		
40	A		
50	A		
60	A		
70	A		
80	A		
90	A		
100	A		

When the same statistical analysis is applied to the TP levels in the pilot DAF unit influent, the levels are all equal (see Fig. 22 and Table 6). This allows comparison between the TP levels in the effluent.

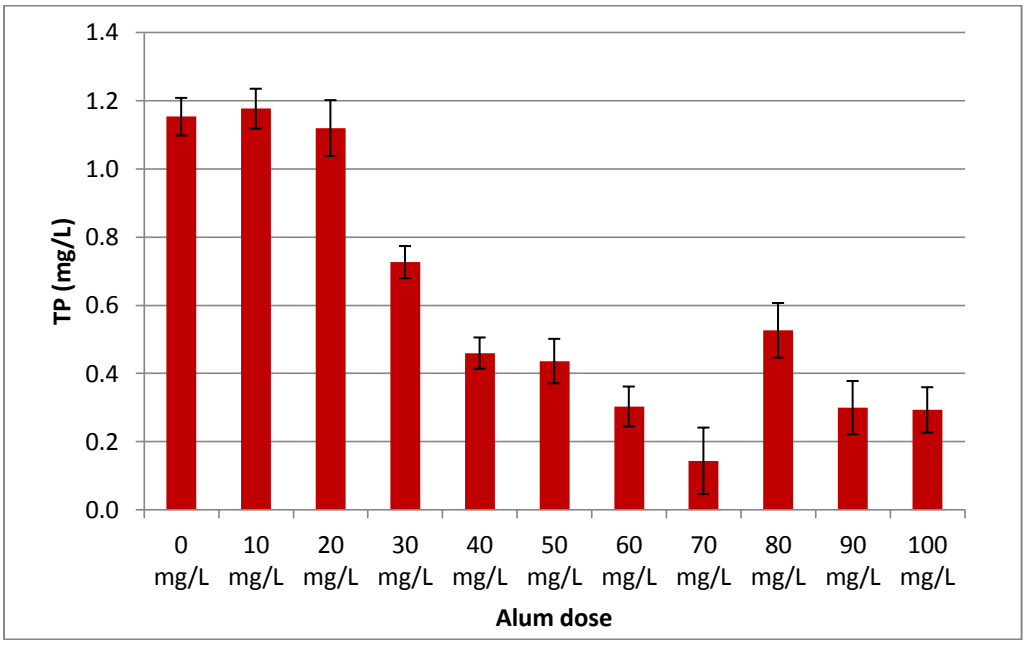

Fig. 23. TP in pilot DAF unit effluent

Table 7
Statistical groupings for TP in pilot DAF unit effluent

Alum dose (mg/L)	Tukey Grouping				
0	A				
10	A				
20	A				
30		B			
40			C	D	
50			C	D	
60				D	E
70					E
80		B	C		
90				D	E
100				D	E

The statistical situation in the effluent in the TP testing isn't quite as clear. The TP concentration in the 0, 10, and 20 mg/L samples are all statistically the same, and the rest of the doses are related in varying degrees (see Fig. 23 and Table 7). Either 30 or 40 mg/L is the optimum alum dose for TP removal. Since 30 mg/L was the optimum dose for TSS removal, and

due to the fact that the chemical dose should be limited if possible, 30 mg/L will be used as the optimum dose for TP removal as well as TSS.

3.4 Conclusion

The alum doses from 30-100 mg/L are statistically similar. Referring back to Fig. 9 (the schematic representation of coagulation), these doses have placed the pilot DAF unit effluent in Zone 2 (where there is a stoichiometric relationship between alum and algae). This is where the pilot DAF unit should operate, in order to minimize chemical usage.

The primary goal of the City of Logan is the removal of phosphorus, and it was demonstrated that the pilot DAF unit is capable of doing this. This unit was able to remove 50-60% of the total phosphorus present, from 1-1.2 mg/L to 0.5-0.7 mg/L. This is low enough to meet the regulations set by the state of Utah.

This phase of testing has also allowed the researcher to become both familiar with the pilot DAF unit and collecting important data. Knowing that the optimum alum dose is 30 mg/L will allow the DAF to run most efficiently and cost effectively in the future. This will also allow the next phase of the project to begin. This next phase was planned to begin in January 2011, but that was before the pilot DAF unit started to function poorly. These problems are discussed in the following chapter.

CHAPTER 4

PILOT DAF UNIT: A TROUBLESHOOTING GUIDE

4.1 Introduction

As was stated earlier, the pilot DAF unit was unable to remove sufficient amount of algae from the months of January to May 2011. This led the author to utilize a bench-scale jar test unit (discussed in the next chapter) for most of the important data collection for this project. However, this time troubleshooting the pilot DAF unit has provided a list of variables that researchers can reference when troubleshooting a DAF system.

4.2 Materials and Methods

After the pilot DAF unit stopped working after in January 2011, a wide range of variables were changed in order to isolate the problem. The operational conditions can be found listed in the Results and Discussion section.

4.3 Results and Discussion

The following is a list of tests performed on the pilot DAF unit. This list can serve as a starting point for troubleshooting a similar DAF unit.

As a more concise summary, Table 9 is a checklist of variables to use while troubleshooting.

Table 8
List of attempts to fix pilot DAF unit

Attempted repair	Result
Installed a static mixer just prior to the alum dosing line, in order to provide a better flash mix of the alum.	Influent flow rate dropped from 67 gpm to 51 gpm, but no improvement in DAF efficiency was observed.
Switched from the air injection pump to the air compressor for the dissolved air source.	When the recycle rate is decreased to the desired amount (~13 gpm), unsaturated air escapes the saturation tank. While working with WesTech on this problem, it was revealed that the compressor was vastly oversized for this application, and the saturation tank was an experimental design that was not fully tested.
A white substance was seen in the bottom of the alum tank. Sent sample of liquid alum stock to chemical supplier to test its concentration.	The solid precipitate seen in the bottom of the tank is an aluminum precipitate. There is no way to get it back in solution. The chemical supplier said that the alum was 7.7% wt/wt Al_2O_3, and the stock should be 8.2-8.3%.
Checked the alum pump for consistent flow rate over time.	No change was observed.
Pulled sample from pilot DAF unit after flocculation tank, check if flocculation was occurring.	Many flocs formed in the sample container, and rapidly settled.
Kept the alum dose consistent while lowering the rate the air was entering the air injection pump.	No algae removed; for some reason, a negative removal rate was observed.
Removed static mixer, and moved alum line back to original dosing location.	No improvement.
Doubled the recycle rate (from 13 gpm to 23 gpm).	TSS removal is still way too low (only removing 25% of what it should be), but the pilot DAF unit is removing almost exactly the right amount of total P.
Visited with several engineers from WesTech at the Logan Lagoons site.	They fixed an airlock in the alum line, but said that the rest of the pilot DAF unit looked like it was operating fine. They decided that there must be something wrong with the alum solution.

Table 9
DAF troubleshooting checklist

Category	Parameters to check
Chemical	Have the coagulants/flocculants been exposed to extremes in temperatures?
	Have the concentrations of the cogaulants/flocculants been checked by an analytical lab?
	Are the dosing calculations correct?
	Is the dosing pump/delievery system working properly?
	Is there proper mixing at the coagulant dosing location?
Physical	Is enough air entering the recycle system?
	Is the recycle rate high enough?
	Is the saturation tank pressure high enough?
	Is there proper saturation occuring in the flotation tank (via visual inspection)?
	Is there unsaturated air entering the flotation tank?
	Has the unit been completely drained and cleaned?
	Have the hoses and piping been thouroughly cleaned or replaced?

4.4 Conclusion

Even though the pilot DAF unit was unable to be fixed during a critical phase of this research, the researcher feels much more comfortable troubleshooting and fixing this piece of equipment. More importantly, a list of parameters was created that should be checked when a DAF system is not performing optimally.

CHAPTER 5

JAR TEST UNIT

5.1 Introduction

A jar test unit is a standard apparatus that allows wastewater engineers and scientists to test different chemical dosing rates for improving water quality. The jar test unit purchased by the Biological Engineering Department at Utah State University has the additional ability to inject air-saturated water, accurately mimicking a DAF system.

Fig. 24. Jar test unit in operation

Fig. 24 shows the jar test unit used in this experimental work. It is manufactured by EC Engineering in Alberta, Canada, and uses six 1-L square jars for the different chemical dosing levels. This many jars allow many different dosing rates to be tested simultaneously. The white backdrop behind and lights underneath the jars allows visual comparison of water quality improvement. (A fan in the base of the unit ensures that there is only a minimal amount of heat transferred to the jars via the lights).

In Fig. 24, the experiment is taking place. The chemicals have been added to each jar, and the mixers are turning at 60 rpm. (The mixer speed is adjustable with the knobs on the right). In front of the jars, resting on the table is the air injection module. One injector goes into each jar, and this replicates the recycle system on the pilot DAF unit. (One difference; the jar test unit injects DI water, instead of wastewater.) The amount of recycle can also be adjusted; all six jars at full recycle amounts to a 12% recycle rate.

The goal of the experimentation with this unit was to duplicate the removal rate data obtained with the pilot DAF unit.

5.2 Materials and Methods

5.2.1 Jar Test Operation

Before starting this experiment, seven 500-mL plastic bottles were cleaned and acid washed (the seventh bottle is for the influent sample). Also, a 5000 mg/L alum stock solution was created by diluting the new stock solution of alum (purchased while troubleshooting the pilot DAF unit).

The remaining six 1-L jars were filled as close to the same time as possible from the Logan Lagoons effluent, using a 1-L volumetric flask. After all the jars were filled, they were placed in the base of the jar test unit, with the mixer module attached. While the mixers were keeping the samples suspended, six 10-mL disposable syringes were filled with the required amount of the 5000 mg/L alum dilution.

At the start of the test, the mixers were turned up to their maximum speed (in this case, 320 rpm). The required amount of alum was injected into the jars as quickly as possible, and the stopwatch started. After 10 seconds elapsed, the mixers were turned down to 60 rpm. The mixers spun at this speed for 15 minutes.

While the mixers were running, several other tasks were completed. First, each of the clean bottles was labeled with a jar number using masking tape. Second, the saturation tank was filled up to the second weld on the inside of the tank with DI water. After the tank was filled, the lid was replaced and the tank was pressurized to 60 psi. After that pressure is reached, the tank was shaken for 10-15 seconds. This ensured that the water was properly saturated with air. Then, the saturation tank was connected to the air injection module.

When the stopwatch read 14 minutes, 45 seconds, the injection module was placed on the jar test unit. For this test, knobs for each injector were turned to 10, the setting for maximum air injection. The unit was also be set to "common start."

At 15 minutes and 10 seconds, the mixer was turned off and any one of the injector buttons on the unit was pressed. All six injectors injected air, providing approximately a 12% recycle. Once the injectors finished, the air injection module was immediately pulled out and the jar test unit was allowed to rest undisturbed for 5 minutes while the bubbles rise. Once this time elapsed, a 500-mL bottle was placed under each sampling port on each jar in order to collect a 400 mL sample. This provided sufficient volume for triplicate TSS and TP samples.

This procedure was completed for the entire range of alum dosing rates, from 0 to 100 mg/L, with increments every 10 mg/L. Also, the alum doses were randomized among the six jars until three replicates of each alum dose were obtained.

5.2.2 Scaled-down total phosphorus testing

For this series of jar test unit runs, a scaled-down phosphorus test was used to save both time and money. The following is a procedure developed by Erick Griffiths, a former graduate student at USU. It uses the same Hach Test 'N Tube Total Phosphorus test kits, but utilizes the supplied chemicals in a much smaller volume, testing 5-6 samples out of 1 tube.

Since this method only reads the absorbance, and is not using the Hach program to automatically calculate the P concentration, a standard curve must be made relating absorbance to P concentration.

1. Mix 1 potassium persulfate pillow in 1 acid vial.
2. In a clean digestion vial, mix 200 µl of the acid and potassium persulfate mixture (from step 1) with 500 µl sample.
3. Cook vials in heating block for 30 minutes at 150 ^{o}C.
4. Cool vials to room temperature.
5. Add 200 µl NaOH to each vial.
6. Mix 1 PhosVer 3 pillow in 1 mL DI H_2O.
7. Add 100 µl of PhosVer 3 mixture to each vial.
8. Briefly mix using vortex.
9. Allow reaction to proceed for at least 2 minutes, but no longer than 8 minutes.
10. Pour each sample into cuvette for absorbance measurement at 890 nm.

5.2.3 Statistical Analysis

Statistical analysis for this section was completed in SAS, a software package commonly used in scientific applications. A slightly different model was used in this portion of the research. Since the researcher was essentially measuring “triplicates of triplicates” (each alum dose was used for three different jars, and each jar was measured in triplicate), a nested experimental design was used, where each group of three measurements was nested within each replicate of each alum dose.

Note that originally, this was not the method of analysis planned. The original plan was to use the generalized linear model, as was used previously. This would allow one to easily

measure the percent removal by averaging the triplicates for both the influent and effluent samples. However, the nested design eliminated the ability to use the percent removal values in the model, since this calculation would cause a loss in resolution. Therefore, the effluent measurements were used in the SAS program, and used to compare the percent removal values.

When data are presented, the same letter on two data points indicates that the two points are considered statistically equal, given the assumption described above. Additionally, when present, error bars are equal to the standard deviation. Since in all previous experiments our assumption of independent and identically distributed error terms was correct, it was assumed that this was the case with this phase of research.

5.3 Results and Discussion

Before any experiments could be completed, a standard curve was created, comparing TP concentration to absorbance. Hach phosphorus standards were diluted and tested using the scaled-down protocol. The standard curve in Fig. 25 has an R^2 value of 0.993. All of the samples should be in the range of the standard curve (0-5 mg/L), allowing interpolation, not extrapolation. This linear regression was used to calculate the TP concentration for all of the tests that use this protocol.

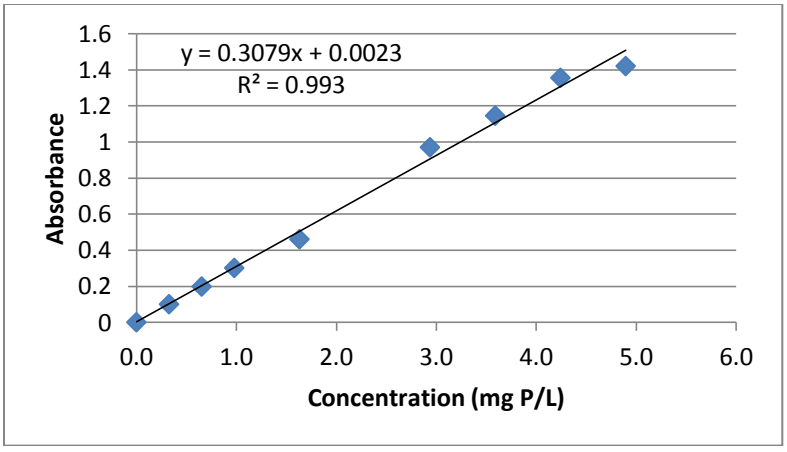

Fig. 25. Standard curve for absorbance vs. TP concentration relationship (scaled-down TP test)

Using this standard curve, the following data were generated for TSS removal and TP removal. As before, error bars indicate the standard deviation.

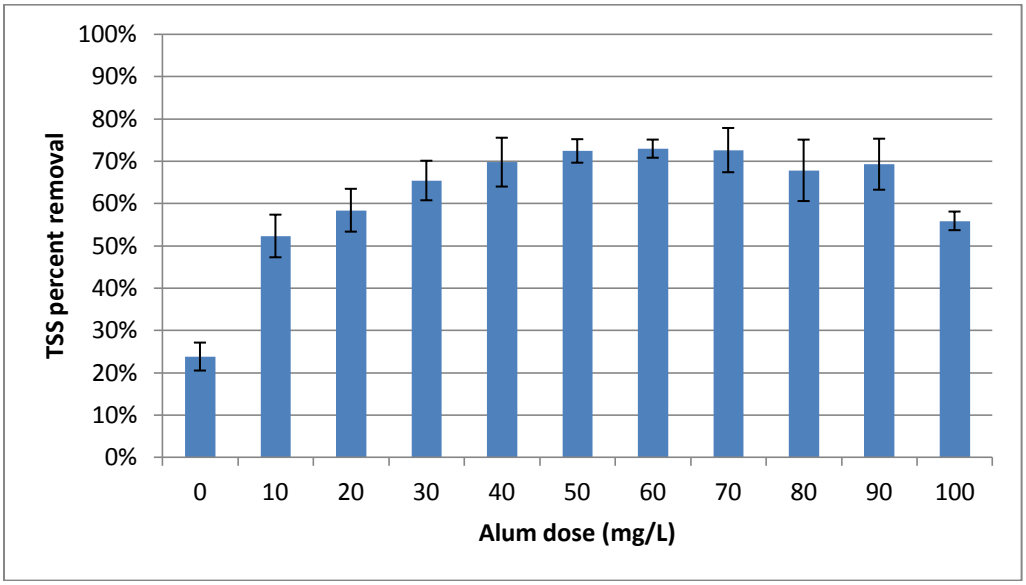

Fig. 26. TSS percent removal vs. alum dose, jar test unit

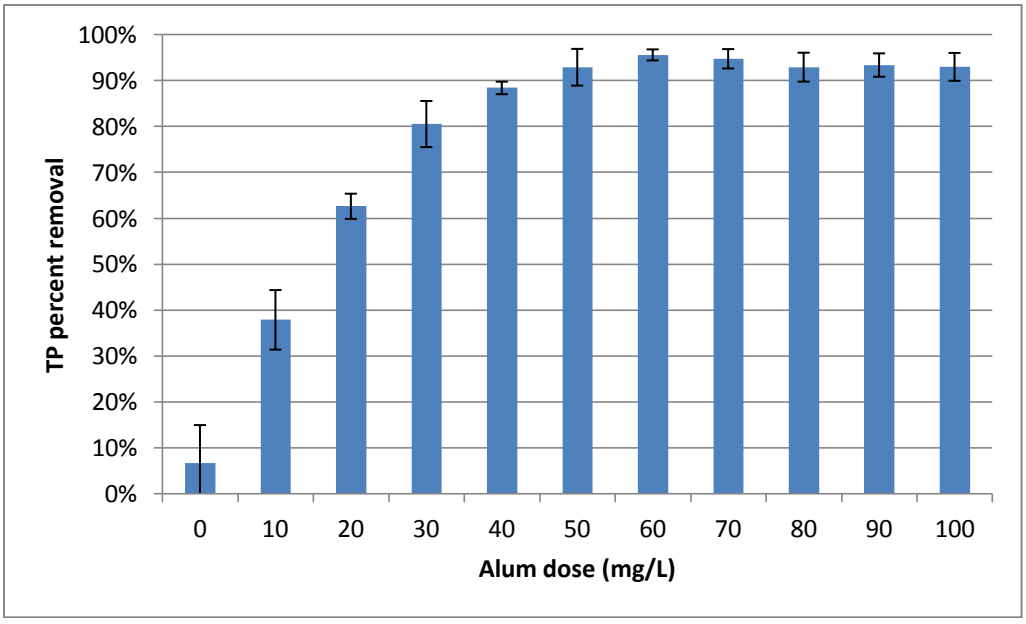

Fig. 27. TP percent removal vs. alum dose, jar test unit

These removal rates are higher than was obtained on the pilot DAF unit. The old alum stock solution must have been substandard even when the pilot DAF was working.

An analysis was performed on the jar test unit data using SAS, a statistical program, in order to determine which of the alum doses produce the same result.

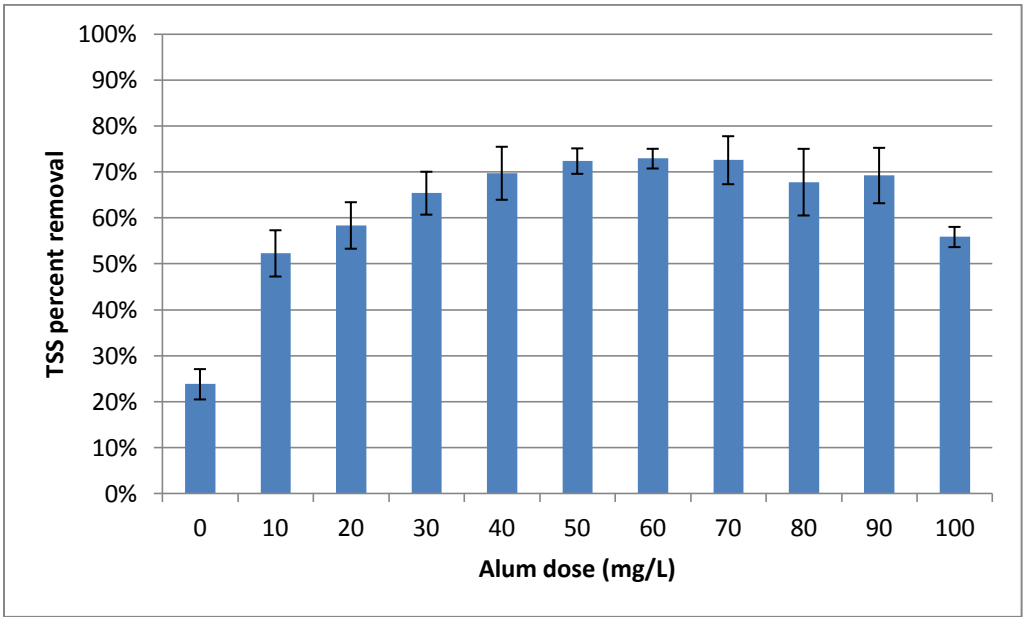

Fig. 28. Statistical analysis of TSS removal data, jar test unit

Table 10
Statistical groupings for TSS removal in jar test unit

Alum dose (mg/L)	Tukey Grouping								
0									
10	A								
20	A	B	C						
30		B	C	D					
40		B		D	E				
50		B		D	E	F			
60						F	G		
70						F	G	H	
80		B		D	E	F	G	H	I
90				D	E	F	G	H	I
100		B							

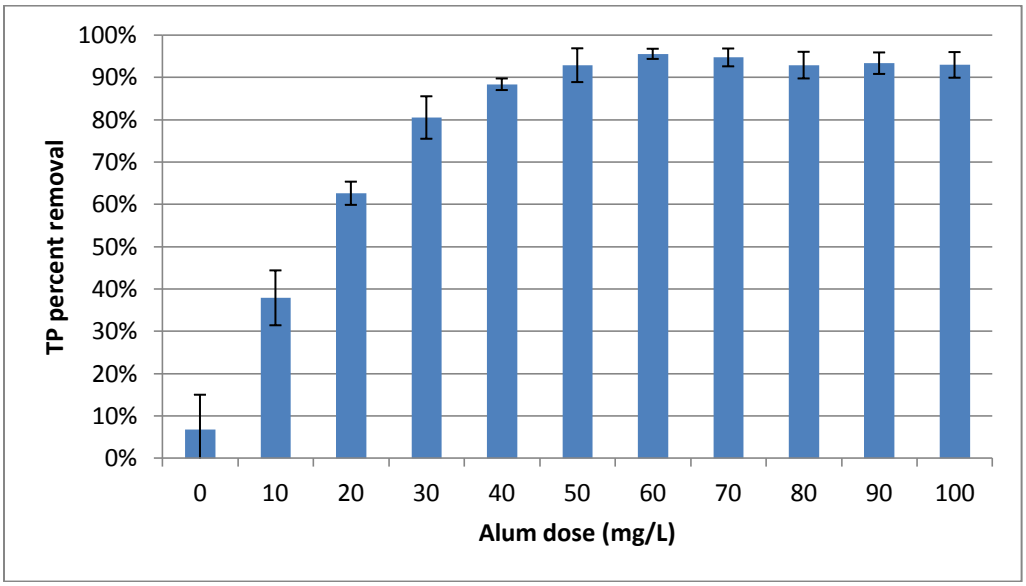

Fig. 29. Statistical analysis of TP removal data, jar test unit

Table 11
Statistical groupings for TP removal in jar test unit

Alum dose (mg/L)	Tukey Grouping						
0							
10							
20							
30	A	B					
40	A	B	C				
50	A		C	D			
60	A		C	D	E		
70	A		C	D	E	F	
80	A		C	D	E	F	G
90	A		C	D	E	F	G
100	A						

On Fig. 28 and in Table 10, some TSS doses can be observed to be statistically similar. Statistical similarity is seen with the 10 and 20 mg/L doses. Additionally, 20-30, 20-50, and many of the higher doses are also statistically the same. In this case, 30 mg/L alum performs just as well as the higher doses. Twenty mg/L performs the same as 30 mg/L, but not as well as 40 mg/L. Because of this, with TSS removal, 30 mg/L is the optimum dose.

The situation is similar when observing TP removal. Statistical similarities can be observed in the range 40-90 mg/L, and 30 and 40 mg/L are also the same. Since the goal is to use as little alum as possible, 30 mg/L also works as the optimum alum dose for TP removal.

5.4 Conclusion

Note that on Fig. 28, the percent removal of TSS actually decreases as the alum dose increases. It is not clear why this is occurring. According to the solubility diagram of aluminum (Fig. 30), for the range of alum doses being used, the alum should be sufficiently high to exceed the solubility constants. (A high pH, greater than 11-11.5, would be required for the system to leave this range). This means that the aluminum ions are free to adsorb to the algal particles, and there should be no reason why the removal efficiency should decrease (Faust and Aly, 1998).

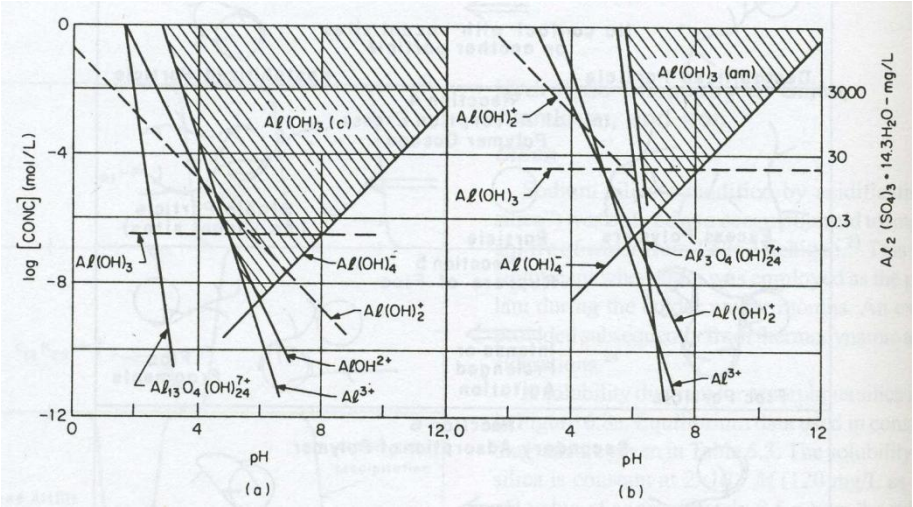

Fig. 30. Solubility of aluminum at equilibrium with (a) gibbsite and (b) amorphous $Al(OH)_3$ (Faust and Aly, 1998)

One possible cause of this decrease in removal efficiency involves the aluminum itself. If there is enough aluminum present, the negatively-charged particles may have their charge

changed from a negative charge to a positive one, instead of just neutralizing the charge. In this case, the algae particles would still repel each other, causing a decrease in removal efficiency.

After completing this part of the project, a procedure was developed for the jar test unit which will allow it to be operated quickly when more testing needs to be completed. Additionally, the researcher became proficient in the scaled-down TP method, which will enable the phosphorus testing to happen more quickly and at a fifth of the cost. This procedure will also be given to the City of Logan, because this could decrease testing expenses significantly. Finally, the optimum dose for TSS and phosphorus removal was determined: 30 mg/L.

CHAPTER 6

THE EFFECT OF ENVIRONMENTAL CONDITIONS ON ALUM AND POLYMER DOSING RATES

6.1 Introduction

The overall goal of this research project was to determine if there was an effect of environmental conditions on the algal harvesting efficiency of a given chemical dose. Previous research has shown that EPS production, a possible substitute for a chemical flocculant, can be higher in periods of higher irradiance and temperature. To determine if this is the case, the following experiment was designed.

The jar test unit was operated to evaluate treatment at different times throughout the day. The alum dose was kept constant while the polymer dose was varied from 0 mg/L to 1 mg/L. Irradiance, temperature, and pH were also monitored throughout the day. The removal efficiencies of the different polymer doses were then related to these environmental conditions in order to try to find a statistically significant relationship. The goal was to find a set of environmental conditions that would allow chemical dosing rates to be lowered.

The polymer used in this experiment is called “T-Floc AE-204,” and is an anionic polymer manufactured by Thatcher Chemical in Salt Lake City, UT. It was recommended by WesTech Engineering for use with their pilot-scale DAF unit.

6.2 Materials and Methods

This experiment provided a number of challenges. First, four different polymer doses were needed for each time point (0, 0.3, 0.6, and 1 mg/L). Since each dose needed to be done in triplicate, this required a total of twelve jars. This meant the jar test unit needs to be operated twice per time point.

In order to collect enough sample for the jar test unit to be run twice, a five gallon bucket was filled with sample at the required time. The first set of jars was filled from the bucket, and then the bucket was sealed. It was then lowered by a rope until it was submerged as much as possible in the Logan Lagoons. This allowed the sample in the bucket to be temperature regulated. Also, since the bucket was sealed, the darkness limited the amount of algae growth and other microbial activity. The turnaround time for the jar test unit was an hour, so this limited the time the sample had to sit in the bucket. Additionally, in order to minimize the effect of the sample staying in the bucket, all twelve samples (4 treatments, in triplicate) were randomly assigned to jars across both runs.

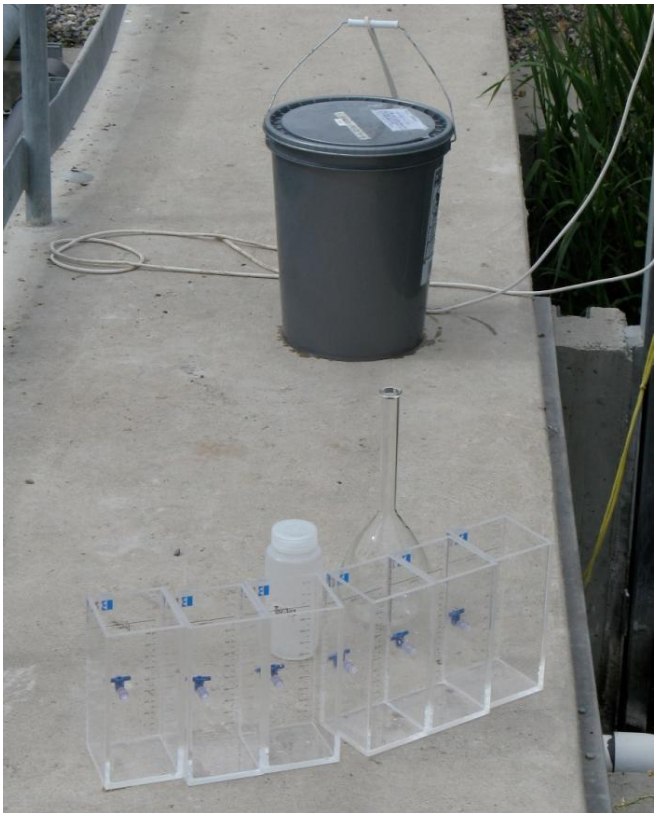

Fig. 31. Filling jars in preparation for jar test unit operation

Fig. 32. Sampling bucket in the Logan Lagoons

After this method was finalized, the testing procedure was developed. Data was collected throughout the course of a day. The time points used were 8 am, 9 am, 11 am, 12 pm, and 2 pm. However, this is too much to do in one day, so these data points were collected on multiple days. Because of the time required for testing, and security concerns with having students working at the Logan Lagoons after 5 pm, the 2 pm sampling time was the latest possible data point.

For the actual jar test unit operation, the same procedure was used as earlier (see chapter 5 JAR TEST UNIT). After a run was completed, the jar test unit was immediately washed with phosphorus-free soap and rinsed with DI water. If this was the first jar test unit run for a time point, the jar test unit was started again as soon as possible.

While the researcher was running the jar test unit, two undergraduate students were doing the lab tests. TSS tests were completed, put in the oven, dried, and weighed, according to Standard Methods. The scaled-down TP test was completed. (Both of these tests were completed in triplicate.) Additionally, since only a limited number of 500 mL plastic bottles were available, these bottles were washed with soap and acid-soaked for 1 hour.

While the testing was occurring, several monitoring equipment was operational. A Hach pH probe was submerged in the Logan Lagoons effluent, monitoring pH and temperature and recording data every 15 minutes. Additionally, a sensor was collecting the photosynthetic photon flux density (PPFD) and irradiance every minute.

6.2.1 Statistical Analysis

Statistical analysis for this section was completed in SAS, a software package commonly used in scientific applications. A slightly different model was used in this portion of the research. Since the researcher was essentially measuring "triplicates of triplicates" (each polymer dose was used on three different jars, and each jar was measured in triplicate), a nested experimental design was used, where each group of three measurements was nested within each replicate of each alum dose.

Note: originally, this was not the method of analysis planned. The original plan was to use the generalized linear model, as was used previously. This would allow one to easily measure the percent removal by averaging the triplicates for both the influent and effluent samples. However, the nested design eliminated the ability to use the percent removal values in the model, since this calculation would cause a loss in resolution. Therefore, the effluent measurements were used in the SAS program, and used to compare the percent removal values.

When data is presented, the same letter on two data points indicates that the two points are considered statistically equal, given the assumption described above. Additionally, when present, error bars are equal to the standard deviation. Since in all previous experiments our assumption of independent and identically distributed error terms was correct, it was assumed that this was the case with this phase of research.

6.3 Results and Discussion

The following two figures (Fig. 33 and Fig. 34) illustrate the overall removal efficiency of the jar test unit throughout the course of a day. The first set of samples was taken on July 21, 2011, at 8:20 am, 11:02 am, and 2:18 pm. The second day of sampling occurred on July 26, 2011, at 9:03 am and 12:01 pm.

In order to observe possible differences between treatment levels, this data will be divided into logical groups. First are the removal rates of total phosphorus (TP).

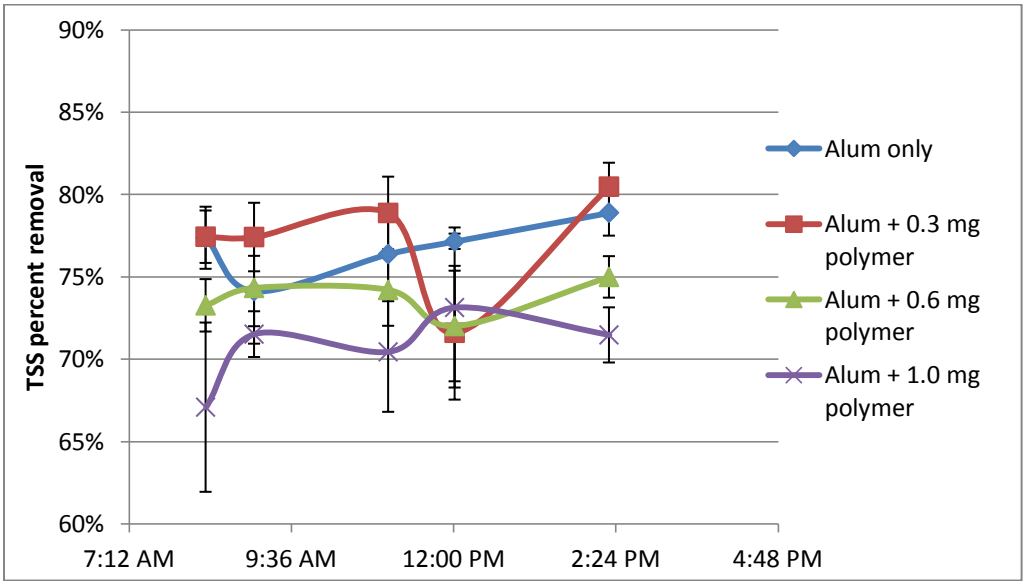

Fig. 33. TSS percent removal rates (July 21 and 26, 2011)

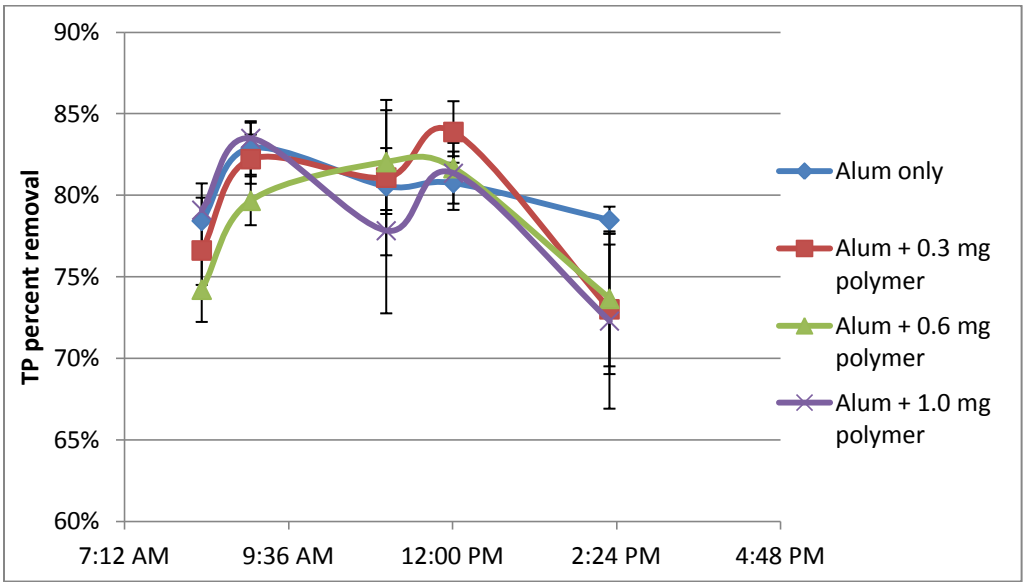

Fig. 34. TP percent removal rates (July 21 and 26, 2011)

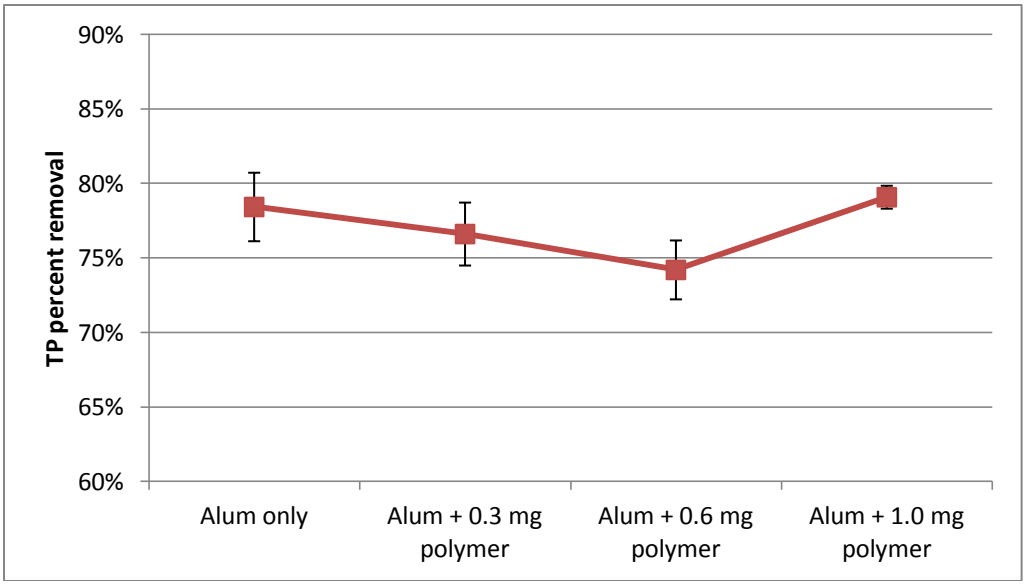

Fig. 35. TP percent removal (July 21, 2011, 8:20 am)

Table 12
Statistical groupings for TP removal, 8:20 AM

Polymer dose (mg/L)	Tukey Grouping		
0	A		
0.3	A	B	
0.6		B	
1.0	A	B	

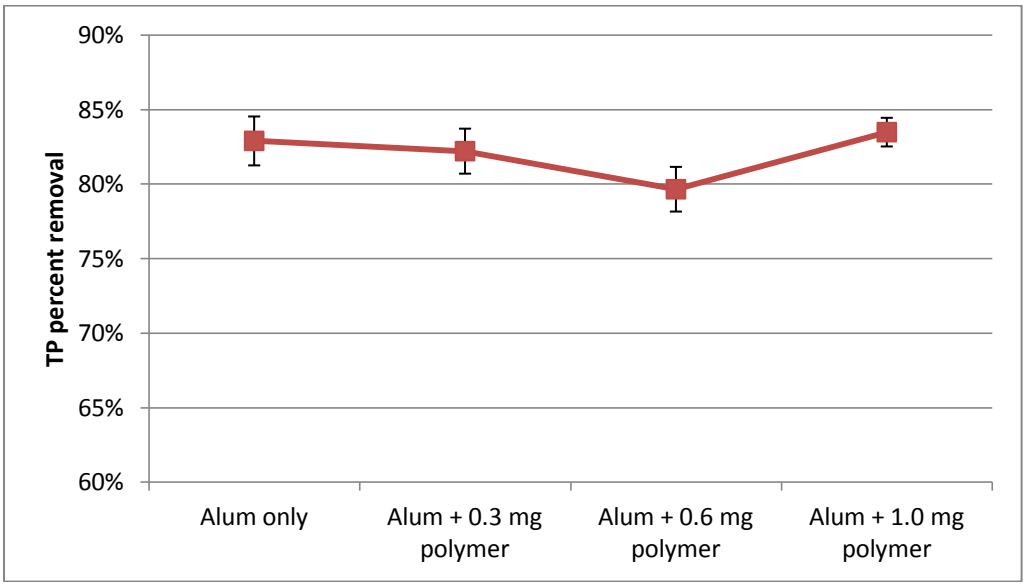

Fig. 36. TP percent removal (July 26, 2011, 9:03 am)

Table 13
Statistical groupings for TP removal, 9:03 AM

Polymer dose (mg/L)	Tukey Grouping		
0	A		
0.3	A	B	
0.6			
1.0	A	B	

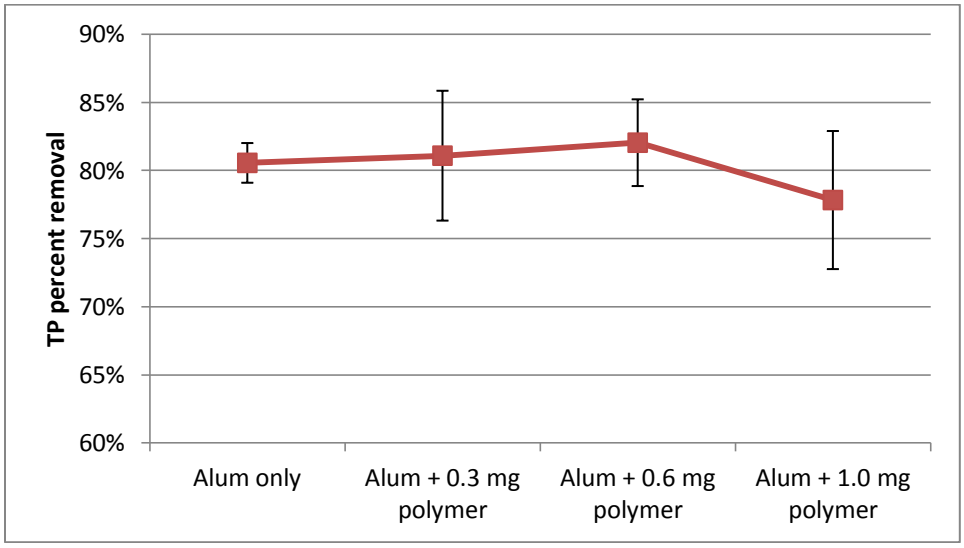

Fig. 37. TP percent removal (July 21, 2011, 11:02 am)

Table 14
Statistical groupings for TP removal, 11:02 AM

Polymer dose (mg/L)	Tukey Grouping		
0	A		
0.3	A	B	
0.6	A	B	C
1.0	A	B	C

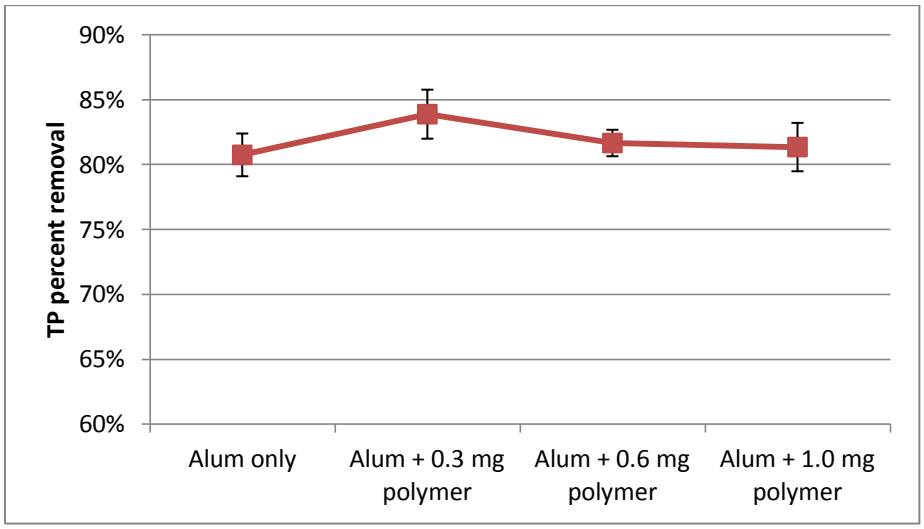

Fig. 38. TP percent removal (July 26, 2011, 12:01 pm)

Table 15
Statistical groupings for TP removal, 12:01 PM

Polymer dose (mg/L)	Tukey Grouping		
0	A		
0.3	A	B	
0.6	A	B	C
1.0	A	B	C

Upon looking at the TP removal data, very little difference in percent removal is seen throughout the day. In most cases, the lowest polymer dose produces statistically equal results as the three higher polymer doses. Even though the higher doses are often related to each other in various ways, the lowest dose is statistically equal to all of the rest.

When TSS percent removal is observed, the results are more interesting.

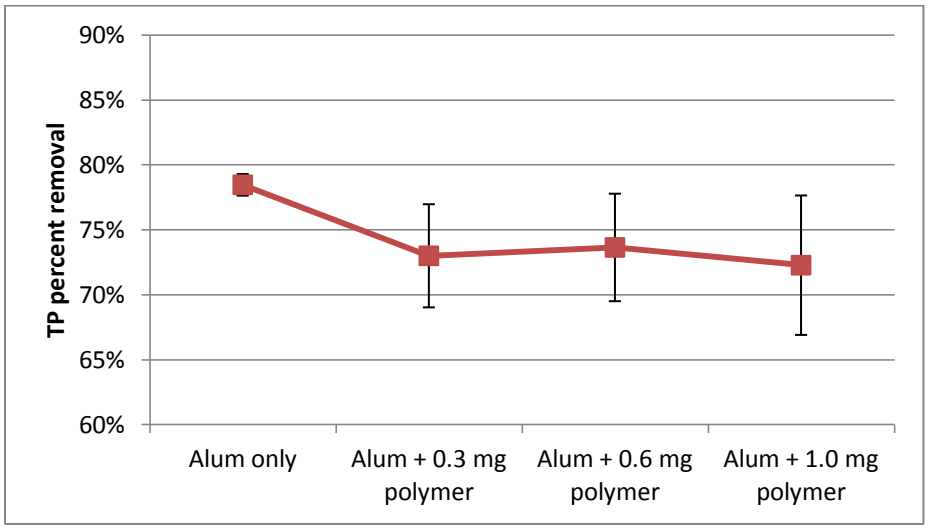

Fig. 39. TP percent removal (July 21, 2011 2:18 pm)

Table 16
Statistical groupings for TP removal, 2:18 PM

Polymer dose (mg/L)	Tukey Grouping		
0	A		
0.3	A	B	
0.6	A	B	
1.0		B	

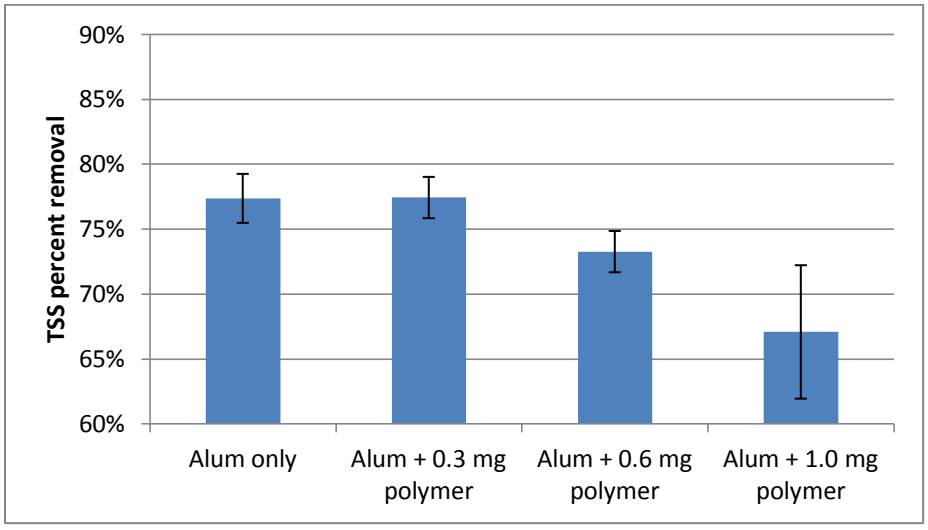

Fig. 40. TSS percent removal (July 21, 2011 8:20 am)

Table 17
Statistical groupings for TSS removal, 8:20 AM

Polymer dose (mg/L)	Tukey Grouping		
0	A		
0.3	A	B	
0.6		B	C
1.0			C

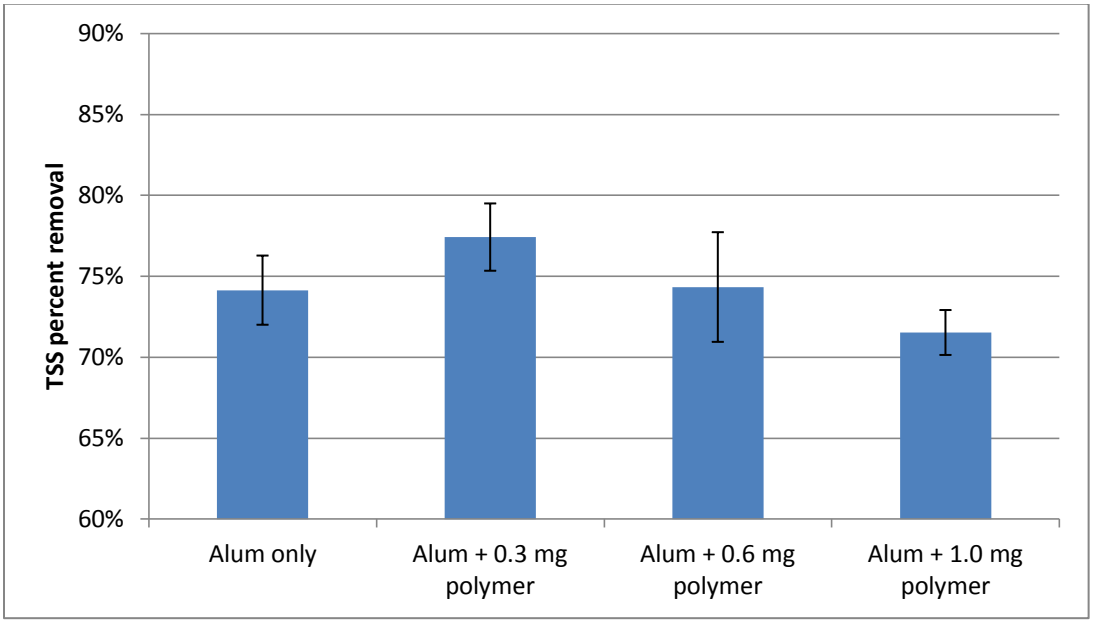

Fig. 41. TSS percent removal (July 26, 2011, 9:03 am)

Table 18
Statistical groupings for TSS removal, 9:03 AM

Polymer dose (mg/L)	Tukey Grouping		
0	A		
0.3	A	B	
0.6	A	B	C
1.0	A		C

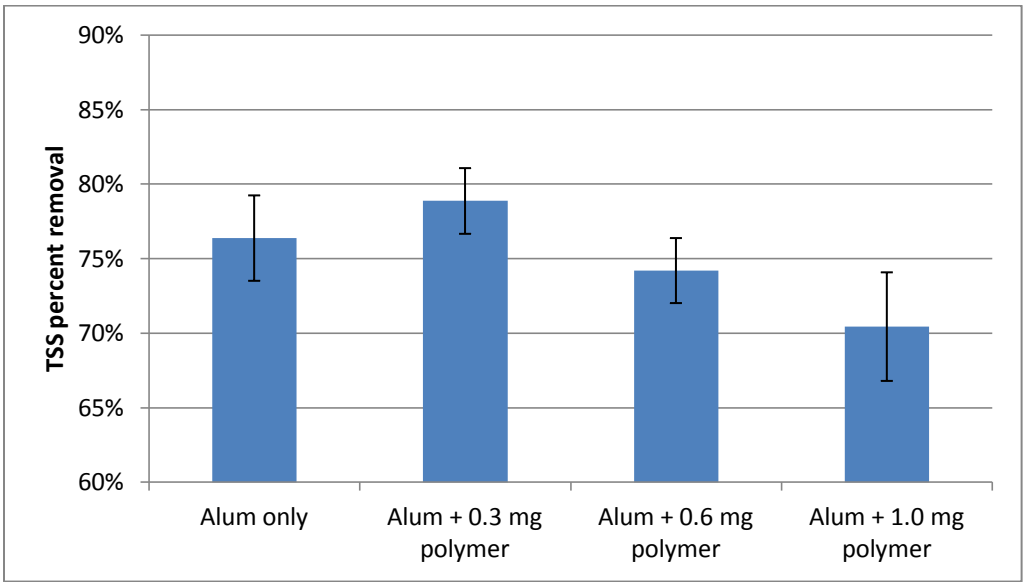

Fig. 42. TSS percent removal (July 21, 2011, 11:02 am)

Table 19
Statistical groupings for TSS removal, 11:02 AM

Polymer dose (mg/L)	Tukey Grouping		
0	A		
0.3	A	B	
0.6	A	B	C
1.0	A	B	C

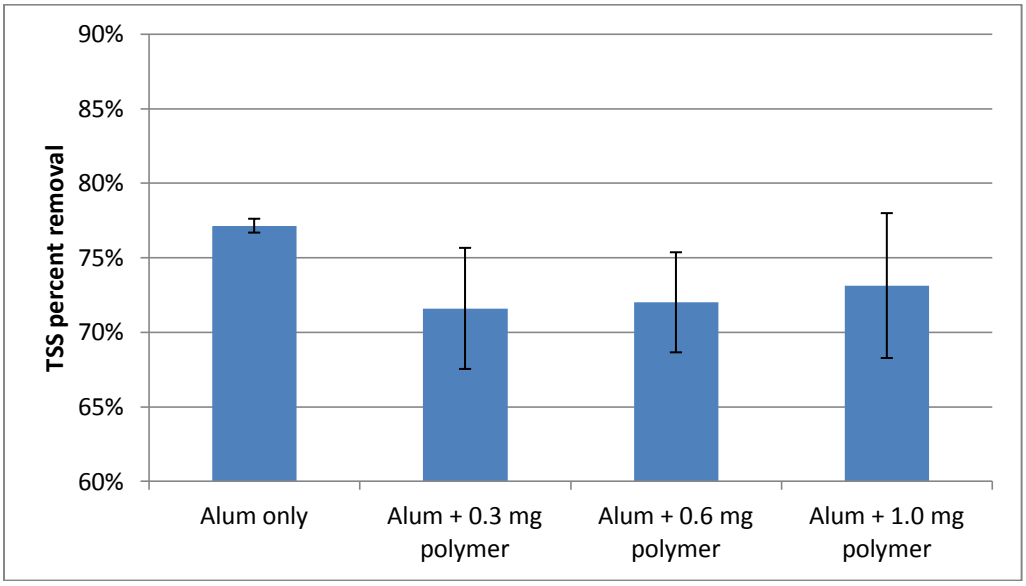

Fig. 43. TSS percent removal (July 26, 2011, 12:01 pm)

Table 20
Statistical groupings for TSS removal, 12:01 PM

Polymer dose (mg/L)	Tukey Grouping		
0	A		
0.3	A	B	
0.6	A	B	C
1.0	A	B	C

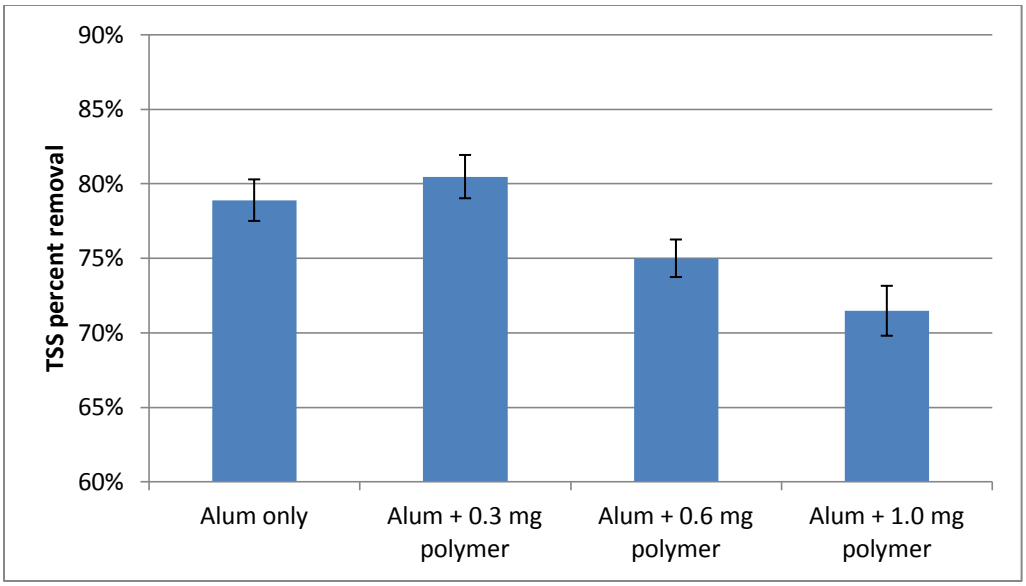

Fig. 44. TSS percent removal (July 21, 2011, 2:18 pm)

Table 21
Statistical groupings for TSS removal, 2:18 PM

Polymer dose (mg/L)	Tukey Grouping		
0	A		
0.3	A	B	
0.6	A	B	C
1.0	A	B	C

According to the data that were collected, adding polymer does not increase TSS removal efficiency. In four of the five time points, all four polymer doses produced a statistically identical result. In the fifth time point, the two larger polymer doses decreased the percent

removal by a significant percentage. This increased dose may have reversed the charge on the particles, lowering the percent removal.

In four of the five tests, the mean for the 0.3 mg/L polymer dose was either equal to or slightly higher than the 30 mg/L alum only treatment, but according to the statistical analysis, they are equal. Further testing to decrease the standard deviation might yield a statistically significant difference, but from this data, no advantage can be seen to using any amount of polymer. Because the polymer only adds cost, the recommended treatment is 30 mg/L alum only.

Even though there was no statistical reason to use the polymer to increase jar test unit efficiency, there was a visual difference seen between the different treatments. The following photographs were taken at the very end of the 15 minute slow mix period, and before the air injection. They show a decrease in the number of flocs, and an increase in the size of the flocs, as the polymer dose increases from 0.3 to 1.0 mg/L.

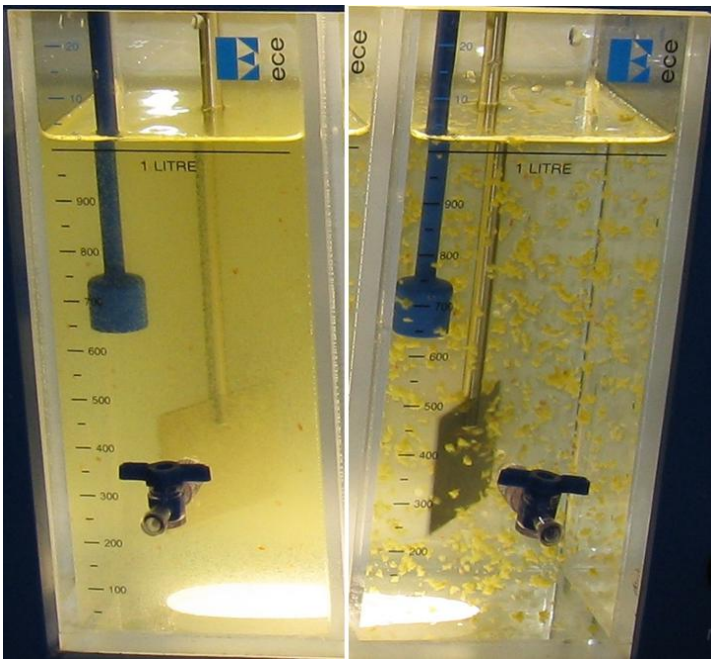

Fig. 45. Algal flocculation in jar test unit; 30 mg/L alum only (left) and 30 mg/L alum with 0.3 mg/L polymer (right)

Fig. 46. Algal flocculation in jar test unit; 30 mg/L alum with 0.6 mg/L polymer (left) and 30 mg/L alum with 1.0 mg/L polymer (right)

A difference between jars can also be seen once the air is injected into the system. In Fig. 47 below, two different treatments are compared. This photograph was taken after the 15 minute slow mix period, after the air insertion, and just prior to sampling. The left jar only received 30 mg/L alum as its treatment, while the right jar received 30 mg/L alum and 1.0 mg/L polymer. While it is difficult to see in this picture, the left jar (alum only) has a noticeable green color to the liquid, while the right jar (alum and polymer) looks very clear. No color can be seen in the liquid. This difference can be seen with any jar that received the polymer treatment.

Another difference is the quality of the float. In the left jar, the algae formed a solid, homogeneous float. This is the type of float that is easily removed by the pilot DAF unit, even though the individual flocs are small. Conversely, in the right jar, much larger flocs were formed. These flocs did not form the solid float, and some of the flocs were even too large to float.

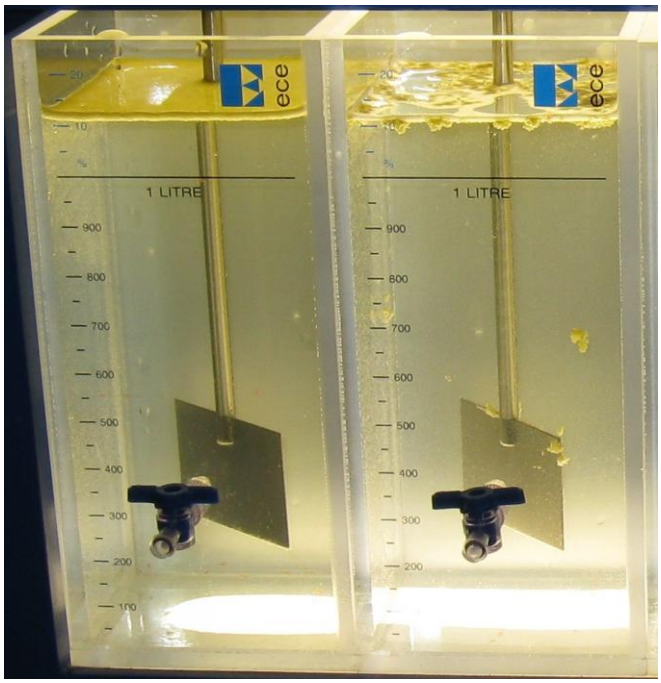

Fig. 47. Float comparison in jar test unit; 30 mg/L alum only (left) and 30 mg/L alum and 1.0 mg/L polymer (right)

Floc behavior is only one way that the jar test unit may operate fundamentally differently than the pilot DAF unit. First, it was assumed that all of the flocs in the jar test unit would have been removed in the pilot DAF unit. The pilot DAF unit has a scraper operating on a conveyor belt, and not all of the algae float is removed. Some escapes out of the effluent. Second, the jar test unit samples were taken from the sampling port on the jars, approximately one third of the way up the jar. It was assumed that this is the effluent of the jar test unit system, even though the jar test unit does not have a true effluent because of its "batch test" nature.

It is possible to compare this optimum dose (30 mg/L alum only) to the environmental conditions in place at the Logan Lagoons. First is the removal rate of this treatment, alongside the air temperature for one day of testing.

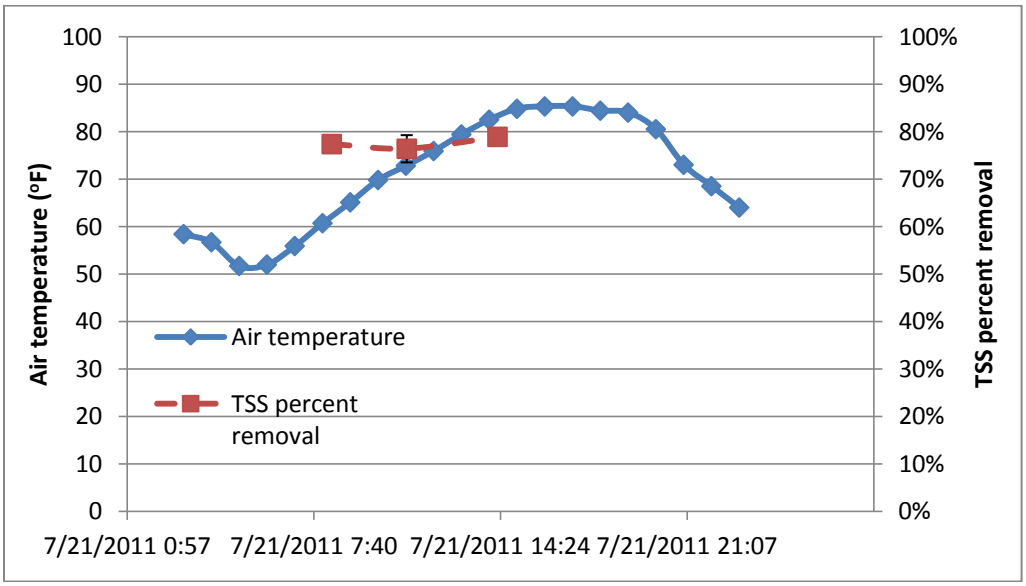

Fig. 48. TSS percent removal with 30mg/L alum vs. air temperature

Next is the sunlight data collected from the data logger on site at the Logan Lagoons. Fig. 49 shows both the PPFD (photosynthetic photon flux density) and irradiance (watts per square meter). These units look at the sunlight differently; PPFD has units of µmoles of photons/m^2/sec, while irradiance is measured in watts/m^2. Since the Campbell Scientific data station records sunlight intensity in irradiance, this unit will be the primary unit used.

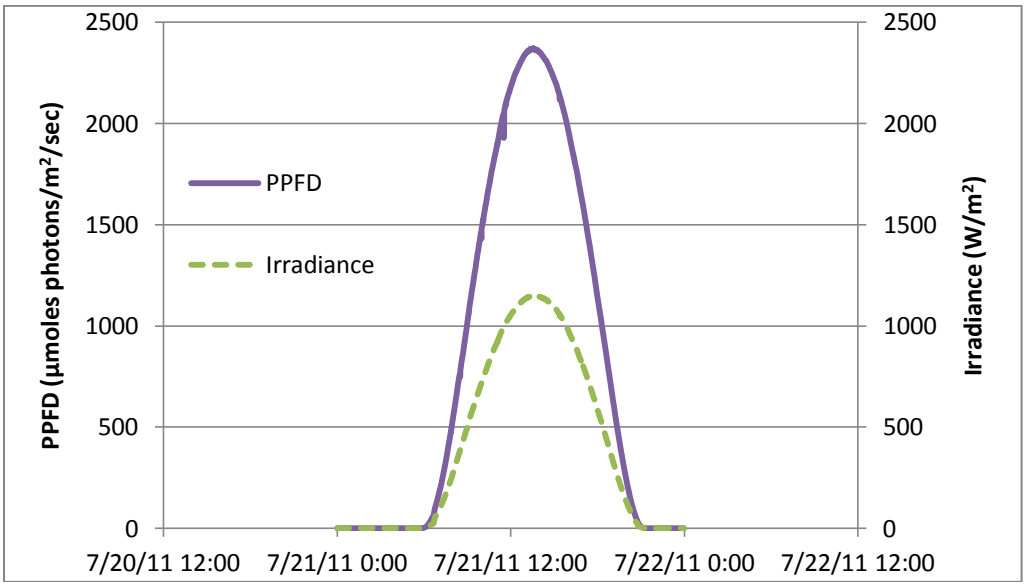

Fig. 49. Light intensity on July 21, 2011

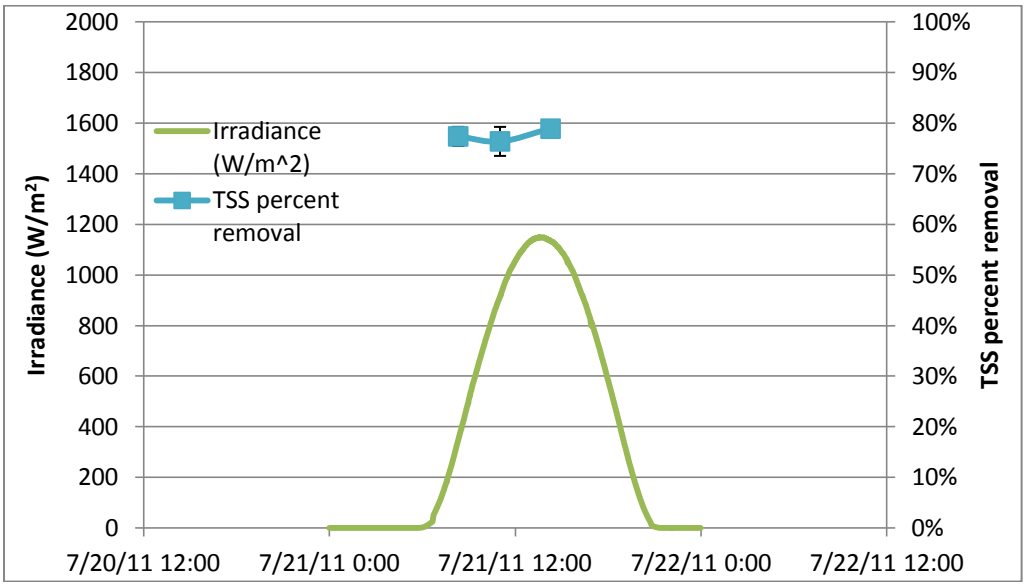

Fig. 50. TSS percent removal with 30 mg/L vs. irradiance

Finally, the effect that pH has on the TSS removal efficiency can be observed. As can be seen below in Fig. 51, there is very little change throughout the day from 8:20 am to 2:18 pm.

The pH probe was not operating correctly the day of testing, but previous days of testing also show little change over a 24 hour period.

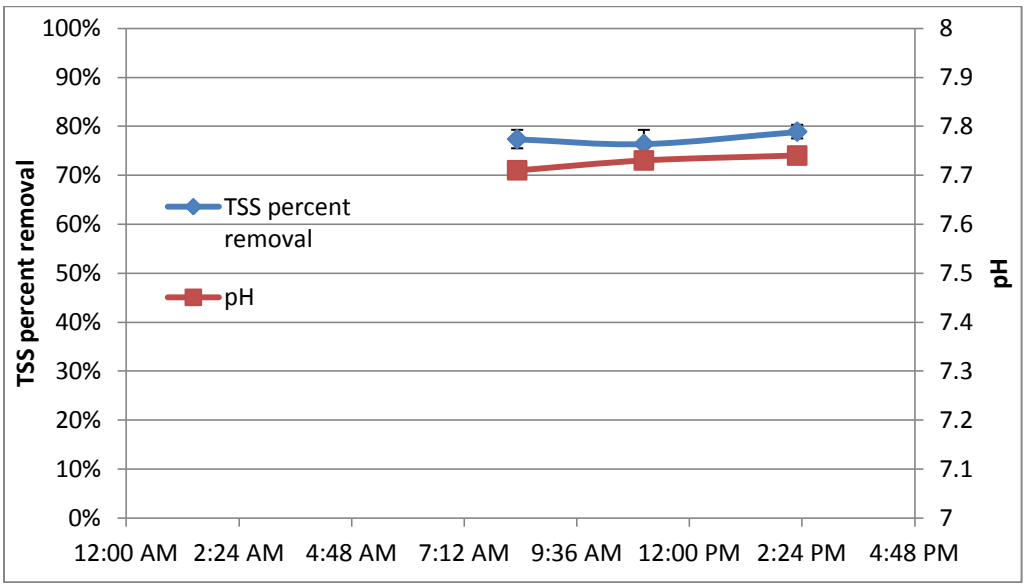

Fig. 51. TSS percent removal with 30 mg/L vs. pH

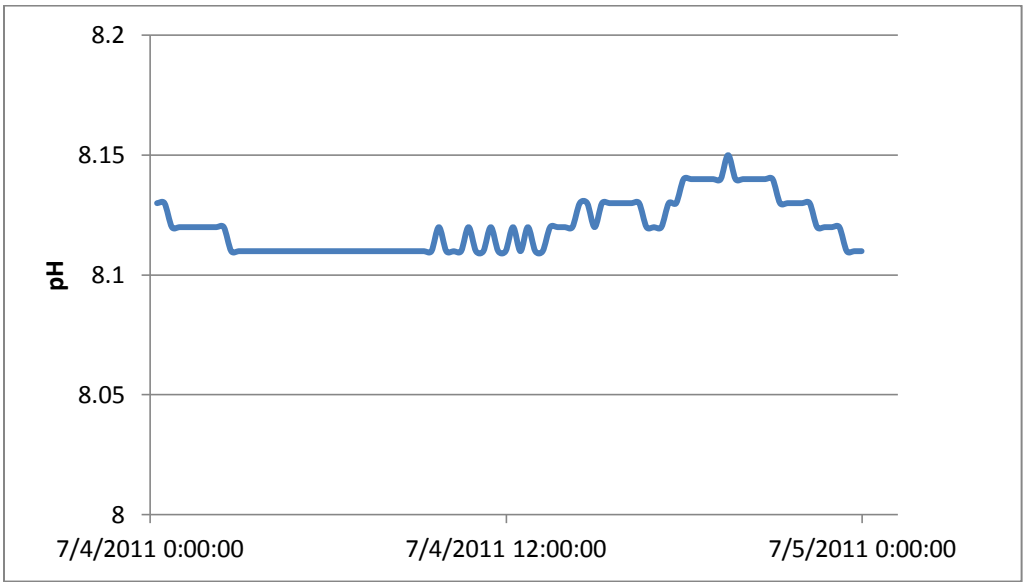

Fig. 52. pH in Logan Lagoons effluent (July 4, 2011)

6.4 Conclusion

After examining the TSS and TP removal efficiencies of several different treatments several times over the course of a day, several facts were determined. First, the amount of polymer added (0.3, 0.6, or 1 mg/L) does not increase the amount of TP removed from the wastewater. This is true across all five time points studied (8:20 am, 9:03 am, 11:02 am, 12:01 pm, and 2:38 pm).

Second, adding polymer does not increase TSS removal efficiency. It actually will decrease the TSS removal efficiency by a statistically significant amount at a concentration exceeding 0.3 mg/L. The "30 mg/L alum and 0.3 mg/L polymer" treatment was always very close to the "30 mg/L" treatment - they were statistically identical. Further replication could produce a noticeable difference between these two points, but this is unknown at this time.

It appears that the algae growing in the Logan Lagoons in the summer do not require additional polymer to increase the removal efficiency. This conclusion was reached during the heat of the summer. On the testing day, air temperatures reached a high of 85 ^{o}F and had only

reached a low of 51.7 ^{o}F the night before. The irradiance had reached a peak of approximately 1100 W/m^2, with a relatively constant pH of 8.1. Different values of temperature, irradiance, and pH would almost certainly change this conclusion.

Advances in our understanding and control of bioflocculation are required before the Logan wastewater treatment plant will be able to avoid some dose of chemical coagulant. The EPS might provide the "finishing step" that the synthetic polymer is currently providing. This also makes the most sense from an economic standpoint; alum is relatively cheap, but the polymer is orders of magnitude more expensive. A large cost benefit could be achieved if the polymer dose can be lessened even by a small percentage, especially when a full-scale DAF unit is installed at the Logan Lagoons.

CHAPTER 7

ECONOMIC ANALYSIS AND RECOMMENDATIONS

7.1 Introduction

The goal of this project was to provide the City of Logan with the most economical and environmentally friendly method of meeting state UDEQ requirements on phosphorus discharge. The City is committed to this goal; their desire to use a DAF system to collect the algae, meeting regulations and harvesting a valuable source of biomass, shows their commitment. However, the City of Logan requires an economic analysis of a DAF system. One of the primary costs for this technology is the chemical cost. The other is the electrical cost, since DAF technology is known to have a high energy requirement. Because of the high O&M costs for a DAF system, this theoretical setup will be compared to that of one based on a series of clarifiers.

7.2 Results and Discussion

It was determined previously that the optimum chemical dosing for Logan Lagoons effluent would be 30 mg/L alum. In order to get a more complete picture of how the chemical cost impacts the final cost of the harvested biomass, further testing was completed on the pilot DAF unit.

While the pilot DAF unit was operating at optimal conditions (31.5 mg/L alum dose, 51 gpm influent rate, 20 gpm recycle, and with a pressure of 70 psi in the recycle system), several tests were completed. These include TSS removal, TP removal, and a volatile solids (VS) measurement on the algae float. The VS measurement will demonstrate the amount of the collected biomass that is actually algae, not inert substances like dirt, sand, and aluminum

sulfate. This will demonstrate how much algae is actually available for biogas or biodiesel production.

Below in Table 22 is a comparison of the chemical costs for the pilot DAF unit at the Logan Lagoons and a proposed full-scale DAF unit. Assuming the same dosage rates for the full-scale unit, running at a flow rate of 15 MGD (million gallons per day), it would cost $1,118.41 in alum stock solution to run for a 24 hour period. This calculation assumes the purchase of the aluminum sulfate in bulk quantities (at least 48,000 lbs) from Thatcher chemical. This quantity of alum sells for $208/ton, which is equal to $0.1038/lb.

Table 22
Chemical costs for pilot and full-scale DAF unit

	Alum dose (mg/L)	Influent flow rate (gpm)	Daily alum cost ($/day)	Daily polymer cost with 0.3 mg/L dose ($/day)	Total cost ($/day)
Pilot-scale DAF unit	31.5	51	$ 5.48	$ 1.24	$ 6.72
Full-scale DAF unit	31.5	10,417	$ 1,118.41	$ 862.34	$ 1,980.75

It was noted previously that additional replication of this testing may reveal that the alum dose along with 0.3 mg/L polymer may yield the best result. The T-Floc AE-204 polymer costs $125 per 5 gallon bucket. This stock polymer is diluted down to a 1% dilution, but the cost is still significant. Adding the polymer to the full-scale DAF unit would add another $862.34/day.

Since the VS, TSS, and TP were calculated with the operation of the pilot DAF unit, the biomass production can be estimated, along with TP and TSS removal, and how much this removal costs on a unit basis. On this test, 68% of the TSS and 65% of the TP was removed, bringing the TSS and TP levels down to acceptable limits (<25 mg/L and <0.5 mg/L, respectively).

Also, the cost was calculated for the removal of each mg/L of TSS and TP. To remove 1 mg/L of TSS, it costs $0.25 worth of alum stock solution. To remove the same amount of TP loading, $7.24 of alum stock is required. See Table 23 for more information.

Table 23
Performance and unit cost values for pilot DAF unit

Performance					
TSS removal (%)	TSS removal (mg/L)	TP removal (%)	TP removal (mg/L)	VS harvested (wt %)	VS harvested (kg/day)
68%	21.7	65%	0.757	0.7%	7.65
Unit cost					
Cost per kg algae harvested ($/kg)		Cost per mg TP removed ($/(mg/L))		Cost per mg TSS removed ($/(mg/L))	
$ 2.15		$ 7.24		$ 0.25	

These calculations also allowed the quantity of biomass created by the pilot DAF unit to be determined. This unit was able to harvest biomass at a 0.7% by weight concentration, and could collect 7.65 kg of dry algae in a 24-hour period. The cost of alum to harvest 1 kg of dry algae is $2.15.

Table 24
Electrical costs on a full-scale DAF unit

Technology	Influent flow rate (gpm)	Recycle flow rate (gpm)	Required pump size (hp)	kW/hp	Required pump size (kW)	Power usage per day (kwh/day)				
Recycle pumps	10417	1250	100	0.7457	74.57	1789.68				
	Recycle flow rate (gpm)	Air flow rate (gpm)	gal/ft^3	Air flow rate (cfm)	Required flow (cfm)	Required pump size (hp)	kW/hp	Required pump size (kW)	Power usage per day (kwh/day)	Actual power usage (Only operates 40%) (kwh/day)
Air compressors	1250	125	7.481	16.709	34.2	10	0.7457	7.457	178.968	71.5872
	Daily electrical use (kwh)	Daily electrical cost ($)								
Total	1861.2672	$ 148.90								

The electrical cost of the DAF unit is also an important consideration. After consulting with engineers at WesTech (David Romer, October 25, 2011), it was determined that the increased electrical cost for a DAF unit (above that of a clarifier system) are from the recycle pumps and the air compressors. All other electrical costs were assumed to be equal.

The data in Table 24 is based on a number of assumptions. First, that the recycle flow rate is 12% of the influent flow rate, and the air flow rate is 10% of the recycle rate. Additionally, the air compressors only run 40% of the time; a factor for this reduction was included. In order to calculate the daily electrical cost, the high value for the range of commercial electricity cost for Utah was used, as displayed on Rocky Mountain Power's website ($0.071 - 0.08/kWh). This results in an increased electrical load from a DAF unit to be 1,861 kWh/day, or $148.90/day.

In order to estimate the construction cost of a DAF unit, in comparison to a clarifier-based system, Carollo Engineers was contacted on August 18, 2011. Dustin Hansen supplied two recent proposals. The first quoted a 15 MGD clarifier system with a total estimated construction cost at $8,778,700. The second detailed a 15 MGD DAF system for the Logan Lagoons, with a final cost of $6,599,000. All of these costs are detailed below in Table 25.

Table 25
Cost comparison of full-scale DAF unit and full-scale clarifier

Technology	Daily alum cost	Electrical cost	Daily O&M	VS harvested (kg/day)	Construction cost	Price of VS required to offset daily O&M cost ($/kg)
Pilot DAF unit	$ 5.48	$ -		7.65	$ -	$ -
Full-scale DAF unit	$ 1,118.41	$ 148.90	$ 1,267.31	1562.55	$ 6,599,000	$ 0.81
Clarifier	$ -	$ -	$ -	0	$ 8,778,700	$ -

Assuming that the amount of algae (volatile solids) will scale up from the pilot DAF unit in a linear fashion, the full-scale DAF unit will produce 1,563 kg of algae per day. In order to offset the additional daily cost of aluminum sulfate and electricity, this algae would have to be worth $0.81/kg.

These cost assumptions, however, are only valid during the environmental conditions when the tests were completed. It is assumed that the removal rates will not be as high when the irradiance and temperature levels are lower.

The first variable to discuss is air temperature. For the jar test unit removal testing done in July, air temperatures had reached into the 80s (^{o}F) during the day, and cooled off into the low 50s (^{o}F) at night. When considering the air temperature data collected from the Campbell Scientific data logger in Fig. A-10, several months have roughly fit these conditions since October 2010. Late June 2011, July 2011, and late October 2010 match this temperature profile. August or September 2010 data is not available, but since that data would come before the October data, it is assumed that it would have a similar (or higher) temperature profile. This can lead us to assume that in general, the removal rates obtained earlier would be similar between late June and early October, at least when air temperature is concerned.

The next variable to look at is the irradiance. According to the irradiance levels recorded at the Campbell Scientific data logger (Fig. A-11), the irradiance in July is very similar to the levels seen in May and June. October 2010 had significantly lower irradiance levels, so it is difficult to make assumptions about August and September. However, from experience, August is as hot and sunny as July. This suggests that the removal rates from previously in this report would be similar at least between May and August, at least with respect to the irradiance.

The final variable to consider is the pH. However, the seasonal variation in pH is small when the standard deviations are considered (see Fig. A-8).

7.3 Conclusion

Using an optimum treatment dose of 30 mg/L alum, the daily alum cost to treat all of the Logan Lagoons effluent would be $1,118.41. The additional electricity need to run a DAF unit instead of a clarifier would cost an additional $148.90 a day. This means that this additional daily cost of $1,267.31 can be offset by the algae production if it is priced at $0.81/kg.

The testing done for this economic analysis was completed in July, one of the warmest, sunniest months of the year in Logan, UT. This would be the best time for EPS production, which was the primary focus of this thesis project. However, this means that any economic conclusions reached here must only apply to this time period.

After looking at the irradiance and temperature levels for October 2010 through July 2011, these economic assumptions would be valid for the months of at least June through August. They may also be correct for the months of May and September, but further testing would be required to confirm this.

CHAPTER 8

FUTURE RESEARCH NEEDS

There are a number of areas where research is still needed. Even though the data collected is representative of warm, summer months, this testing should be completed over the course of the year. The Logan Lagoons effluent likely behaves differently under different environmental conditions with the same alum and polymer dosing rates. Summer is when EPS production is the highest; how well different dosing rates work in the winter should also be observed. Additionally, the TSS is significantly higher in the winter months as compared to the summer; a difference in algae concentration may require a different alum/polymer dose.

The pilot DAF unit should be operated with the conditions and the optimum dosing rates that were found with the jar test unit. It is necessary to replicate what was found at a small scale with the jar test unit; the pilot DAF unit should also be run with varying polymer doses. No improvements in TSS or TP removal efficiencies were seen, but a visible difference in floc size was observed. These larger, more stable flocs may make a bigger difference in the pilot DAF unit than the jar test unit.

Also, testing to determine the environmental impacts on chemical dosing rates should be completed on a batch culture of algae growing in a raceway. Autoflocculation has been observed occurring in raceways at the Logan Lagoons; it would be very informative to see how this could affect jar test unit operation. Ideally, the hourly testing would be done at different points along the culture's life cycle. If testing throughout the day was done every three days, for example, the effect of the age of the algal culture could also be taken into effect. It would be advantageous to know if, for example, if an algal culture is allowed to age for 10 days, only half of the chemical is required for proper DAF removal rates.

Finally, research needs to be completed into the proper molar ratio of algae to alum. The optimum alum dose found in this project of 30 mg/L depended on the range of algae seen in the effluent of the Logan Lagoons (20-40 mg/L). Aluminum sulfate is able to coagulate the algae because the alum is able to physically neutralize the negative charges of each individual algae cell. If a raceway system were installed, in order to bring the algae concentration up to 300 mg/L, much more alum would be needed. Research into the optimum molar ratio of algae to alum would need to be completed before a higher feedstock is run through the DAF unit.

CHAPTER 9

CONCLUSIONS

As part of the first objective of this research, the optimum alum dose for TSS and TP removal was found to be 30 mg/L, on both the pilot DAF unit and the jar test unit. It was determined that the addition of the polymer T-Floc AE-204 did not increase the percent removal of either TSS or TP. The percent removal actually decreased when the polymer was used, indicating that the polymer was reversing the charge, not neutralizing it.

Data collected during the economic analysis of this project provided the molar ratios of aluminum to TP and aluminum to TSS. During this testing, 21.7 mg/L TSS and 0.757 mg/L TP was removed, while using a 31.5 mg/L alum dose. Using the assumption that the molar weight of algae is 3,550 g/mole, the molar ratio of Al/TSS was found to be 30.1. The molar ratio of Al/TP was found to be 7.5.

An additional objective was to determine if the algal species living in the Logan Lagoons will flocculate without the addition of chemicals. Initial data obtained with the pilot DAF unit demonstrated that even without alum or polymer addition, approximately 7% of the TSS was able to be removed. No phosphorus was removed at the same time. The jar test unit, however, was able to remove 24% of the TSS and 7% of the TP without using any chemical addition.

Even though the jar test unit was able to remove 24% of the TSS and 7% of the TP without chemical addition, this is not enough to assume that we can run a full-scale DAF without chemical addition.

The second objective of this research project was to determine if autoflocculation and bioflocculation can improve DAF efficiency when chemical coagulants are used. While using a constant, optimum alum dose (30 mg/L), and using varying amount of synthetic polymer, it was

determined that adding the polymer either made the removal rates worse, or matched the alum dose for removal efficiencies. This indicates that during warm, summer months, no synthetic polymer is required to get the best TSS and TP removal efficiencies.

The final objective for this project was to conduct an economic analysis for DAF operation with and without chemical addition. It was determined that some chemical was required, and this 30 mg/L alum dose would have a chemical cost of $1,118.41/day. The necessary electrical cost of the DAF unit would add an additional $148.90 to the daily cost. It was determined that this treatment/pricing combination would be valid at least for the months of June through August. If 0.3 mg/L polymer is needed during non-summer months, then another $862.34 in polymer cost would need to be added per day.

REFERENCES

Adelman, M.A., 1990. Mineral depletion, with special reference to petroleum. Rev. Econ. Stat. 72, 1-10.

Bare, W.F.R., Jones, N.B., Middlebrooks, E.J., 1975. Algae removal using dissolved air flotation. J. Water Pollut. Control Fed. 47, 153-169.

Behzadi, S., Farid, M.M., 2007. Review: examining the use of different feedstock for the production of biodiesel. Asia Pac. J. Chem. Eng. 2, 480-486.

Benson, A., 2007. Sewage lagoons on way out? The Herald Journal.

Brandt, A.R., Farrell, A.E., 2007. Scraping the bottom of the barrel: greenhouse gas emission consequences of a transition to low-quality and synthetic petroleum resources. Climatic Change 84, 241-263.

Chisti, Y., 2007. Biodiesel from microalgae. Biotechnol. Adv. 25, 294-306.

Chisti, Y., 2008. Biodiesel from microalgae beats bioethanol. Trends Biotechnol. 26, 126-131.

Chung, Y., Choi, Y.C., Choi, Y.H., Kang, H.S., 2000. A demonstration scaling-up of the dissolved air flotation. Water Res. 34, 817-824.

City of Logan, UT, 2008. City of Logan, Monthly Operation Report, Wastewater Treatment Facility.

Decho, A., 1990. Microbial exopolymer secretions in ocean environments: their role(s) in food webs and marine processes. Oceanogr. Mar. Biol. Annual Review 28, 73-153.

DeLuchi, M.A., 1991. Emissions of greenhouse gases from the use of transportation fuels and electricity.

Demirbas, A., 2009. Biofuels: Securing the Planet's Future Energy Needs. Springer, London.

Dismukes, G.C., Carrieri, D., Bennette, N., Ananyev, G.M., Posewitz, M.C., 2008. Aquatic phototrophs: efficient alternatives to land-based crops for biofuels. Curr. Opin. Biotechnol. 19, 235-240.

Eaton, A., Clesceri, L., Rice, E., Greenberg, A., Franson, M., 2005a. 2540-D Total Suspended Solids Dried at 103-105 C, in: Standard Methods for the Examination of Water & Wastewater: Centennial ed. American Public Health Association, Washington.

Eaton, A., Clesceri, L., Rice, E., Greenberg, A., Franson, M., 2005b. 4500-P E. Phosphorus, in: Standard Methods for the Examination of Water & Wastewater: Centennial ed.

American Public Health Association, Washington.

Eaton, A., Clesceri, L., Rice, E., Greenberg, A., Franson, M., 2005c. 4500-N Nitrogen, in: Standard Methods for the Examination of Water & Wastewater: Centennial ed. American Public Health Association, Washington.

Eaton, A., Clesceri, L., Rice, E., Greenberg, A., Franson, M., 2005d. 2540-F Settleable Solids, in: Standard Methods for the Examination of Water & Wastewater: Centennial ed. American Public Health Association, Washington.

Fargione, J., Hill, J., Tilman, D., Polasky, S., Hawthorne, P., 2008. Land clearing and the biofuel carbon debt. Science 319, 1235-1238.

Faust, S.D., Aly, O.M., 1998. Chemistry of Water Treatment, 2nd ed. Ann Arbor Press, Ann Arbor.

Goldman, J., Carpenter, E., 1974. A kinetic approach to the effect of temperature on algal growth. Limnol. Oceanogr. 756-766.

Golueke, C.G., Oswald, W.J., 1965. Harvesting and processing sewage-grown planktonic algae. J. Water Pollut. Control Fed. 37, 471-498.

Gregory, J., 2006. Particles in Water: Properties and Processes. CRC Press, Baca Racon, FL.

Griffiths, E., Viamajala, S., Thompson. R., Jones, J., Sims, R., Hamud, I., 2009. Evaluation of biofuel potential through wastewater treatment using algae. Presented at the 31st Symposium on Biotechnology for Fuels and Chemicals, San Francisco, CA.

Harrison, R.G., Todd, P., Rudge, S.R., Petrides, D.P., 2003. Bioseparations Science and Engineering. Oxford University Press, New York.

Hill, J., Nelson, E., Tilman, D., Polasky, S., Tiffany, D., 2006. Environmental, economic, and energetic costs and benefits of biodiesel and ethanol biofuels. Proceedings of the National Academy of Sciences 103, 11206 -11210.

Hirsch, R.L., 2008. Mitigation of maximum world oil production: shortage scenarios. Energy Policy 36, 881-889.

Hsu, P.H., 1975. Precipitation of phosphate from solution using aluminum salt. Water Res. 9, 1155-1161.

Kilian, L., 2008. Exogenous oil supply shocks: how big are they and how much do they matter for the U.S. economy? Review Econ. Stat. 90, 216-240.

Kim, S., Dale, B.E., 2005. Life cycle assessment of various cropping systems utilized for producing biofuels: bioethanol and biodiesel. Biomass Bioenergy 29, 426-439.

Larsdotter, K., Jansen, J. la C., Dalhammar, G., 2007. Biologically mediated phosphorus precipitation in wastewater treatment with microalgae. Environ. Technol. 28, 953.

Lavoie, A., de la Noue, J., 1987. Harvesting of Scenedesmus obliquus in Wastewaters: Auto- or Bioflocculation? Biotechnol. Bioengin. 30, 852-859.

Moellmer, W., 1974. Factors Controlling Autoflocculation for Algae and Algal Nutrient Removal (Ph.D. Dissertation), University of California, Berkeley.

Pavoni, J.L., Keiber, S.W., Boblitt, G.T., 1974. The harvesting of algae as a food source from wastewater using natural and induced flocculation techniques, in: Wastewater Use in the Production of Food and Fiber - - Proceedings, Environmental Protection Technology Series. Presented at the Conference on the Use of Wastewater in the Production of Food and Fiber, Office of Research and Development, U.S. Environmental Protection Agency, Oklahoma City, Oklahoma, pp. 435-496.

Pimentel, D., Patzek, T., 2005. Ethanol Production Using Corn, Soybeans, Switchgrass, and Wood; Biodiesel Production Using Soybean and Sunflower. Nat. Resour. Res. 14, 65-76.

Ragauskas, A., Williams, C., Davison, B., Britovsek, G., Cairney, J., Eckert, C., Frederick, W., Hallett, J., Leak, D., Liotta, C., Mielenz, J., Murphy, R., Templer, R., Tschaplinski, T., 2006. The path forward for biofuels and biomaterials. Science 311, 484-489.

Richmond, A., 2004. Handbook of Microalgal Culture - Biotechnology and Applied Phycology. Blackwell Science Ltd., Oxford.

Rubio, J., Souza, M.L., Smith, R.W., 2002. Overview of flotation as a wastewater treatment technique. Miner. Eng. 15, 139-155.

Sawyer, C., McCarty, P., Parkin, G., 2003. Chemistry for Environmental Engineering and Science, 5th ed. McGraw-Hill., Boston.

Schuessler, R.G., 1967. An Investigation of the Chemical Flocculation and Auto-Flocculation of Algae (Master's Thesis), University of Notre Dame.

Sheehan, J., Dunahay, T., Benemann, J., Roessler, P., 1998. A Look Back at the U.S. Department of Energy's Aquatic Species Program - Biodiesel from Algae. National Renewable Energy Laboratory, Golden, Colorado.

Smith, D.J., Underwood, G.J.C., 2000. The production of extracellular carbohydrates by estuarine benthic diatoms: the effects of growth phase and light and dark treatment. J. Phycol. 36, 321-333.

Staats, N., Stal, L., Mur, L., 2000. Exopolysaccharide production by the epipelic diatom Cylindrotheca closterium: effects of nutrient conditions. J. Exp. Mar. Biol. Ecol. 249, 13-27.

Sukenik, A., Shelef, G., 1984. Algal autoflocculation - verification and proposed mechanism. Biotechnol. Bioeng. 26, 142-147.

SWCA Environmental Consultants, 2010. Middle Bear River and Cutler Reservoir: Total Maximum Daily Load (TMDL). Utah Division of Water Quality.

Teixeira, M.R., Rosa, M.J., 2006. Comparing dissolved air flotation and conventional sedimentation to remove cyanobacterial cells of Microcystis aeruginosa: Part I: The key operating conditions. Sep. Purif. Technol. 52, 84-94.

Tian, Y., Zheng, L., Sun, D.-zhi, 2006. Functions and behaviors of activated sludge extracellular polymeric substances (EPS): a promising environmental interest. J. Environ. Sci. 18, 420-427.

Tilman, D., Hill, J., Lehman, C., 2006. Carbon-negative biofuels from low-input high-diversity grassland biomass. Science 314, 1598-1600.

Wang, B., Li, Y., Wu, N., Lan, C.Q., 2008. CO2 bio-mitigation using microalgae. Appl. Microbiol. Biotechnol 79, 707-718.

Wolfstein, K., Stal, L.J., 2002. Production of extracellular polymeric substances (EPS) by benthic diatoms: effect of irradiance and temperature. Mar. Ecol. Prog. Ser. 236, 13-22.

Wolverton, B.C., McDonald, R.C., 1979. Upgrading facultative wastewater lagoons with vascular aquatic plants. J. Water Pollut. Control Fed. 51, 305-313.

Zhang, X., Hu, Q., Sommerfeld, M., Puruhito, E., Chen, Y., 2010. Harvesting algal biomass for biofuels using ultrafiltration techniques. Bioresour. Technol. 101, 5297-5304.

APPENDICES

APPENDIX A: NUTRIENT AND ENVIRONMENTAL DATA AT THE LOGAN LAGOONS

A1.1 Introduction

Since it has been previously shown that temperature, irradiance, and nutrient levels have a positive effect on EPS production in algae, it is important to know how these variables change and how they impact the algae growing in the Logan Lagoons. In order to determine the range of these values, several monitoring tests were designed and run at different points throughout the year. The first of these tests involved a small-scale, indoor, raceway filled with Logan Lagoons effluent. This raceway was constructed by a previous graduate student, and was used twice to collect two separate sets of data. First, the algae culture was given daily nutrient addition of nitrogen and phosphorus and allowed to increase to the capacity of the raceway. The raceway was refilled, and this time, did not receive additional nutrients. The response of the raceway was monitored, and was used for the second set of data.

The second test involved a wide range of nutrient testing done by undergraduate students on the Logan Lagoons effluent from July 2010 to August 2011. A range of tests were performed on the effluent three times a week, including total suspended solids (TSS), total and soluble P, total and soluble N, orthophosphate, ammonia, total and soluble COD, and pH. The tests that are the most relevant are TSS, TP, and pH.

The third test involved observing the settleable solids of the wastewater. Using an Imhoff cone, the amount of settleable solids in the Logan Lagoons effluent was determined over the course of a day.

The fourth and final test involved a weather station located in Logan, UT. This weather station, run by Campbell Scientific, is approximately 2.75 miles from the Logan Lagoons research site. This weather station publishes a variety of environmental conditions on the Campbell

Scientific website, including air temperature, precipitation, solar radiation, relative humidity, and wind speed. This data is published hourly for the last 24 hours, but a computer script was written which downloads this data on a daily basis, providing hourly weather data starting in October 2010.

A1.2 Materials and Methods

A1.2.1 Indoor raceway with and without nutrient addition

The raceway used in this experiment was constructed by Nathan Israelsen and Erick Griffiths, who permitted it to be used for this experiment. It measures 8 feet long by 3 feet wide by 3 feet tall, and holds a volume of 450 L. This raceway has curved corners to eliminate locations of low flow, and a paddlewheel to keep the culture flowing smoothly. It is surrounded by natural wavelength fluorescent bulbs on two sides and the bottom, in order to provide sufficient light for algal growth.

The first time the raceway was operated, nutrients were added on a regular basis. In order to properly monitor this raceway, a number of steps were completed 5 days a week (Monday through Friday). The water level was measured at a specific point, and water was added to bring the total depth up to 10 inches. The calibration of a pH meter was checked, and if no recalibration was required, then the pH and temperature of the raceway was measured at the same location as the water. Three 250 mL samples were then pulled from the raceway surface at the same location.

Following Standard Methods for the Examination of Water & Wastewater (Eaton, Clesceri, Rice, Greenberg, and Franson, 2005a), a TSS test was performed on each of the three samples. Additionally, a total nitrogen test (using the persulfate digestion method (Eaton, Clesceri, Rice, Greenberg, and Franson, 2005c)) and total phosphorus test (using the acid

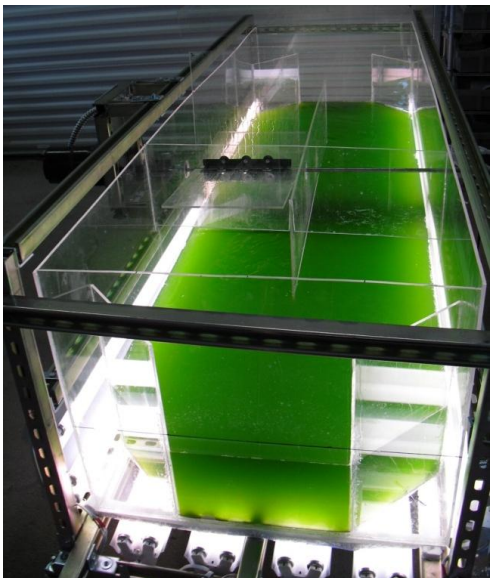

Fig. A-1: Small-scale raceway growing an algal culture

persulfate digestion method (Eaton, Clesceri, Rice, Greenberg, and Franson, 2005b)) were performed in triplicate on these samples. These tests were performed using Hach Test 'N Tube kits, which are based on the Standard Methods procedures. After these values are obtained, calculations were performed in order to determine the proper amount of nutrients to add to the raceway. For this raceway batch, the target nutrient level was 5 mg P/L and 80 mg N/L (maintaining a 16:1 N:P ratio). Nitrogen was added in the form of sodium nitrate ($NaNO_3$). Phosphorus was added as a combination of 25% dibasic potassium phosphate (K_2HPO_4) and 75% monobasic potassium phosphate (KH_2PO_4).

For the second raceway run, the same procedure was followed as before, only no nutrients were added to the system. An initial balance of the nutrients was performed, however, with the total phosphorus levels brought up to 5 mg/L and total nitrogen brought up to 80 mg/L. Also for this run, a Hach pH probe was used for continuous pH measurement, in order to get a more accurate pH profile.

A1.2.3 Logan Lagoons Effluent Nutrient Analysis

This testing was completed from July 2010 to August 2011. For the first few months of operation (July and August 2010), multiple people were scheduled to complete this testing, which introduced a large amount of error into the data set. Once two undergraduate researchers were assigned with this as their sole task, the error in the data was greatly reduced.

The following tests were completed using their appropriate Hach testing kits; total and soluble phosphorus, total and soluble nitrogen, orthophosphate, ammonia, and total and soluble chemical oxygen demand. Temperature, pH, dissolved oxygen, and total suspended solids were completed using the procedure outlined in Standard Methods. Additionally, in the summer of 2011, the following tests were added to the testing: volatile suspended solids, total nitrate, and total nitrite.

A1.2.4 Settleable solids testing

In order to determine the settleable solids of the Logan Lagoons effluent, the Standard Methods procedure was followed (Eaton, Clesceri, Rice, Greenberg, and Franson, 2005d). An Imhoff cone was filled with the liquid in question to the 1 L mark. The liquid was passed through a rough filter. This removes the larger daphnia present, preventing them from eating the algae during the test. The cone then sat undisturbed for 45 minutes; after this time had elapsed, the cone was gently swirled to break loose any particles from the side of the cone and sat back down. After 1 hour total time, the amount of settled solids was read off of the cone, in units of mL/L.

This test was first done on the Logan Lagoons effluent throughout the course of a day, in order to determine a baseline for settleabilty of the Logan Lagoons algae. This procedure was performed throughout the course of the day, from 5 am to 11 pm, every three hours. Two

Imhoff cones were available, so duplicate data was obtained. According to Standard Methods, duplicate data are not normally required, but this data was collected for completeness.

A1.2.4 Weather Station Data

A computer script was written that would access the hourly weather data on the Campbell Scientific website and save the website to a computer as an html file. This data could then be extracted and added to an Excel spreadsheet for further analysis.

A1.3 Results and Discussion

A1.3.1 Indoor raceway with and without nutrient addition

The goal of this phase of testing was observe the pH changes of a batch culture of algae over time, while also monitoring the TSS increase. This would show the possibility for autoflocculation to occur in a future large-scale raceway at the Logan Lagoons.

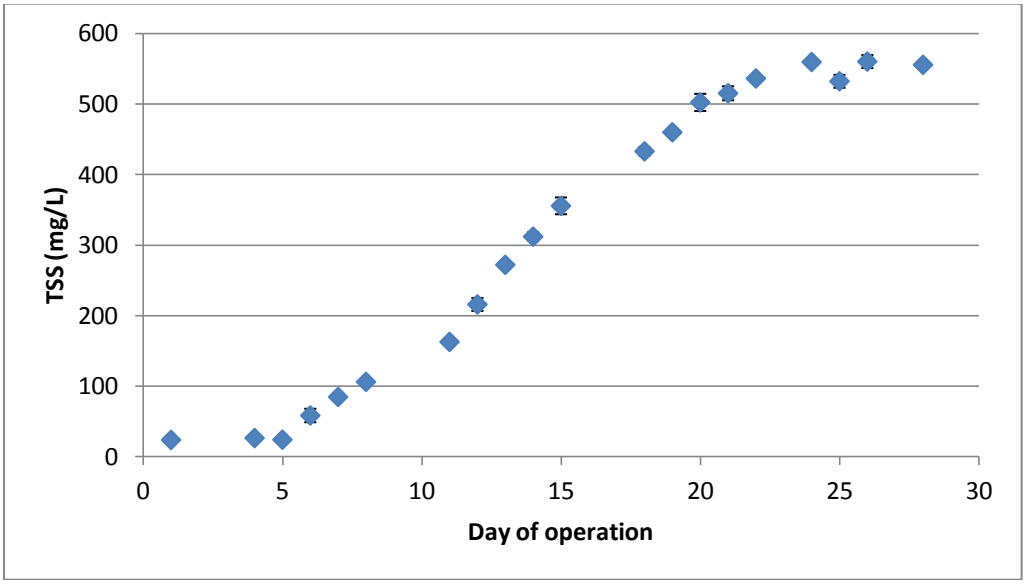

Fig. A-2: TSS vs. day of operation, small raceway with nutrient addition (Sept 16 - Oct 15, 2010)

Fig. A-2 shows the growth curve in this raceway (error bars are equal to 1 standard deviation). The regular nutrient addition helped increase the total suspended solids from

approximately 25 mg/L to over 500 mg/L in less than a month. The growth leveled off at this point because the carrying capacity of this raceway had been met. Since this culture is not nutrient limited, the growth plateau is most likely caused by a light limitation.

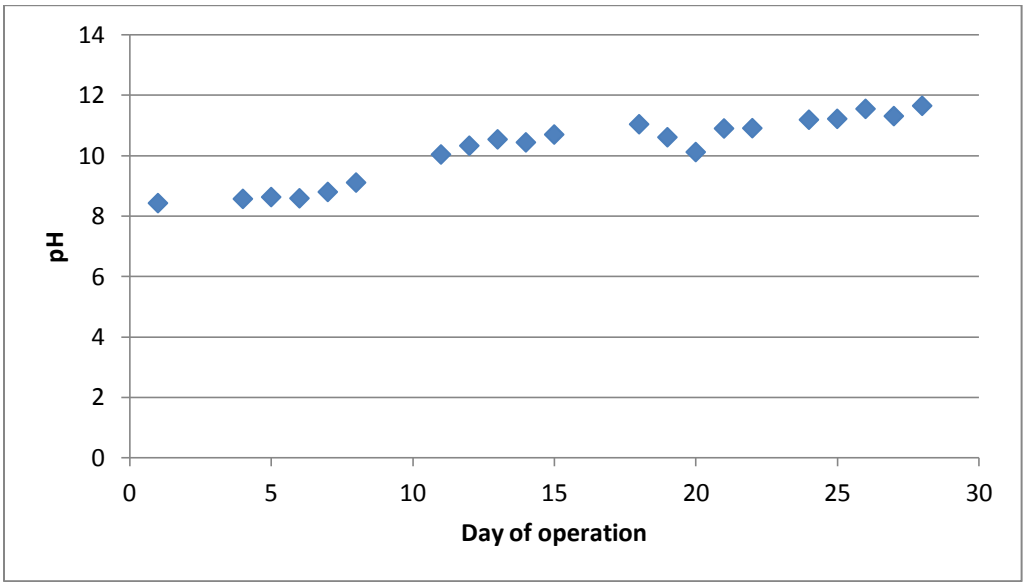

Fig. A-3: pH vs. day of operation, small raceway with nutrient addition (Sept 16 - Oct 15 2010)

In Fig. A-3 it is illustrated how the pH of the algal culture quickly increased. By the time the algae concentration had reached 500 mg/L, the pH of the system was almost 12. This indicates that this culture would have been easily autoflocculated.

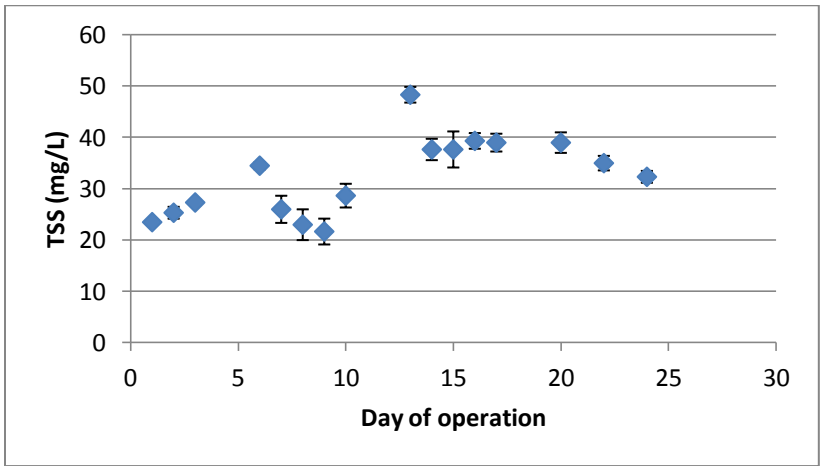

Fig. A-4: TSS vs. day of operation, small raceway without nutrient addition (Nov 3-26 2010)

When these graphs are compared to the raceway run without nutrient addition, a number of interesting comparisons can be made. In Fig. A-4, the TSS level did not increase nearly as high; the amount of algae did increase from 23 mg/L to 39 mg/L at the peak, but never higher. In this situation, the algal culture was nutrient limited, not light limited.

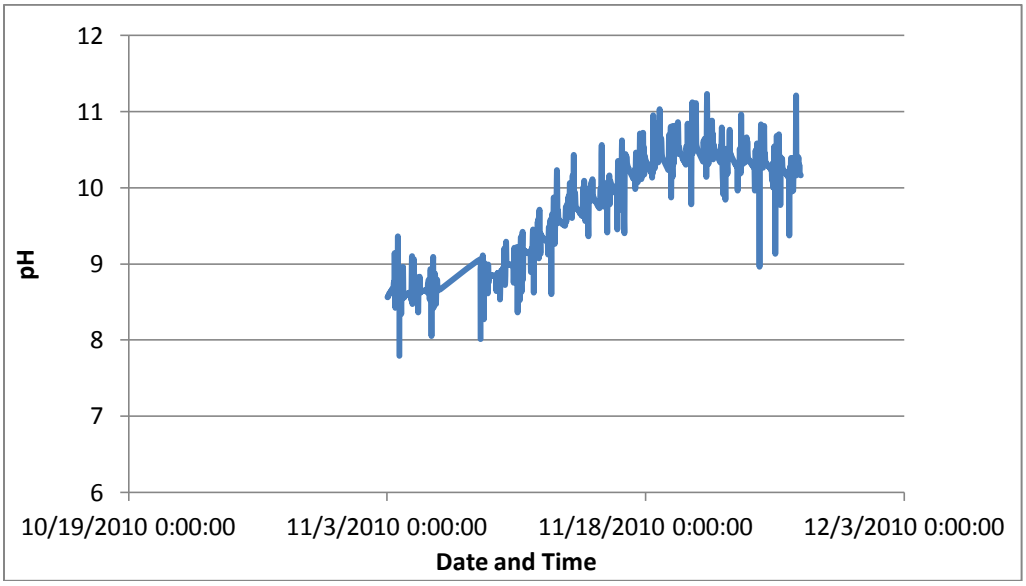

Fig. A-5: pH vs. date, small raceway without nutrient addition (Nov 3-26 2010)

In Fig. A-5, the pH of the raceway behaved very similar to the pH when there was regular nutrient addition. It didn't reach quite as high without nutrient addition (only pH 11 at its highest), but this is still high enough to cause autoflocculation.

A1.3.2 Logan Lagoons Effluent Nutrient Analysis

The following graphs detail the season average values for TSS, TP, and pH. The error bars are equal to one standard deviation.

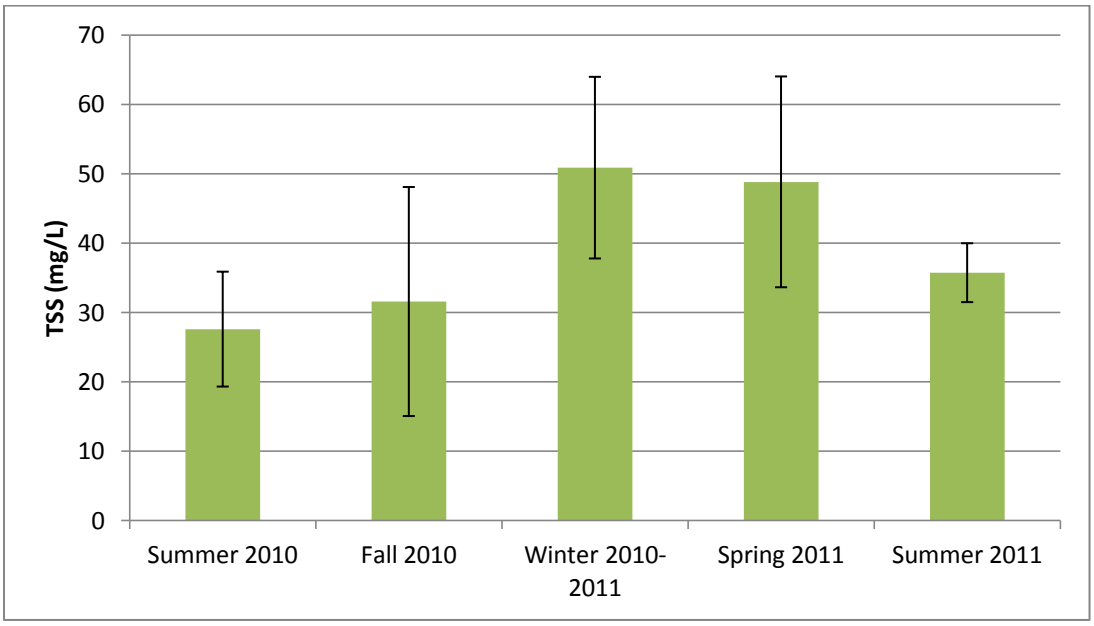

Fig. A-6: Seasonal TSS averages in the Logan Lagoons

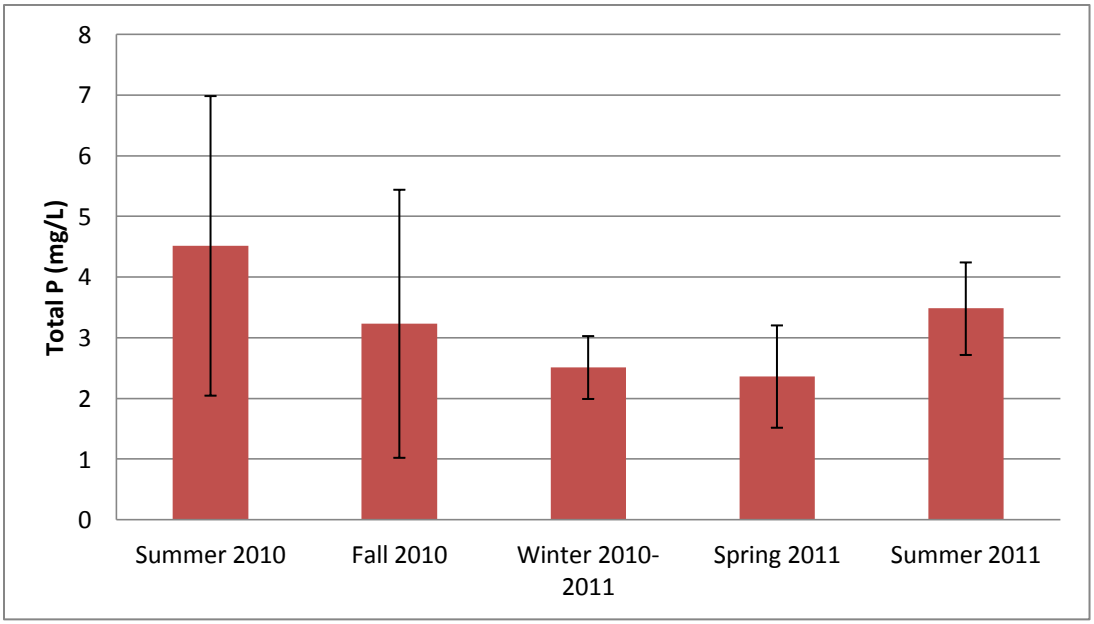

Fig. A-7: Seasonal TP averages in the Logan Lagoons

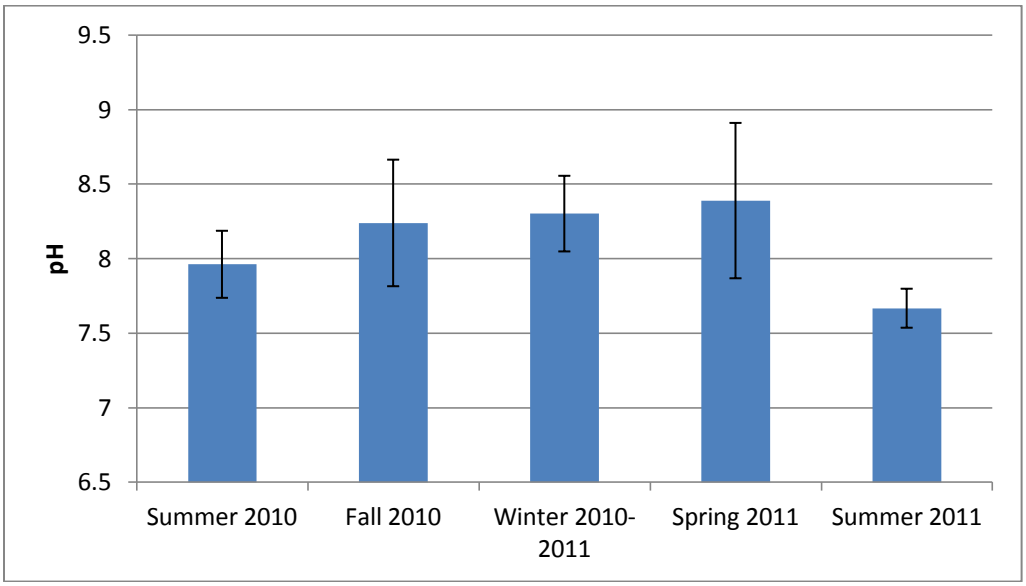

Fig. A-8: Seasonal pH averages in the Logan Lagoons

A1.3.3 Settleable solids testing

The amount of settleable solids was first tested using the Logan Lagoons effluent as a baseline. As can be seen in Fig. A-9, there is virtually no settleability in the effluent as it emerges from the Logan Lagoons.

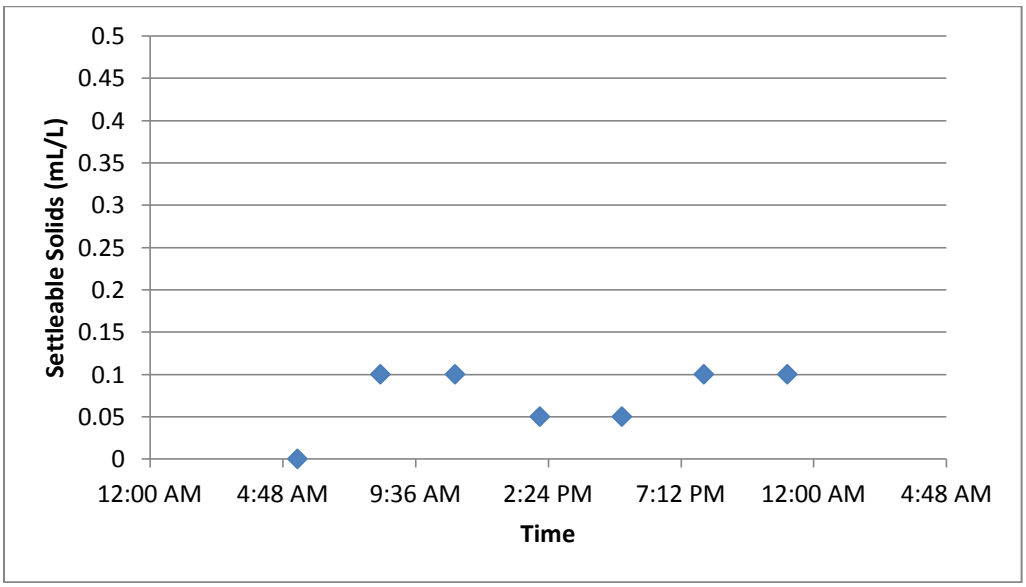

Fig. A-9: Settleable solids in Logan Lagoons effluent (July 6, 2011)

A1.3.4 Weather station data

The weather station data collected for the months of October 2010 through July 2011 has provided an overview of the temperature and solar radiation ranges for the fall – summer months.

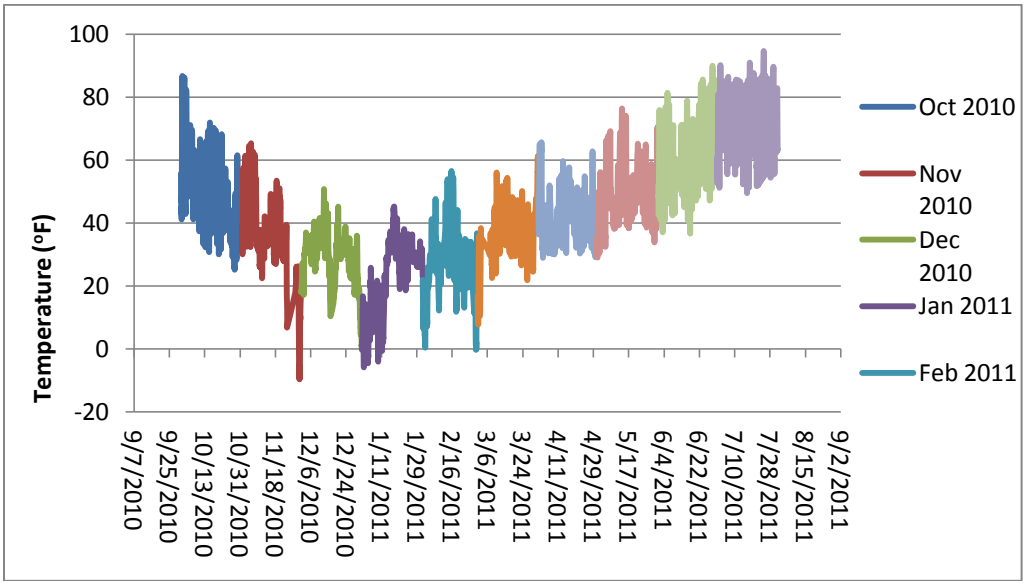

Fig. A-10: Air temperature in Logan, UT (Oct 2010 - July 2011)

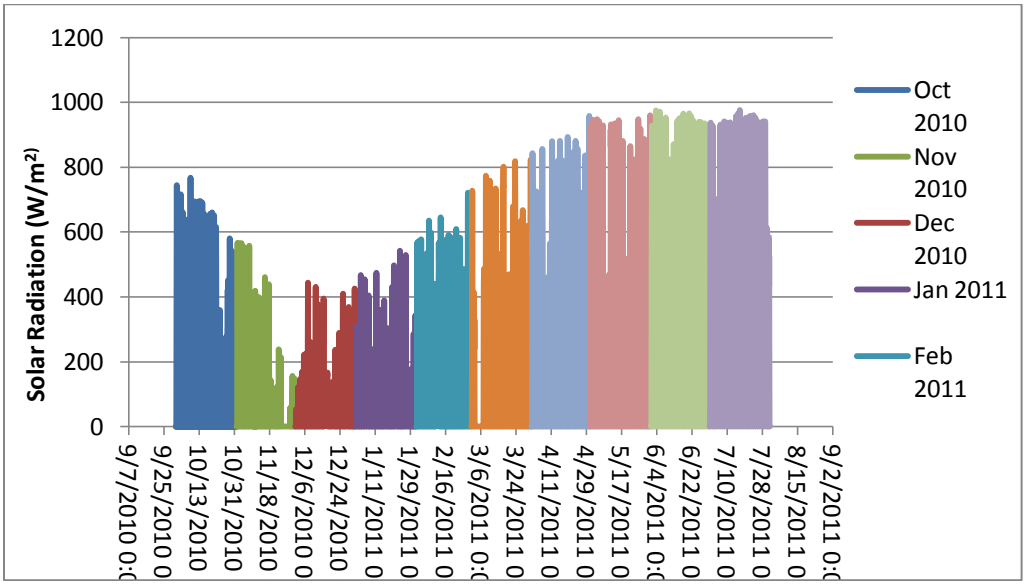

Fig. A-11: Solar radiation in Logan, UT (Oct 2010 - July 2011)

A1.4 Conclusion

These monitoring tests will be helpful for predictions in other parts of this project. A batch algal culture will reach a high pH value (10-11) whether or not nutrients are added. If nutrients are added to the system, however, the TSS will rise significantly, until the carrying capacity of the raceway is reached, which is advantageous for purposes of algal harvesting. This high pH indicates that autoflocculation should be a possibility with the algal species found at the Logan Lagoons.

It was also observed that even though the TSS is highest in the winter months, the TP loading is highest in the summer. Since there is a higher volume of water flowing into the plant during warmer months, from both snow runoff and rainfall, it makes sense that the algae is being diluted by this stormwater. Also, any fertilizer runoff during the summer months would be contributing to the TP levels, but not the algae concentration. This is actually good news for the purposes of harvesting algae. A batch algae culture, in the summer heat and sun, along with increased phosphorus levels, should grow very well. It can be determined from the weather data that both July and October have the highest air temperatures, and it can be assumed that August and September have similar levels. Additionally, the solar radiation during May, June, and July is the highest among the available data. It is not known how long this trend will last, because October is significantly lower, but most likely August is also this sunny.

Finally, with the Imhoff cones, on can look at the baseline data and see that there is virtually no natural settling occurring without any treatment of the water in the effluent.

APPENDIX B: SCRIPT FOR WEATHER DATA COLLECTION FROM CAMPBELL SCIENTIFIC

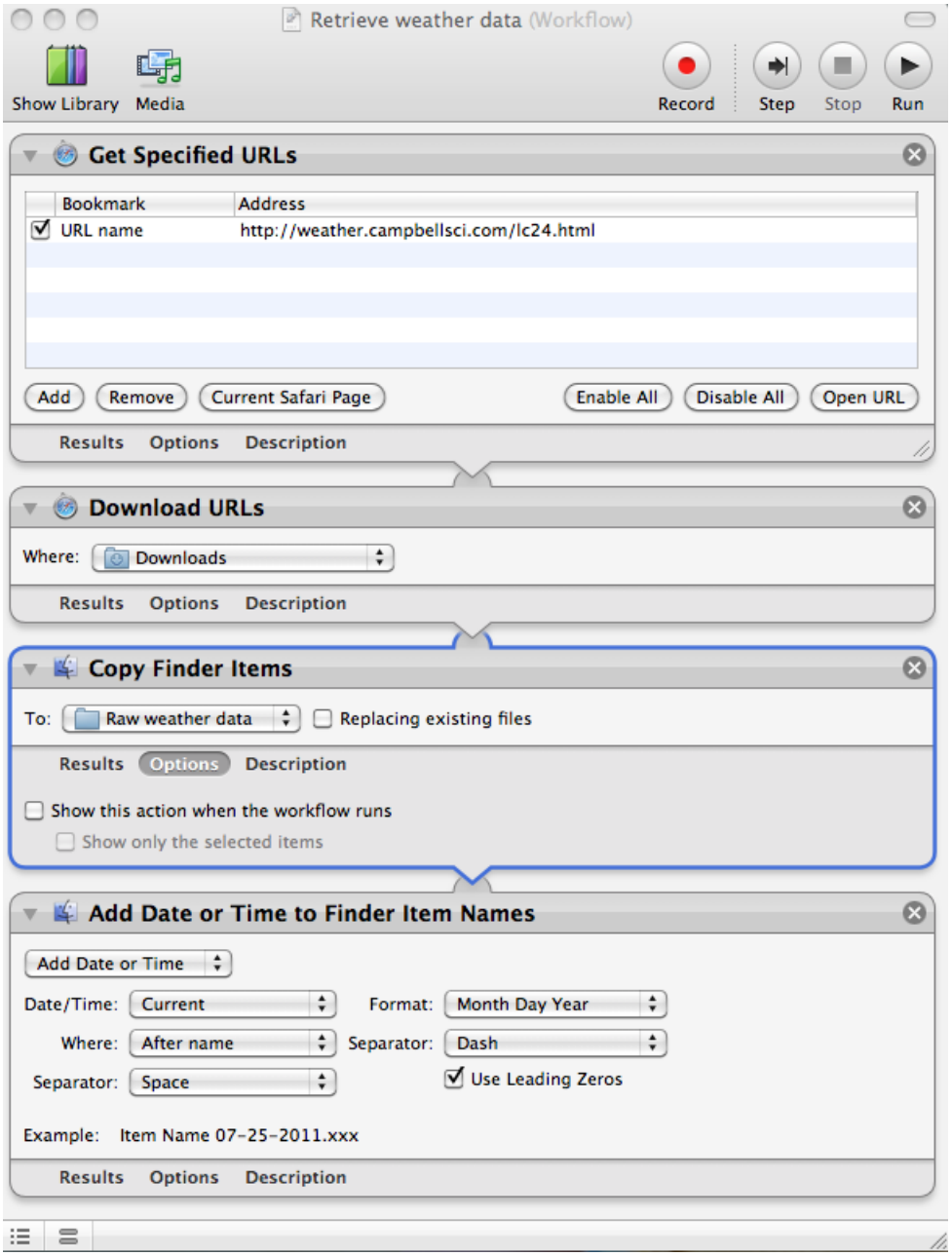

Fig. B-1: Computer script for daily weather data collection

APPENDIX C: SAS PROGRAMS

Note: for Part C1, all of the output for Run #1 is included, including graphical assumption checks. For subsequent SAS work, only the relevant code will be included.

C1: Steady state calculations for pilot DAF unit

```
/*Steady-state determination, pilot-scale DAF unit*/
/*formatting options*/
options ls=80 nodate pageno=1 formdlim='~';
goptions ftext=swiss ftitle=swissb htitle=3 htext=3 vorigin=1 in
    hsize=8 in vsize=8 in device=win rotate=portrait;
run;

/*data entry*/
/*Run #1*/
data SteadyState;
    input Time $ TSS @@;
    datalines;
0 26.5 0 27 0 28        15 18.5 15 17 15 17.5       30 12.5 30 13 30 12
45 11.5 45 10.5 45 12   60 10.5 60 13 60 12         75 11 75 11 75 14
90 10.5 90 11 90 12
;
run;

/*Time of operation comparison*/
proc glm data=SteadyState;
    class Time;
    model TSS = Time;
    output out = out1 p=pred r=resid;
    means Time / Tukey;
run;

/*graphical checks of assumptions*/
proc gplot data=out1;
    plot resid*(Time pred) / vaxis=axis1;
    symbol1 v=dot;
    axis1 label=(angle=90);
    title1 'Check Heteroscedasticity';
run;

proc univariate data=out1 normal plots;
    var resid;
    histogram resid / normal(color=blue) cfill=yellow;
    probplot resid / normal (mu=est sigma=est color=red w=3 L=2);
    title1 'Check Normality';
run;
```

Fig. C-1: Steady-state calculations for pilot DAF unit, input code (1 of 3)

```
/*data entry*/
/*Run #2*/
data SteadyState2;
     input Time2 $ TSS2 @@;
     datalines;
0 32.5 0 31.5 0 33.1        15 27.8 15 28.4 15 27.8     30 28.0 30 22.3 30 24.9
45 21.7 45 18.9 45 20.8     60 26.5 60 21.6 60 22.2
75 23.0 75 22.5 75 22.9     90 28.1 90 26.3 90 25.5
;
run;

/*Time of operation comparison*/
proc glm data=SteadyState2;
     class Time2;
     model TSS2 = Time2;
     output out = out1 p=pred r=resid;
     means Time2 / Tukey;
run;

/*graphical checks of assumptions*/
proc gplot data=out1;
     plot resid*(Time2 pred) / vaxis=axis1;
     symbol1 v=dot;
     axis1 label=(angle=90);
     title1 'Check Heteroscedasticity';
run;

proc univariate data=out1 normal plots;
     var resid;
     histogram resid / normal(color=blue) cfill=yellow;
     probplot resid / normal (mu=est sigma=est color=red w=3 L=2);
     title1 'Check Normality';
run;
```

Fig. C-2: Steady-state calculations for pilot DAF unit, input code (2 of 3)

```
/*data entry*/
/*Run #4*/
data SteadyState4;
     input Time4 $ TSS4 @@;
     datalines;
0 54.5 0 35.8 0 36.5        15 25.5 15 27.8 15 28.5     30 23.4 30 22.8 30 23.0
45 23.1 45 21.0 45 24.1     60 22.2 60 23.6 60 17.4
75 23.5 75 25.0 75 23.0     90 24.4 90 24.4 90 24.6
;
run;

/*Time of operation comparison*/
proc glm data=SteadyState4;
     class Time4;
     model TSS4 = Time4;
     output out = out1 p=pred r=resid;
     means Time4 / Tukey;
run;

/*graphical checks of assumptions*/
proc gplot data=out1;
     plot resid*(Time4 pred) / vaxis=axis1;
     symbol1 v=dot;
     axis1 label=(angle=90);
     title1 'Check Heteroscedasticity';
run;

proc univariate data=out1 normal plots;
     var resid;
     histogram resid / normal(color=blue) cfill=yellow;
     probplot resid / normal (mu=est sigma=est color=red w=3 L=2);
     title1 'Check Normality';
run;
```

Fig. C-3: Steady-state calculations for pilot DAF unit, input code (3 of 3)

```
                                Check Normality                                1

                                The GLM Procedure

                            Class Level Information

                  Class         Levels    Values

                  Time               7    0 15 30 45 60 75 90

                    Number of Observations Read          21
                    Number of Observations Used          21
```

```
                                Check Normality                                2

                                The GLM Procedure

Dependent Variable: TSS

                                           Sum of
 Source                     DF           Squares      Mean Square    F Value    Pr > F

 Model                       6      624.9047619      104.1507937     101.73    <.0001

 Error                      14       14.3333333        1.0238095

 Corrected Total            20      639.2380952

               R-Square     Coeff Var      Root MSE      TSS Mean

               0.977577      6.832325      1.011835      14.80952

 Source                     DF         Type I SS      Mean Square    F Value    Pr > F

 Time                        6      624.9047619      104.1507937     101.73    <.0001

 Source                     DF        Type III SS      Mean Square    F Value    Pr > F

 Time                        6      624.9047619      104.1507937     101.73    <.0001
```

```
                                Check Normality                                3

                                The GLM Procedure

                    Tukey's Studentized Range (HSD) Test for TSS
```

Fig. C-4: Steady-state calculations for pilot DAF unit, output code (1 of 5)

```
NOTE: This test controls the Type I experimentwise error rate, but it generally
      has a higher Type II error rate than REGWQ.

                    Alpha                                0.05
                    Error Degrees of Freedom               14
                    Error Mean Square                 1.02381
                    Critical Value of Studentized Range 4.82895
                    Minimum Significant Difference       2.821

          Means with the same letter are not significantly different.

           Tukey Grouping          Mean      N    Time

                        A       27.1667      3    0

                        B       17.6667      3    15

                        C       12.5000      3    30
                        C
                        C       12.0000      3    75
                        C
                        C       11.8333      3    60
                        C
                        C       11.3333      3    45
                        C
                        C       11.1667      3    90

-------------------------------------------------------------------------------

                               Check Normality                              4

                          The UNIVARIATE Procedure
                             Variable:  resid

                                 Moments

        N                          21    Sum Weights                21
        Mean                        0    Sum Observations            0
        Std Deviation      0.84656167    Variance           0.71666667
        Skewness           0.52628468    Kurtosis           -0.1078345
        Uncorrected SS     14.3333333    Corrected SS       14.3333333
        Coeff Variation             .    Std Error Mean      0.1847349

                       Basic Statistical Measures

              Location                        Variability

          Mean      0.00000     Std Deviation            0.84656
          Median   -0.16667     Variance                 0.71667
          Mode     -1.00000     Range                    3.33333
                                Interquartile Range      1.33333
```

Fig. C-5: Steady-state calculations for pilot DAF unit, output code (2 of 5)

Note: The mode displayed is the smallest of 2 modes with a count of 2.

Tests for Location: Mu0=0

Test	-Statistic-		-----p Value------	
Student's t	t	0	Pr > |t|	1.0000
Sign	M	-1	Pr >= |M|	0.8238
Signed Rank	S	-6.5	Pr >= |S|	0.8194

Tests for Normality

Test	--Statistic---		-----p Value------	
Shapiro-Wilk	W	0.961495	Pr < W	0.5468
Kolmogorov-Smirnov	D	0.117838	Pr > D	>0.1500
Cramer-von Mises	W-Sq	0.046955	Pr > W-Sq	>0.2500
Anderson-Darling	A-Sq	0.310852	Pr > A-Sq	>0.2500

Quantiles (Definition 5)

Quantile	Estimate
100% Max	2.000000
99%	2.000000
95%	1.166667
90%	0.833333
75% Q3	0.666667
50% Median	-0.166667

Check Normality 5

The UNIVARIATE Procedure
Variable: resid

Quantiles (Definition 5)

Quantile	Estimate
25% Q1	-0.666667
10%	-1.000000
5%	-1.000000
1%	-1.333333
0% Min	-1.333333

Extreme Observations

------Lowest------ ------Highest-----

Fig. C-6: Steady-state calculations for pilot DAF unit, output code (3 of 5)

Value	Obs	Value	Obs
-1.333333	13	0.833333	21
-1.000000	17	0.833333	4
-1.000000	16	0.833333	3
-0.833333	11	1.166667	14
-0.666667	19	2.000000	18

Stem	Leaf	#	Boxplot
2	0	1	
1			
1	2	1	
0	57888	5	
0	022	3	
-0	222	3	
-0	87775	5	
-1	300	3	

----+----+----+----+

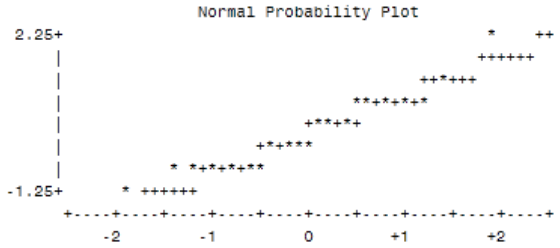

Check Normality 6

The UNIVARIATE Procedure
Fitted Normal Distribution for resid

Parameters for Normal Distribution

Parameter	Symbol	Estimate
Mean	Mu	0
Std Dev	Sigma	0.846562

Goodness-of-Fit Tests for Normal Distribution

Test		----Statistic-----	------p Value------	
Kolmogorov-Smirnov	D	0.11783849	Pr > D	>0.150
Cramer-von Mises	W-Sq	0.04695516	Pr > W-Sq	>0.250

Fig. C-7: Steady-state calculations for pilot DAF unit, output code (4 of 5)

Anderson-Darling	A-Sq	0.31085156	Pr > A-Sq	>0.250

Quantiles for Normal Distribution

Percent	Quantile Observed	Quantile Estimated
1.0	-1.33E+00	-1.96940
5.0	-1.00E+00	-1.39247
10.0	-1.00E+00	-1.08491
25.0	-6.67E-01	-0.57100
50.0	-1.67E-01	0.00000
75.0	6.67E-01	0.57100
90.0	8.33E-01	1.08491
95.0	1.17E+00	1.39247
99.0	2.00E+00	1.96940

Fig. C-8: Steady-state calculations for pilot DAF unit, output code (5 of 5)

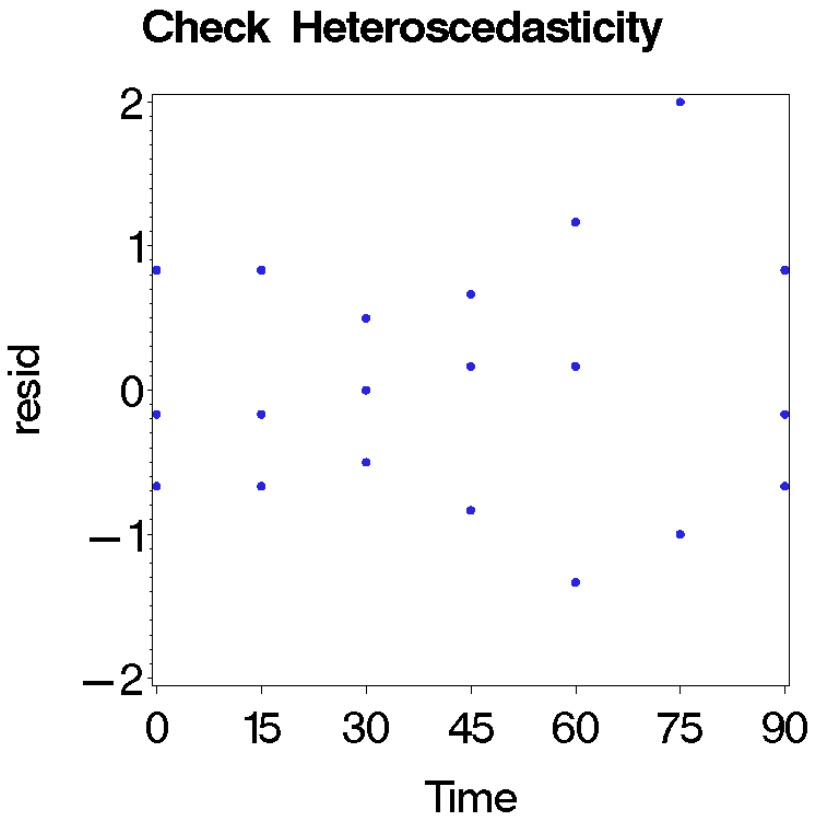

Fig. C-9: Steady-state calculations for pilot DAF unit, output graphs (1 of 2)

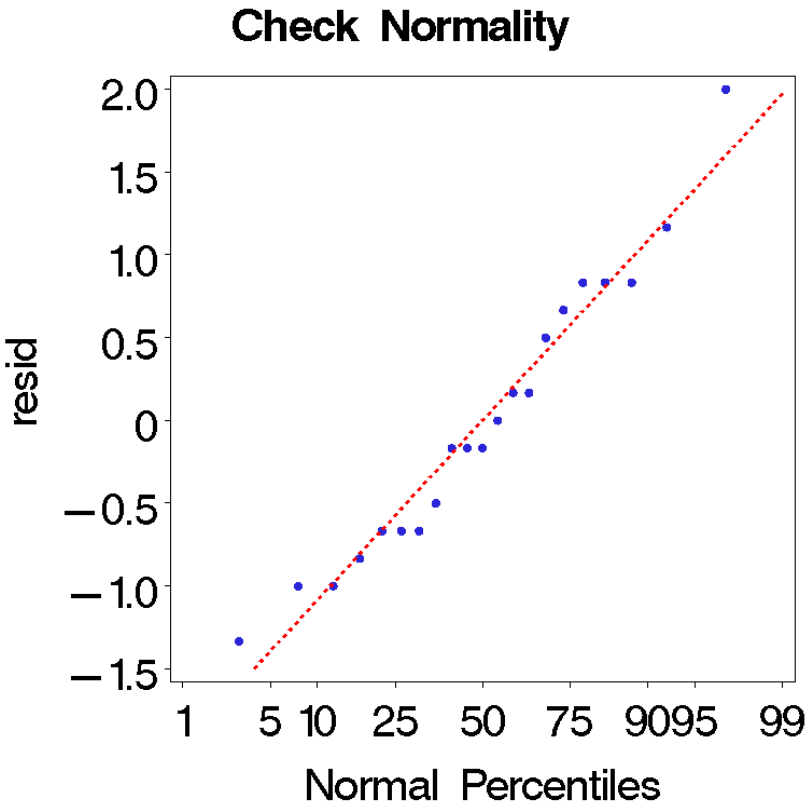

Fig. C-10: Steady-state calculations for pilot DAF unit, output graphs (2 of 2)

C2: Initial data for pilot DAF unit

```
/*Alum dose determination, pilot-scale DAF unit*/
/*formatting options*/
options ls=80 nodate pageno=1 formdlim='~';
goptions ftext=swiss ftitle=swissb htitle=3 htext=3 vorigin=1 in
    hsize=8 in vsize=8 in device=win rotate=portrait;
run;

/*data entry*/
/*TSS of the influent*/
data Influent;
    input Dose $ TSS_inf @@;
    datalines;
0 24.0 0 23.5 0 26.0    10 29.5 10 25.5 10 25   20 23 20 25 20 25.5     30 25 30 24.5 30 25.5
40 26.5 40 25 40 23     50 23.5 50 24 50 23     60 25 60 24.5 60 24.5   70 29 70 34 70 28.5
80 27 80 27.4 80 29.7   90 26.9 90 26.4 90 27.2     100 28.3 100 24.6 100 26.4
;
run;

proc glm data=Influent;
    class Dose;
    model TSS_inf = Dose;
    output out = out1 p=pred r=resid;
    means Dose / Tukey;
run;

/*graphical checks of assumptions*/
proc gplot data=out1;
    plot resid*(Dose pred) / vaxis=axis1;
    symbol1 v=dot;
    axis1 label=(angle=90);
    title1 'Check Heteroscedasticity';
run;

proc univariate data=out1 normal plots;
    var resid;
    histogram resid / normal(color=blue) cfill=yellow;
    probplot resid / normal (mu=est sigma=est color=red w=3 L=2);
    title1 'Check Normality';
run;
```

Fig. C-11: Initial data for pilot DAF unit, input code (1 of 4)

```
/*data entry*/
/*TSS of the effluent*/
data Influent;
    input Dose2 $ TSS_eff @@;
    datalines;
0 22.0 0 24.5 0 22.0        10 29 10 27.5 10 25.8    20 22 20 21.2 20 25.5        30 14.3 30 13.5 30 12.3
40 13.9 40 13.9 40 12.3     50 15.8 50 13.7 50 14.2 60 10.9 60 14.9 60 16.5     70 16.7 70 15.9 70 16
80 16.6 80 14.1 80 17.3     90 13.3 90 15.0 90 13.4     100 13.0 100 11.3 100 12.3
;
run;

proc glm data=Influent;
    class Dose2;
    model TSS_eff = Dose2;
    output out = out1 p=pred r=resid;
    means Dose2 / Tukey;
run;

/*graphical checks of assumptions*/
proc gplot data=out1;
    plot resid*(Dose2 pred) / vaxis=axis1;
    symbol1 v=dot;
    axis1 label=(angle=90);
    title1 'Check Heteroscedasticity';
run;

proc univariate data=out1 normal plots;
    var resid;
    histogram resid / normal(color=blue) cfill=yellow;
    probplot resid / normal (mu=est sigma=est color=red w=3 L=2);
    title1 'Check Normality';
run;
```

Fig. C-12: Initial data for pilot DAF unit, input code (2 of 4)

```
/*data entry*/
/*TP of the influent*/
data Influent;
    input Dose3 $ TP_inf @@;
    datalines;
0 1.13 0 1.11 0 1.16        10 1.11 10 1.29 10 1.15     20 1.46 20 1.35 20 1.41
30 1.31 30 1.43 30 1.57     40 1.34 40 1.19 40 1.29     50 1.25 50 1.18 50 1.11
60 1.38 60 1.34 60 1.30     70 1.48 70 1.05 70 1.21     80 1.06 80 1.24 80 1.13
90 2.25 90 1.36 90 1.18     100 1.25 100 1.36 100 1.18
;
run;

proc glm data=Influent;
    class Dose3;
    model TP_inf = Dose3;
    output out = out1 p=pred r=resid;
    means Dose3 / Tukey;
run;

/*graphical checks of assumptions*/
proc gplot data=out1;
    plot resid*(Dose3 pred) / vaxis=axis1;
    symbol1 v=dot;
    axis1 label=(angle=90);
    title1 'Check Heteroscedasticity';
run;

proc univariate data=out1 normal plots;
    var resid;
    histogram resid / normal(color=blue) cfill=yellow;
    probplot resid / normal (mu=est sigma=est color=red w=3 L=2);
    title1 'Check Normality';
run;
```

Fig. C-13: Initial data for pilot DAF unit, input code (3 of 4)

```
/*data entry*/
/*TP of the effluent*/
data Influent;
    input Dose4 $ TP_eff @@;
    datalines;
0 1.19 0 1.09 0 1.18        10 1.22 10 1.20 10 1.11     20 1.19 20 1.03 20 1.14
30 0.78 30 0.71 30 0.69     40 0.50 40 0.47 40 0.41     50 0.37 50 0.44 50 0.50
60 0.26 60 0.37 60 0.28     70 0.03 70 0.19 70 0.21     80 0.45 80 0.61 80 0.52
90 0.25 90 0.39 90 0.26     100 0.35 100 0.31 100 0.22
;
run;

proc glm data=Influent;
    class Dose4;
    model TP_eff = Dose4;
    output out = out1 p=pred r=resid;
    means Dose4 / Tukey;
run;

/*graphical checks of assumptions*/
proc gplot data=out1;
    plot resid*(Dose4 pred) / vaxis=axis1;
    symbol1 v=dot;
    axis1 label=(angle=90);
    title1 'Check Heteroscedasticity';
run;

proc univariate data=out1 normal plots;
    var resid;
    histogram resid / normal(color=blue) cfill=yellow;
    probplot resid / normal (mu=est sigma=est color=red w=3 L=2);
    title1 'Check Normality';
run;
```

Fig. C-14: Initial data for pilot DAF unit, input code (4 of 4)

Check Normality 3

The GLM Procedure

Tukey's Studentized Range (HSD) Test for TSS_inf

NOTE: This test controls the Type I experimentwise error rate, but it generally has a higher Type II error rate than REGWQ.

Alpha	0.05
Error Degrees of Freedom	22
Error Mean Square	2.564545
Critical Value of Studentized Range	5.05555
Minimum Significant Difference	4.6743

Means with the same letter are not significantly different.

Tukey Grouping	Mean	N	Dose
A	30.500	3	70
A			
B A	28.033	3	80
B A			
B A	26.833	3	90
B A			
B A	26.667	3	10
B A			
B A	26.433	3	100
B			
B	25.000	3	30
B			
B	24.833	3	40
B			
B	24.667	3	60
B			
B	24.500	3	0
B			
B	24.500	3	20
B			
B	23.500	3	50

Fig. C-15: Initial data for pilot DAF unit, output code (1 of 4)

Check Normality 10

The GLM Procedure

Tukey's Studentized Range (HSD) Test for TSS_eff

NOTE: This test controls the Type I experimentwise error rate, but it generally has a higher Type II error rate than REGWQ.

Alpha	0.05
Error Degrees of Freedom	22
Error Mean Square	2.35697
Critical Value of Studentized Range	5.05555
Minimum Significant Difference	4.4811

Means with the same letter are not significantly different.

Tukey Grouping	Mean	N	Dose2
A	27.433	3	10
B	22.900	3	20
B			
B	22.833	3	0
C	16.200	3	70
C			
C	16.000	3	80
C			
C	14.567	3	50
C			
C	14.100	3	60
C			
C	13.900	3	90
C			
C	13.367	3	30
C			
C	13.367	3	40
C			
C	12.200	3	100

Fig. C-16: Initial data for pilot DAF unit, output code (2 of 4)

Check Normality 17

The GLM Procedure

Tukey's Studentized Range (HSD) Test for TP_inf

NOTE: This test controls the Type I experimentwise error rate, but it generally has a higher Type II error rate than REGWQ.

Alpha	0.05
Error Degrees of Freedom	22
Error Mean Square	0.039436
Critical Value of Studentized Range	5.05555
Minimum Significant Difference	0.5796

Means with the same letter are not significantly different.

Tukey Grouping	Mean	N	Dose3
A	1.5967	3	90
A			
A	1.4367	3	30
A			
A	1.4067	3	20
A			
A	1.3400	3	60
A			
A	1.2733	3	40
A			
A	1.2633	3	100
A			
A	1.2467	3	70
A			
A	1.1833	3	10
A			
A	1.1800	3	50
A			
A	1.1433	3	80
A			
A	1.1333	3	0

Fig. C-17: Initial data for pilot DAF unit, output code (3 of 4)

Check Normality 24

The GLM Procedure

Tukey's Studentized Range (HSD) Test for TP_eff

NOTE: This test controls the Type I experimentwise error rate, but it generally has a higher Type II error rate than REGWQ.

Alpha	0.05
Error Degrees of Freedom	22
Error Mean Square	0.004715
Critical Value of Studentized Range	5.05555
Minimum Significant Difference	0.2004

Means with the same letter are not significantly different.

Tukey Grouping	Mean	N	Dose4
A	1.17667	3	10
A			
A	1.15333	3	0
A			
A	1.12000	3	20
B	0.72667	3	30
B			
C B	0.52667	3	80
C			
C D	0.46000	3	40
C D			
C D	0.43667	3	50
D			
E D	0.30333	3	60
E D			
E D	0.30000	3	90
E D			
E D	0.29333	3	100
E			
E	0.14333	3	70

Fig. C-18: Initial data for pilot DAF unit, output code (4 of 4)

C3: Alum dose determination with jar test unit

```
/*Optimum alum dose determination of jar test unit, according to TSS and Total P removal efficiency*/
/*Corrected SAS procedure, using a nested experimental design*/

/*formatting options*/
options ls=80 nodate pageno=1 formdlim='~';
goptions ftext=swiss ftitle=swissb htitle=3 htext=3 vorigin=1 in
    hsize=8 in vsize=8 in device=win rotate=portrait;
run;

/*data entry of TSS removal data*/
data jartestTSS;
    input Dose $ Run Rep TSS @@;
    cards;
0   1   1   37
0   1   2   37
0   1   3   38
0   2   1   30
0   2   2   31
0   2   3   30
0   3   1   34
0   3   2   33
0   3   3   33
10  1   1   22
10  1   2   23
10  1   3   23
10  2   1   18
10  2   2   17
10  2   3   17
10  3   1   22
10  3   2   24
10  3   3   24
20  1   1   19
20  1   2   22
20  1   3   21
20  2   1   14
20  2   2   15
20  2   3   15
20  3   1   21
20  3   2   22
20  3   3   17
30  1   1   16
30  1   2   16
30  1   3   19
30  2   1   12
30  2   2   13
30  2   3   11
30  3   1   18
30  3   2   17
```

Fig. C-19: Alum dose determination with jar test unit, input code (1 of 6)

```
30  3   3   16
40  1   1   15
40  1   2   15
40  1   3   17
40  2   1   10
40  2   2   10
40  2   3   9
40  3   1   16
40  3   2   14
40  3   3   15
50  1   1   14
50  1   2   15
50  1   3   12
50  2   1   10
50  2   2   10
50  2   3   10
50  3   1   13
50  3   2   15
50  3   3   11
60  1   1   7
60  1   2   7
60  1   3   7
60  2   1   6
60  2   2   13
60  2   3   9
60  3   1   9
60  3   2   12
60  3   3   10
70  1   1   7
70  1   2   9
70  1   3   9
70  2   1   6
70  2   2   10
70  2   3   7
70  3   1   11
70  3   2   10
70  3   3   11
80  1   1   5
80  1   2   10
80  1   3   12
80  2   1   15
80  2   2   10
80  2   3   11
80  3   1   12
80  3   2   12
80  3   3   6
90  1   1   10
```

Fig. C-20: Alum dose determination with jar test unit, input code (2 of 6)

```
90  1   2   9
90  1   3   9
90  2   1   11
90  2   2   8
90  2   3   6
90  3   1   11
90  3   2   13
90  3   3   13
100 1   1   8
100 1   2   12
100 1   3   15
100 2   1   16
100 2   2   14
100 2   3   12
100 3   1   20
100 3   2   18
100 3   3   16
;
run;
```

```
/*Calculate the Expected Mean Squares*/
proc mixed data=jartestTSS method=type3;
    class Dose Run Rep;
    model TSS=Dose;
    random Run(Dose);
    title1 'EMS using Type3 option - TSS Data';
run;
```

```
/*Perform tests*/
proc mixed data=jartestTSS covtest;
    class Dose Run Rep;
    model TSS=Dose / ddfm=satterthwaite outp=out1;
    lsmeans Dose / pdiff=all adjust=Tukey;
    title1 'Using REML estimation - TSS Data';
run;
```

Fig. C-21: Alum dose determination with jar test unit, input code (3 of 6)

```
/*data entry of Total P removal data*/
data jartestTP;
    input Dose2 $ Run2 Rep2 TP @@;
    cards;
0   1   1   2.222
0   1   2   2.611
0   1   3   2.494
0   2   1   1.818
0   2   2   2.285
0   2   3   2.376
0   3   1   2.703
0   3   2   2.931
0   3   3   2.918
10  1   1   1.702
10  1   2   1.575
10  1   3   1.692
10  2   1   1.425
10  2   2   1.584
10  2   3   1.292
10  3   1   1.713
10  3   2   1.846
10  3   3   2.031
20  1   1   1.039
20  1   2   0.809
20  1   3   0.760
20  2   1   1.113
20  2   2   1.061
20  2   3   0.860
20  3   1   1.092
20  3   2   1.047
20  3   3   1.170
30  1   1   0.335
30  1   2   0.744
30  1   3   0.685
30  2   1   0.584
30  2   2   0.314
30  2   3   0.200
30  3   1   0.420
30  3   2   0.673
30  3   3   0.703
40  1   1   0.432
40  1   2   0.240
40  1   3   0.270
40  2   1   0.106
40  2   2   0.454
40  2   3   0.262
40  3   1   0.177
40  3   2   0.368
```

Fig. C-22: Alum dose determination with jar test unit, input code (4 of 6)

```
40  3   3   0.459
50  1   1   0.201
50  1   2   0.318
50  1   3   0.312
50  2   1   0.109
50  2   2   0.093
50  2   3   0.103
50  3   1   0.125
50  3   2   0.157
50  3   3   0.245
60  1   1   0.143
60  1   2   0.150
60  1   3   0.143
60  2   1   0.037
60  2   2   0.144
60  2   3   0.079
60  3   1   0.101
60  3   2   0.068
60  3   3   0.062
70  1   1   0.143
70  1   2   0.179
70  1   3   0.169
70  2   1   0.040
70  2   2   0.060
70  2   3   0.073
70  3   1   0.078
70  3   2   0.166
70  3   3   0.214
80  1   1   0.208
80  1   2   0.201
80  1   3   0.205
80  2   1   0.060
80  2   2   0.089
80  2   3   0.069
80  3   1   0.250
80  3   2   0.208
80  3   3   0.218
90  1   1   0.195
90  1   2   0.211
90  1   3   0.179
90  2   1   0.069
90  2   2   0.063
90  2   3   0.095
90  3   1   0.091
90  3   2   0.250
90  3   3   0.253
100 1   1   1.137
100 1   2   0.153
```

Fig. C-23: Alum dose determination with jar test unit, input code (5 of 6)

```
100 1   3   0.169
100 2   1   0.069
100 2   2   0.099
100 2   3   0.102
100 3   1   0.296
100 3   2   0.198
100 3   3   0.231
;
run;

/*Calculate the Expected Mean Squares*/
proc mixed data=jartestTP method=type3;
    class Dose2 Run2 Rep2;
    model TP=Dose2;
    random Run2(Dose2);
    title1 'EMS using Type3 option - TP Data';
run;

/*Perform tests*/
proc mixed data=jartestTP covtest;
    class Dose2 Run2 Rep2;
    model TP=Dose2 / ddfm=satterthwaite outp=out1;
    lsmeans Dose2 / pdiff=all adjust=Tukey;
    title1 'Using REML estimation - TP Data';
run;
```

Fig. C-24: Alum dose determination with jar test unit, input code (6 of 6)

Using REML estimation - TSS Data 4

The Mixed Procedure

Type 3 Tests of Fixed Effects

Effect	Num DF	Den DF	F Value	Pr > F
Dose	10	88	60.67	<.0001

Least Squares Means

Effect	Dose	Estimate	Standard Error	DF	t Value	Pr > |t|
Dose	0	33.6667	0.9340	88	36.05	<.0001
Dose	10	21.1111	0.9340	88	22.60	<.0001
Dose	100	14.5556	0.9340	88	15.58	<.0001
Dose	20	18.4444	0.9340	88	19.75	<.0001
Dose	30	15.3333	0.9340	88	16.42	<.0001
Dose	40	13.4444	0.9340	88	14.39	<.0001
Dose	50	12.2222	0.9340	88	13.09	<.0001
Dose	60	8.8889	0.9340	88	9.52	<.0001
Dose	70	8.8889	0.9340	88	9.52	<.0001
Dose	80	10.3333	0.9340	88	11.06	<.0001
Dose	90	10.0000	0.9340	88	10.71	<.0001

Differences of Least Squares Means

Effect	Dose	_Dose	Estimate	Standard Error	DF	t Value	Pr > |t|	Adjustment
Dose	0	10	12.5556	1.3209	88	9.51	<.0001	Tukey
Dose	0	100	19.1111	1.3209	88	14.47	<.0001	Tukey
Dose	0	20	15.2222	1.3209	88	11.52	<.0001	Tukey
Dose	0	30	18.3333	1.3209	88	13.88	<.0001	Tukey
Dose	0	40	20.2222	1.3209	88	15.31	<.0001	Tukey
Dose	0	50	21.4444	1.3209	88	16.24	<.0001	Tukey
Dose	0	60	24.7778	1.3209	88	18.76	<.0001	Tukey

Differences of Least Squares Means

Effect	Dose	_Dose	Adj P
Dose	0	10	<.0001
Dose	0	100	<.0001
Dose	0	20	<.0001
Dose	0	30	<.0001
Dose	0	40	<.0001
Dose	0	50	<.0001
Dose	0	60	<.0001

Fig. C-25: Alum dose determination with jar test unit, output code (1 of 6)

Using REML estimation - TSS Data 6

The Mixed Procedure

Differences of Least Squares Means

Effect	Dose	_Dose	Adj P
Dose	0	70	<.0001
Dose	0	80	<.0001
Dose	0	90	<.0001
Dose	10	100	0.0002
Dose	10	20	0.6365
Dose	10	30	0.0016
Dose	10	40	<.0001
Dose	10	50	<.0001
Dose	10	60	<.0001
Dose	10	70	<.0001
Dose	10	80	<.0001
Dose	10	90	<.0001
Dose	100	20	0.1263
Dose	100	30	1.0000
Dose	100	40	0.9989
Dose	100	50	0.7960
Dose	100	60	0.0022
Dose	100	70	0.0022
Dose	100	80	0.0670
Dose	100	90	0.0333
Dose	20	30	0.4070
Dose	20	40	0.0119
Dose	20	50	0.0005
Dose	20	60	<.0001
Dose	20	70	<.0001
Dose	20	80	<.0001
Dose	20	90	<.0001
Dose	30	40	0.9374
Dose	30	50	0.4070
Dose	30	60	0.0002
Dose	30	70	0.0002
Dose	30	80	0.0119
Dose	30	90	0.0052
Dose	40	50	0.9975
Dose	40	60	0.0333
Dose	40	70	0.0333
Dose	40	80	0.4070
Dose	40	90	0.2609
Dose	50	60	0.3057
Dose	50	70	0.3057
Dose	50	80	0.9374
Dose	50	90	0.8403
Dose	60	70	1.0000
Dose	60	80	0.9904
Dose	60	90	0.9989
Dose	70	80	0.9904
Dose	70	90	0.9989

Fig. C-26: Alum dose determination with jar test unit, output code (2 of 6)

Using REML estimation - TSS Data 7

The Mixed Procedure

Differences of Least Squares Means

Effect	Dose	_Dose	Estimate	Standard Error	DF	t Value	Pr > |t|	Adjustment
Dose	80	90	0.3333	1.3209	88	0.25	0.8014	Tukey

Differences of Least Squares Means

Effect	Dose	_Dose	Adj P
Dose	80	90	1.0000

Fig. C-27: Alum dose determination with jar test unit, output code (3 of 6)

Using REML estimation - TP Data 11

The Mixed Procedure

Type 3 Tests of Fixed Effects

Effect	Num DF	Den DF	F Value	Pr > F
Dose2	10	88	153.79	<.0001

Least Squares Means

Effect	Dose2	Estimate	Standard Error	DF	t Value	Pr > |t|
Dose2	0	2.4842	0.06261	88	39.68	<.0001
Dose2	10	1.6511	0.06261	88	26.37	<.0001
Dose2	100	0.2727	0.06261	88	4.36	<.0001
Dose2	20	0.9946	0.06261	88	15.89	<.0001
Dose2	30	0.5176	0.06261	88	8.27	<.0001
Dose2	40	0.3076	0.06261	88	4.91	<.0001
Dose2	50	0.1848	0.06261	88	2.95	0.0041
Dose2	60	0.1030	0.06261	88	1.65	0.1035
Dose2	70	0.1247	0.06261	88	1.99	0.0495
Dose2	80	0.1676	0.06261	88	2.68	0.0089
Dose2	90	0.1562	0.06261	88	2.50	0.0144

Differences of Least Squares Means

Effect	Dose2	_Dose2	Estimate	Standard Error	DF	t Value	Pr > |t|	Adjustment
Dose2	0	10	0.8331	0.08854	88	9.41	<.0001	Tukey
Dose2	0	100	2.2116	0.08854	88	24.98	<.0001	Tukey
Dose2	0	20	1.4897	0.08854	88	16.83	<.0001	Tukey
Dose2	0	30	1.9667	0.08854	88	22.21	<.0001	Tukey
Dose2	0	40	2.1767	0.08854	88	24.58	<.0001	Tukey
Dose2	0	50	2.2994	0.08854	88	25.97	<.0001	Tukey
Dose2	0	60	2.3812	0.08854	88	26.90	<.0001	Tukey

Differences of Least Squares Means

Effect	Dose2	_Dose2	Adj P
Dose2	0	10	<.0001
Dose2	0	100	<.0001
Dose2	0	20	<.0001
Dose2	0	30	<.0001
Dose2	0	40	<.0001
Dose2	0	50	<.0001
Dose2	0	60	<.0001

Fig. C-28: Alum dose determination with jar test unit, output code (4 of 6)

Using REML estimation - TP Data 13

The Mixed Procedure

Differences of Least Squares Means

Effect	Dose2	_Dose2	Adj P
Dose2	0	70	<.0001
Dose2	0	80	<.0001
Dose2	0	90	<.0001
Dose2	10	100	<.0001
Dose2	10	20	<.0001
Dose2	10	30	<.0001
Dose2	10	40	<.0001
Dose2	10	50	<.0001
Dose2	10	60	<.0001
Dose2	10	70	<.0001
Dose2	10	80	<.0001
Dose2	10	90	<.0001
Dose2	100	20	<.0001
Dose2	100	30	0.1889
Dose2	100	40	1.0000
Dose2	100	50	0.9955
Dose2	100	60	0.7050
Dose2	100	70	0.8456
Dose2	100	80	0.9824
Dose2	100	90	0.9637
Dose2	20	30	<.0001
Dose2	20	40	<.0001
Dose2	20	50	<.0001
Dose2	20	60	<.0001
Dose2	20	70	<.0001
Dose2	20	80	<.0001
Dose2	20	90	<.0001
Dose2	30	40	0.3964
Dose2	30	50	0.0130
Dose2	30	60	0.0005
Dose2	30	70	0.0013
Dose2	30	80	0.0069
Dose2	30	90	0.0045
Dose2	40	50	0.9485
Dose2	40	60	0.4363
Dose2	40	70	0.6043
Dose2	40	80	0.8859
Dose2	40	90	0.8268
Dose2	50	60	0.9975
Dose2	50	70	0.9998
Dose2	50	80	1.0000
Dose2	50	90	1.0000
Dose2	60	70	1.0000
Dose2	60	80	0.9997
Dose2	60	90	0.9999
Dose2	70	80	1.0000
Dose2	70	90	1.0000

Fig. C-29: Alum dose determination with jar test unit, output code (5 of 6)

Using REML estimation - TP Data 14

The Mixed Procedure

Differences of Least Squares Means

Effect	Dose2	_Dose2	Estimate	Standard Error	DF	t Value	Pr > |t|	Adjustment
Dose2	80	90	0.01133	0.08854	88	0.13	0.8984	Tukey

Differences of Least Squares Means

Effect	Dose2	_Dose2	Adj P
Dose2	80	90	1.0000

Fig. C-30: Alum dose determination with jar test unit, output code (6 of 6)

C4: Environmental effects on jar test unit operation

```
/*Determination of the effect of time of day on jar test removal efficiency*/
/*Corrected SAS procedure, using a nested experimental design*/

/*formatting options*/
options ls=80 nodate pageno=1 formdlim='~';
goptions ftext=swiss ftitle=swissb htitle=3 htext=3 vorigin=1 in
    hsize=8 in vsize=8 in device=win rotate=portrait;
run;

/*data entry of TSS removal data*/
/*8:20 AM */
data jartestTSS;
    input PolyDose Run Rep TSS @@;
    cards;
0.0     1   1   6
0.0     1   2   8
0.0     1   3   6
0.0     2   1   7
0.0     2   2   6
0.0     2   3   5
0.0     3   1   7
0.0     3   2   4
0.0     3   3   6
0.3     1   1   9
0.3     1   2   7
0.3     1   3   7
0.3     2   1   9
0.3     2   2   7
0.3     2   3   6
0.3     3   1   6
0.3     3   2   6
0.3     3   3   8
0.6     1   1   9
0.6     1   2   11
0.6     1   3   6
0.6     2   1   9
0.6     2   2   9
0.6     2   3   9
0.6     3   1   7
0.6     3   2   8
0.6     3   3   9
1.0     1   1   10
1.0     1   2   9
1.0     1   3   9
1.0     2   1   10
1.0     2   2   11
1.0     2   3   9
1.0     3   1   7
```

Fig. C-31: Environmental effects on jar test operation, 8:20 am, input code (1 of 4)

```
1.0     3   1   7
1.0     3   2   8
1.0     3   3   7
;
run;

/*Calculate the Expected Mean Squares*/
proc mixed data=jartestTSS method=type3;
    class PolyDose Run Rep;
    model TSS=PolyDose;
    random Run(PolyDose);
    title1 'Get EMS using Type3 option - TSS Data';
run;

/*Perform tests*/
proc mixed data=jartestTSS covtest;
    class PolyDose Run Rep;
    model TSS=PolyDose / ddfm=satterthwaite outp=out1;
    lsmeans PolyDose / pdiff=all adjust=Tukey;
    title1 'Using REML estimation - TSS Data';
run;
```

Fig. C-32: Environmental effects on jar test operation, 8:20 am, input code (2 of 4)

```
/*data entry of TP removal data*/
/*8:20 AM */
data jartestTP;
    input PolyDose2 Run2 Rep2 TP @@;
    cards;
0.0     1   1   0.620
0.0     1   2   0.572
0.0     1   3   0.520
0.0     2   1   0.604
0.0     2   2   0.815
0.0     2   3   0.523
0.0     3   1   0.705
0.0     3   2   0.715
0.0     3   3   0.702
0.3     1   1   0.610
0.3     1   2   0.626
0.3     1   3   0.658
0.3     2   1   0.691
0.3     2   2   0.772
0.3     2   3   0.785
0.3     3   1   0.681
0.3     3   2   0.662
0.3     3   3   0.639
0.6     1   1   0.710
0.6     1   2   0.671
0.6     1   3   0.671
0.6     2   1   0.775
0.6     2   2   0.759
0.6     2   3   0.834
0.6     3   1   0.788
0.6     3   2   0.753
0.6     3   3   0.791
1.0     1   1   0.637
1.0     1   2   0.601
1.0     1   3   0.594
1.0     2   1   0.542
1.0     2   2   0.617
1.0     2   3   0.663
1.0     3   1   0.604
1.0     3   2   0.676
1.0     3   3   0.666
;
run;
```

Fig. C-33: Environmental effects on jar test operation, 8:20 am, input code (3 of 4)

```
/*Calculate the Expected Mean Squares*/
proc mixed data=jartestTP method=type3;
     class PolyDose2 Run2 Rep2;
     model TP=PolyDose2;
     random Run(PolyDose2);
     title1 'Get EMS using Type3 option - TP Data';
run;

/*Perform tests*/
proc mixed data=jartestTP covtest;
     class PolyDose2 Run2 Rep2;
     model TP=PolyDose2 / ddfm=satterthwaite outp=out1;
     lsmeans PolyDose2 / pdiff=all adjust=Tukey;
     title1 'Using REML estimation - TP Data';
run;
```

Fig. C-34: Environmental effects on jar test operation, 8:20 am, input code (4 of 4)

Using REML estimation - TSS Data 4

The Mixed Procedure

Type 3 Tests of Fixed Effects

Effect	Num DF	Den DF	F Value	Pr > F
PolyDose	3	32	8.78	0.0002

Least Squares Means

Effect	Poly Dose	Estimate	Standard Error	DF	t Value	Pr > |t|
PolyDose	0	6.1111	0.4312	32	14.17	<.0001
PolyDose	0.3	7.2222	0.4312	32	16.75	<.0001
PolyDose	0.6	8.5556	0.4312	32	19.84	<.0001
PolyDose	1	8.8889	0.4312	32	20.61	<.0001

Differences of Least Squares Means

Effect	Poly Dose	$\overline{\text{Poly}}$ Dose	Estimate	Standard Error	DF	t Value	Pr > |t|	Adjustment
PolyDose	0	0.3	-1.1111	0.6098	32	-1.82	0.0778	Tukey
PolyDose	0	0.6	-2.4444	0.6098	32	-4.01	0.0003	Tukey
PolyDose	0	1	-2.7778	0.6098	32	-4.55	<.0001	Tukey
PolyDose	0.3	0.6	-1.3333	0.6098	32	-2.19	0.0362	Tukey
PolyDose	0.3	1	-1.6667	0.6098	32	-2.73	0.0101	Tukey
PolyDose	0.6	1	-0.3333	0.6098	32	-0.55	0.5885	Tukey

Differences of Least Squares Means

Effect	Poly Dose	$\overline{\text{Poly}}$ Dose	Adj P
PolyDose	0	0.3	0.2820
PolyDose	0	0.6	0.0019
PolyDose	0	1	0.0004
PolyDose	0.3	0.6	0.1488
PolyDose	0.3	1	0.0474
PolyDose	0.6	1	0.9468

Fig. C-35: Environmental effects on jar test operation, 8:20 am, output code (1 of 2)

Using REML estimation - TP Data 6

The Mixed Procedure

Type 3 Tests of Fixed Effects

Effect	Num DF	Den DF	F Value	Pr > F
PolyDose2	3	32	6.19	0.0019

Least Squares Means

Effect	Poly Dose2	Estimate	Standard Error	DF	t Value	Pr > |t|
PolyDose2	0	0.6418	0.02269	32	28.28	<.0001
PolyDose2	0.3	0.6804	0.02269	32	29.98	<.0001
PolyDose2	0.6	0.7502	0.02269	32	33.06	<.0001
PolyDose2	1	0.6222	0.02269	32	27.42	<.0001

Differences of Least Squares Means

Effect	Poly Dose2	$\overline{\text{Poly}}$ Dose2	Estimate	Standard Error	DF	t Value	Pr > |t|
PolyDose2	0	0.3	-0.03867	0.03209	32	-1.20	0.2371
PolyDose2	0	0.6	-0.1084	0.03209	32	-3.38	0.0019
PolyDose2	0	1	0.01956	0.03209	32	0.61	0.5466
PolyDose2	0.3	0.6	-0.06978	0.03209	32	-2.17	0.0372
PolyDose2	0.3	1	0.05822	0.03209	32	1.81	0.0790
PolyDose2	0.6	1	0.1280	0.03209	32	3.99	0.0004

Differences of Least Squares Means

Effect	Poly Dose2	$\overline{\text{Poly}}$ Dose2	Adjustment	Adj P
PolyDose2	0	0.3	Tukey	0.6284
PolyDose2	0	0.6	Tukey	0.0099
PolyDose2	0	1	Tukey	0.9284
PolyDose2	0.3	0.6	Tukey	0.1523
PolyDose2	0.3	1	Tukey	0.2855
PolyDose2	0.6	1	Tukey	0.0020

Fig. C-36: Environmental effects on jar test operation, 8:20 am, output code (2 of 2)

```
/*Determination of the effect of time of day on jar test removal efficiency*/
/*Corrected SAS procedure, using a nested experimental design*/

/*formatting options*/
options ls=80 nodate pageno=1 formdlim='~';
goptions ftext=swiss ftitle=swissb htitle=3 htext=3 vorigin=1 in
    hsize=8 in vsize=8 in device=win rotate=portrait;
run;

/*data entry of TSS removal data*/
/*9:03 AM */
data jartestTSS;
    input PolyDose Run Rep TSS @@;
    cards;
0.0     1   1   10
0.0     1   2   10
0.0     1   3   11
0.0     2   1   9
0.0     2   2   10
0.0     2   3   9
0.0     3   1   10
0.0     3   2   10
0.0     3   3   9
0.3     1   1   9
0.3     1   2   10
0.3     1   3   11
0.3     2   1   8
0.3     2   2   7
0.3     2   3   10
0.3     3   1   10
0.3     3   2   9
0.3     3   3   8
0.6     1   1   10
0.6     1   2   10
0.6     1   3   12
0.6     2   1   10
0.6     2   2   11
0.6     2   3   10
0.6     3   1   10
0.6     3   2   9
0.6     3   3   8
1.0     1   1   10
1.0     1   2   10
1.0     1   3   10
1.0     2   1   9
1.0     2   2   11
1.0     2   3   11
```

Fig. C-37: Environmental effects on jar test operation, 9:03 am, input code (1 of 4)

```
1.0     3   1   10
1.0     3   2   11
1.0     3   3   12
;
run;

/*Calculate the Expected Mean Squares*/
proc mixed data=jartestTSS method=type3;
    class PolyDose Run Rep;
    model TSS=PolyDose;
    random Run(PolyDose);
    title1 'Get EMS using Type3 option - TSS Data';
run;

/*Perform tests*/
proc mixed data=jartestTSS covtest;
    class PolyDose Run Rep;
    model TSS=PolyDose / ddfm=satterthwaite outp=out1;
    lsmeans PolyDose / pdiff=all adjust=Tukey;
    title1 'Using REML estimation - TSS Data';
run;
```

Fig. C-38: Environmental effects on jar test operation, 9:03 am, input code (2 of 4)

```
/*data entry of TP removal data*/
/*9:03 AM */
data jartestTP;
     input PolyDose2 Run2 Rep2 TP @@;
     cards;
0.0     1   1   0.462
0.0     1   2   0.407
0.0     1   3   0.531
0.0     2   1   0.349
0.0     2   2   0.407
0.0     2   3   0.414
0.0     3   1   0.410
0.0     3   2   0.488
0.0     3   3   0.472
0.3     1   1   0.443
0.3     1   2   0.362
0.3     1   3   0.427
0.3     2   1   0.475
0.3     2   2   0.479
0.3     2   3   0.466
0.3     3   1   0.508
0.3     3   2   0.469
0.3     3   3   0.466
0.6     1   1   0.547
0.6     1   2   0.469
0.6     1   3   0.511
0.6     2   1   0.446
0.6     2   2   0.456
0.6     2   3   0.566
0.6     3   1   0.579
0.6     3   2   0.557
0.6     3   3   0.553
1.0     1   1   0.430
1.0     1   2   0.440
1.0     1   3   0.482
1.0     2   1   0.384
1.0     2   2   0.433
1.0     2   3   0.430
1.0     3   1   0.323
1.0     3   2   0.420
1.0     3   3   0.466
;
run;
```

Fig. C-39: Environmental effects on jar test operation, 9:03 am, input code (3 of 4)

```
/*Calculate the Expected Mean Squares*/
proc mixed data=jartestTP method=type3;
     class PolyDose2 Run2 Rep2;
     model TP=PolyDose2;
     random Run(PolyDose2);
     title1 'Get EMS using Type3 option - TP Data';
run;

/*Perform tests*/
proc mixed data=jartestTP covtest;
     class PolyDose2 Run2 Rep2;
     model TP=PolyDose2 / ddfm=satterthwaite outp=out1;
     lsmeans PolyDose2 / pdiff=all adjust=Tukey;
     title1 'Using REML estimation - TP Data';
run;
```

Fig. C-40: Environmental effects on jar test operation, 9:03 am, input code (4 of 4)

Using REML estimation - TSS Data 4

The Mixed Procedure

Type 3 Tests of Fixed Effects

Effect	Num DF	Den DF	F Value	Pr > F
PolyDose	3	32	2.72	0.0607

Least Squares Means

Effect	Poly Dose	Estimate	Standard Error	DF	t Value	Pr > |t|
PolyDose	0	9.7778	0.3368	32	29.03	<.0001
PolyDose	0.3	9.1111	0.3368	32	27.05	<.0001
PolyDose	0.6	10.0000	0.3368	32	29.69	<.0001
PolyDose	1	10.4444	0.3368	32	31.01	<.0001

Differences of Least Squares Means

Effect	Poly Dose	$\overline{\text{Poly}}$ Dose	Estimate	Standard Error	DF	t Value	Pr > |t|	Adjustment
PolyDose	0	0.3	0.6667	0.4763	32	1.40	0.1712	Tukey
PolyDose	0	0.6	-0.2222	0.4763	32	-0.47	0.6440	Tukey
PolyDose	0	1	-0.6667	0.4763	32	-1.40	0.1712	Tukey
PolyDose	0.3	0.6	-0.8889	0.4763	32	-1.87	0.0712	Tukey
PolyDose	0.3	1	-1.3333	0.4763	32	-2.80	0.0086	Tukey
PolyDose	0.6	1	-0.4444	0.4763	32	-0.93	0.3577	Tukey

Differences of Least Squares Means

Effect	Poly Dose	$\overline{\text{Poly}}$ Dose	Adj P
PolyDose	0	0.3	0.5087
PolyDose	0	0.6	0.9658
PolyDose	0	1	0.5087
PolyDose	0.3	0.6	0.2624
PolyDose	0.3	1	0.0407
PolyDose	0.6	1	0.7874

Fig. C-41: Environmental effects on jar test operation, 9:03 am, output code (1 of 2)

Using REML estimation - TP Data 6

The Mixed Procedure

Type 3 Tests of Fixed Effects

Effect	Num DF	Den DF	F Value	Pr > F
PolyDose2	3	32	6.96	0.0010

Least Squares Means

Effect	Poly Dose2	Estimate	Standard Error	DF	t Value	Pr > |t|
PolyDose2	0	0.4378	0.01627	32	26.90	<.0001
PolyDose2	0.3	0.4550	0.01627	32	27.96	<.0001
PolyDose2	0.6	0.5204	0.01627	32	31.98	<.0001
PolyDose2	1	0.4231	0.01627	32	26.00	<.0001

Differences of Least Squares Means

Effect	Poly Dose2	$\bar{P}$oly Dose2	Estimate	Standard Error	DF	t Value	Pr > |t|
PolyDose2	0	0.3	-0.01722	0.02301	32	-0.75	0.4597
PolyDose2	0	0.6	-0.08267	0.02301	32	-3.59	0.0011
PolyDose2	0	1	0.01467	0.02301	32	0.64	0.5285
PolyDose2	0.3	0.6	-0.06544	0.02301	32	-2.84	0.0077
PolyDose2	0.3	1	0.03189	0.02301	32	1.39	0.1754
PolyDose2	0.6	1	0.09733	0.02301	32	4.23	0.0002

Differences of Least Squares Means

Effect	Poly Dose2	$\bar{P}$oly Dose2	Adjustment	Adj P
PolyDose2	0	0.3	Tukey	0.8767
PolyDose2	0	0.6	Tukey	0.0057
PolyDose2	0	1	Tukey	0.9192
PolyDose2	0.3	0.6	Tukey	0.0368
PolyDose2	0.3	1	Tukey	0.5172
PolyDose2	0.6	1	Tukey	0.0010

Fig. C-42: Environmental effects on jar test operation, 9:03 am, output code (2 of 2)

```
/*Determination of the effect of time of day on jar test removal efficiency*/
/*Corrected SAS procedure, using a nested experimental design*/

/*formatting options*/
options ls=80 nodate pageno=1 formdlim='~';
goptions ftext=swiss ftitle=swissb htitle=3 htext=3 vorigin=1 in
    hsize=8 in vsize=8 in device=win rotate=portrait;
run;

/*data entry of TSS removal data*/
/*11:02 AM */
data jartestTSS;
    input PolyDose Run Rep TSS @@;
    cards;
0.0     1   1   7
0.0     1   2   9
0.0     1   3   4
0.0     2   1   13
0.0     2   2   9
0.0     2   3   3
0.0     3   1   7
0.0     3   2   4
0.0     3   3   9
0.3     1   1   7
0.3     1   2   7
0.3     1   3   7
0.3     2   1   7
0.3     2   2   6
0.3     2   3   5
0.3     3   1   7
0.3     3   2   4
0.3     3   3   8
0.6     1   1   7
0.6     1   2   7
0.6     1   3   7
0.6     2   1   7
0.6     2   2   9
0.6     2   3   7
0.6     3   1   9
0.6     3   2   9
0.6     3   3   8
1.0     1   1   9
1.0     1   2   12
1.0     1   3   9
1.0     2   1   9
1.0     2   2   8
1.0     2   3   8
```

Fig. C-43: Environmental effects on jar test operation, 11:02 am, input code (1 of 4)

```
1.0     2   3   8
1.0     3   1   8
1.0     3   2   7
1.0     3   3   10
;
run;

/*Calculate the Expected Mean Squares*/
proc mixed data=jartestTSS method=type3;
    class PolyDose Run Rep;
    model TSS=PolyDose;
    random Run(PolyDose);
    title1 'Get EMS using Type3 option - TSS Data';
run;

/*Perform tests*/
proc mixed data=jartestTSS covtest;
    class PolyDose Run Rep;
    model TSS=PolyDose / ddfm=satterthwaite outp=out1;
    lsmeans PolyDose / pdiff=all adjust=Tukey;
    title1 'Using REML estimation - TSS Data';
run;
```

Fig. C-44: Environmental effects on jar test operation, 11:02 am, input code (2 of 4)

```
/*data entry of TP removal data*/
/*11:02 AM */
data jartestTP;
    input PolyDose2 Run2 Rep2 TP @@;
    cards;
0.0     1   1   0.174
0.0     1   2   0.580
0.0     1   3   0.593
0.0     2   1   0.591
0.0     2   2   0.555
0.0     2   3   0.585
0.0     3   1   0.559
0.0     3   2   0.549
0.0     3   3   0.536
0.3     1   1   0.360
0.3     1   2   0.200
0.3     1   3   0.450
0.3     2   1   0.568
0.3     2   2   0.552
0.3     2   3   0.650
0.3     3   1   0.604
0.3     3   2   0.607
0.3     3   3   0.669
0.6     1   1   0.434
0.6     1   2   0.493
0.6     1   3   0.382
0.6     2   1   0.304
0.6     2   2   0.327
0.6     2   3   0.499
0.6     3   1   0.663
0.6     3   2   0.562
0.6     3   3   0.578
1.0     1   1   0.418
1.0     1   2   0.697
1.0     1   3   0.626
1.0     2   1   0.408
1.0     2   2   0.275
1.0     2   3   0.567
1.0     3   1   0.737
1.0     3   2   0.737
1.0     3   3   0.773
;
run;
```

Fig. C-45: Environmental effects on jar test operation, 11:02 am, input code (3 of 4)

```
/*Calculate the Expected Mean Squares*/
proc mixed data=jartestTP method=type3;
    class PolyDose2 Run2 Rep2;
    model TP=PolyDose2;
    random Run(PolyDose2);
    title1 'Get EMS using Type3 option - TP Data';
run;

/*Perform tests*/
proc mixed data=jartestTP covtest;
    class PolyDose2 Run2 Rep2;
    model TP=PolyDose2 / ddfm=satterthwaite outp=out1;
    lsmeans PolyDose2 / pdiff=all adjust=Tukey;
    title1 'Using REML estimation - TP Data';
run;
```

Fig. C-46: Environmental effects on jar test operation, 11:02 am, input code (4 of 4)

Using REML estimation - TSS Data 4

The Mixed Procedure

Type 3 Tests of Fixed Effects

Effect	Num DF	Den DF	F Value	Pr > F
PolyDose	3	32	2.57	0.0712

Least Squares Means

Effect	Poly Dose	Estimate	Standard Error	DF	t Value	Pr > |t|
PolyDose	0	7.2222	0.6407	32	11.27	<.0001
PolyDose	0.3	6.4444	0.6407	32	10.06	<.0001
PolyDose	0.6	7.7778	0.6407	32	12.14	<.0001
PolyDose	1	8.8889	0.6407	32	13.87	<.0001

Differences of Least Squares Means

Effect	Poly Dose	$\overline{\text{Poly}}$ Dose	Estimate	Standard Error	DF	t Value	Pr > |t|	Adjustment
PolyDose	0	0.3	0.7778	0.9061	32	0.86	0.3971	Tukey
PolyDose	0	0.6	-0.5556	0.9061	32	-0.61	0.5441	Tukey
PolyDose	0	1	-1.6667	0.9061	32	-1.84	0.0751	Tukey
PolyDose	0.3	0.6	-1.3333	0.9061	32	-1.47	0.1509	Tukey
PolyDose	0.3	1	-2.4444	0.9061	32	-2.70	0.0110	Tukey
PolyDose	0.6	1	-1.1111	0.9061	32	-1.23	0.2290	Tukey

Differences of Least Squares Means

Effect	Poly Dose	$\overline{\text{Poly}}$ Dose	Adj P
PolyDose	0	0.3	0.8260
PolyDose	0	0.6	0.9271
PolyDose	0	1	0.2742
PolyDose	0.3	0.6	0.4659
PolyDose	0.3	1	0.0513
PolyDose	0.6	1	0.6151

Fig. C-47: Environmental effects on jar test operation, 11:02 am, output code (1 of 2)

Using REML estimation - TP Data 6

The Mixed Procedure

Type 3 Tests of Fixed Effects

Effect	Num DF	Den DF	F Value	Pr > F
PolyDose2	3	32	0.85	0.4775

Least Squares Means

Effect	Poly Dose2	Estimate	Standard Error	DF	t Value	Pr > |t|
PolyDose2	0	0.5247	0.04925	32	10.65	<.0001
PolyDose2	0.3	0.5178	0.04925	32	10.51	<.0001
PolyDose2	0.6	0.4713	0.04925	32	9.57	<.0001
PolyDose2	1	0.5820	0.04925	32	11.82	<.0001

Differences of Least Squares Means

Effect	Poly Dose2	$\bar{P}$oly Dose2	Estimate	Standard Error	DF	t Value	Pr > |t|
PolyDose2	0	0.3	0.006889	0.06965	32	0.10	0.9218
PolyDose2	0	0.6	0.05333	0.06965	32	0.77	0.4495
PolyDose2	0	1	-0.05733	0.06965	32	-0.82	0.4165
PolyDose2	0.3	0.6	0.04644	0.06965	32	0.67	0.5097
PolyDose2	0.3	1	-0.06422	0.06965	32	-0.92	0.3634
PolyDose2	0.6	1	-0.1107	0.06965	32	-1.59	0.1219

Differences of Least Squares Means

Effect	Poly Dose2	$\bar{P}$oly Dose2	Adjustment	Adj P
PolyDose2	0	0.3	Tukey	0.9996
PolyDose2	0	0.6	Tukey	0.8692
PolyDose2	0	1	Tukey	0.8431
PolyDose2	0.3	0.6	Tukey	0.9088
PolyDose2	0.3	1	Tukey	0.7933
PolyDose2	0.6	1	Tukey	0.3991

Fig. C-48: Environmental effects on jar test operation, 11:02 am, output code (2 of 2)

```
/*Determination of the effect of time of day on jar test removal efficiency*/
/*Corrected SAS procedure, using a nested experimental design*/

/*formatting options*/
options ls=80 nodate pageno=1 formdlim='~';
goptions ftext=swiss ftitle=swissb htitle=3 htext=3 vorigin=1 in
    hsize=8 in vsize=8 in device=win rotate=portrait;
run;

/*data entry of TSS removal data*/
/*12:01 PM */
data jartestTSS;
    input PolyDose Run Rep TSS @@;
    cards;
0.0     1   1   10
0.0     1   2   8
0.0     1   3   10
0.0     2   1   10
0.0     2   2   9
0.0     2   3   10
0.0     3   1   9
0.0     3   2   10
0.0     3   3   9
0.3     1   1   19
0.3     1   2   11
0.3     1   3   11
0.3     2   1   11
0.3     2   2   10
0.3     2   3   10
0.3     3   1   10
0.3     3   2   10
0.3     3   3   10
0.6     1   1   11
0.6     1   2   10
0.6     1   3   10
0.6     2   1   10
0.6     2   2   11
0.6     2   3   11
0.6     3   1   13
0.6     3   2   12
0.6     3   3   12
1.0     1   1   12
1.0     1   2   10
1.0     1   3   8
1.0     2   1   13
1.0     2   2   13
1.0     2   3   12
```

Fig. C-49: Environmental effects on jar test operation, 12:01 pm, input code (1 of 4)

```
1.0     2   3   12
1.0     3   1   10
1.0     3   2   10
1.0     3   3   8
;
run;

/*Calculate the Expected Mean Squares*/
proc mixed data=jartestTSS method=type3;
    class PolyDose Run Rep;
    model TSS=PolyDose;
    random Run(PolyDose);
    title1 'Get EMS using Type3 option - TSS Data';
run;

/*Perform tests*/
proc mixed data=jartestTSS covtest;
    class PolyDose Run Rep;
    model TSS=PolyDose / ddfm=satterthwaite outp=out1;
    lsmeans PolyDose / pdiff=all adjust=Tukey;
    title1 'Using REML estimation - TSS Data';
run;
```

Fig. C-50: Environmental effects on jar test operation, 12:01 pm, input code (2 of 4)

```
/*data entry of TP removal data*/
/*12:01 PM */
data jartestTP;
    input PolyDose2 Run2 Rep2 TP @@;
    cards;
0.0     1   1   0.417
0.0     1   2   0.440
0.0     1   3   0.420
0.0     2   1   0.352
0.0     2   2   0.232
0.0     2   3   0.602
0.0     3   1   0.164
0.0     3   2   0.300
0.0     3   3   0.612
0.3     1   1   0.375
0.3     1   2   0.362
0.3     1   3   0.384
0.3     2   1   0.388
0.3     2   2   0.316
0.3     2   3   0.342
0.3     3   1   0.440
0.3     3   2   0.271
0.3     3   3   0.332
0.6     1   1   0.365
0.6     1   2   0.378
0.6     1   3   0.368
0.6     2   1   0.472
0.6     2   2   0.433
0.6     2   3   0.446
0.6     3   1   0.404
0.6     3   2   0.453
0.6     3   3   0.355
1.0     1   1   0.326
1.0     1   2   0.313
1.0     1   3   0.378
1.0     2   1   0.495
1.0     2   2   0.488
1.0     2   3   0.423
1.0     3   1   0.482
1.0     3   2   0.440
1.0     3   3   0.407
;
run;
```

Fig. C-51: Environmental effects on jar test operation, 12:01 pm, input code (3 of 4)

```
/*Calculate the Expected Mean Squares*/
proc mixed data=jartestTP method=type3;
    class PolyDose2 Run2 Rep2;
    model TP=PolyDose2;
    random Run(PolyDose2);
    title1 'Get EMS using Type3 option - TP Data';
run;

/*Perform tests*/
proc mixed data=jartestTP covtest;
    class PolyDose2 Run2 Rep2;
    model TP=PolyDose2 / ddfm=satterthwaite outp=out1;
    lsmeans PolyDose2 / pdiff=all adjust=Tukey;
    title1 'Using REML estimation - TP Data';
run;
```

Fig. C-52: Environmental effects on jar test operation, 12:01 pm, input code (4 of 4)

Using REML estimation - TSS Data 4

The Mixed Procedure

Type 3 Tests of Fixed Effects

Effect	Num DF	Den DF	F Value	Pr > F
PolyDose	3	32	1.84	0.1593

Least Squares Means

Effect	Poly Dose	Estimate	Standard Error	DF	t Value	Pr > |t|
PolyDose	0	9.4444	0.6211	32	15.21	<.0001
PolyDose	0.3	11.3333	0.6211	32	18.25	<.0001
PolyDose	0.6	11.1111	0.6211	32	17.89	<.0001
PolyDose	1	10.6667	0.6211	32	17.17	<.0001

Differences of Least Squares Means

Effect	Poly Dose	$\overline{\text{Poly}}$ Dose	Estimate	Standard Error	DF	t Value	Pr > |t|	Adjustment
PolyDose	0	0.3	-1.8889	0.8784	32	-2.15	0.0392	Tukey
PolyDose	0	0.6	-1.6667	0.8784	32	-1.90	0.0668	Tukey
PolyDose	0	1	-1.2222	0.8784	32	-1.39	0.1737	Tukey
PolyDose	0.3	0.6	0.2222	0.8784	32	0.25	0.8019	Tukey
PolyDose	0.3	1	0.6667	0.8784	32	0.76	0.4534	Tukey
PolyDose	0.6	1	0.4444	0.8784	32	0.51	0.6163	Tukey

Differences of Least Squares Means

Effect	Poly Dose	$\overline{\text{Poly}}$ Dose	Adj P
PolyDose	0	0.3	0.1592
PolyDose	0	0.6	0.2493
PolyDose	0	1	0.5137
PolyDose	0.3	0.6	0.9942
PolyDose	0.3	1	0.8722
PolyDose	0.6	1	0.9571

Fig. C-53: Environmental effects on jar test operation, 12:01 pm, output code (1 of 2)

Using REML estimation - TP Data 6

The Mixed Procedure

Type 3 Tests of Fixed Effects

Effect	Num DF	Den DF	F Value	Pr > F
PolyDose2	3	32	0.80	0.5035

Least Squares Means

Effect	Poly Dose2	Estimate	Standard Error	DF	t Value	Pr > |t|
PolyDose2	0	0.3932	0.02974	32	13.22	<.0001
PolyDose2	0.3	0.3567	0.02974	32	11.99	<.0001
PolyDose2	0.6	0.4082	0.02974	32	13.73	<.0001
PolyDose2	1	0.4169	0.02974	32	14.02	<.0001

Differences of Least Squares Means

Effect	Poly Dose2	$\overline{\text{Poly}}$ Dose2	Estimate	Standard Error	DF	t Value	Pr > |t|
PolyDose2	0	0.3	0.03656	0.04206	32	0.87	0.3912
PolyDose2	0	0.6	-0.01500	0.04206	32	-0.36	0.7237
PolyDose2	0	1	-0.02367	0.04206	32	-0.56	0.5775
PolyDose2	0.3	0.6	-0.05156	0.04206	32	-1.23	0.2292
PolyDose2	0.3	1	-0.06022	0.04206	32	-1.43	0.1619
PolyDose2	0.6	1	-0.00867	0.04206	32	-0.21	0.8380

Differences of Least Squares Means

Effect	Poly Dose2	$\overline{\text{Poly}}$ Dose2	Adjustment	Adj P
PolyDose2	0	0.3	Tukey	0.8206
PolyDose2	0	0.6	Tukey	0.9842
PolyDose2	0	1	Tukey	0.9423
PolyDose2	0.3	0.6	Tukey	0.6154
PolyDose2	0.3	1	Tukey	0.4894
PolyDose2	0.6	1	Tukey	0.9968

Fig. C-54: Environmental effects on jar test operation, 12:01 pm, output code (2 of 2)

```
/*Determination of the effect of time of day on jar test removal efficiency*/
/*Corrected SAS procedure, using a nested experimental design*/

/*formatting options*/
options ls=80 nodate pageno=1 formdlim='~';
goptions ftext=swiss ftitle=swissb htitle=3 htext=3 vorigin=1 in
    hsize=8 in vsize=8 in device=win rotate=portrait;
run;

/*data entry of TSS removal data*/
/*2:18 PM */
data jartestTSS;
    input PolyDose Run Rep TSS @@;
    cards;
0.0     1   1   8
0.0     1   2   8
0.0     1   3   8
0.0     2   1   8
0.0     2   2   8
0.0     2   3   -27
0.0     3   1   10
0.0     3   2   6
0.0     3   3   7
0.3     1   1   6
0.3     1   2   6
0.3     1   3   7
0.3     2   1   6
0.3     2   2   9
0.3     2   3   7
0.3     3   1   9
0.3     3   2   8
0.3     3   3   6
0.6     1   1   11
0.6     1   2   10
0.6     1   3   6
0.6     2   1   9
0.6     2   2   8
0.6     2   3   8
0.6     3   1   9
0.6     3   2   10
0.6     3   3   11
1.0     1   1   13
1.0     1   2   8
1.0     1   3   11
1.0     2   1   10
1.0     2   2   10
1.0     2   3   11
```

Fig. C-55: Environmental effects on jar test operation, 2:18 pm, input code (1 of 4)

```
1.0     2   3   11
1.0     3   1   10
1.0     3   2   11
1.0     3   3   12
;
run;

/*Calculate the Expected Mean Squares*/
proc mixed data=jartestTSS method=type3;
    class PolyDose Run Rep;
    model TSS=PolyDose;
    random Run(PolyDose);
    title1 'Get EMS using Type3 option - TSS Data';
run;

/*Perform tests*/
proc mixed data=jartestTSS covtest;
    class PolyDose Run Rep;
    model TSS=PolyDose / ddfm=satterthwaite outp=out1;
    lsmeans PolyDose / pdiff=all adjust=Tukey;
    title1 'Using REML estimation - TSS Data';
run;
```

Fig. C-56: Environmental effects on jar test operation, 2:18 pm, input code (2 of 4)

```
/*data entry of TP removal data*/
/*2:18 PM */
data jartestTP;
     input PolyDose2 Run2 Rep2 TP @@;
     cards;
0.0     1   1   0.345
0.0     1   2   0.469
0.0     1   3   0.443
0.0     2   1   0.605
0.0     2   2   0.482
0.0     2   3   0.561
0.0     3   1   0.622
0.0     3   2   0.599
0.0     3   3   0.583
0.3     1   1   0.501
0.3     1   2   0.566
0.3     1   3   0.696
0.3     2   1   0.469
0.3     2   2   0.449
0.3     2   3   0.488
0.3     3   1   0.719
0.3     3   2   0.654
0.3     3   3   0.703
0.6     1   1   0.563
0.6     1   2   0.596
0.6     1   3   0.521
0.6     2   1   0.514
0.6     2   2   0.472
0.6     2   3   0.531
0.6     3   1   0.644
0.6     3   2   0.602
0.6     3   3   0.625
1.0     1   1   0.631
1.0     1   2   0.641
1.0     1   3   0.618
1.0     2   1   0.651
1.0     2   2   0.703
1.0     2   3   0.673
1.0     3   1   0.755
1.0     3   2   0.703
1.0     3   3   0.735
;
run;
```

Fig. C-57: Environmental effects on jar test operation, 2:18 pm, input code (3 of 4)

```
/*Calculate the Expected Mean Squares*/
proc mixed data=jartestTP method=type3;
     class PolyDose2 Run2 Rep2;
     model TP=PolyDose2;
     random Run(PolyDose2);
     title1 'Get EMS using Type3 option - TP Data';
run;

/*Perform tests*/
proc mixed data=jartestTP covtest;
     class PolyDose2 Run2 Rep2;
     model TP=PolyDose2 / ddfm=satterthwaite outp=out1;
     lsmeans PolyDose2 / pdiff=all adjust=Tukey;
     title1 'Using REML estimation - TP Data';
run;
```

Fig. C-58: Environmental effects on jar test operation, 2:18 pm, input code (4 of 4)

Using REML estimation - TSS Data 4

The Mixed Procedure

Type 3 Tests of Fixed Effects

Effect	Num DF	Den DF	F Value	Pr > F
PolyDose	3	32	2.09	0.1209

Least Squares Means

Effect	Poly Dose	Estimate	Standard Error	DF	t Value	Pr > |t|
PolyDose	0	4.0000	1.9894	32	2.01	0.0528
PolyDose	0.3	7.1111	1.9894	32	3.57	0.0011
PolyDose	0.6	9.1111	1.9894	32	4.58	<.0001
PolyDose	1	10.6667	1.9894	32	5.36	<.0001

Differences of Least Squares Means

Effect	Poly Dose	$\overline{\text{Poly}}$ Dose	Estimate	Standard Error	DF	t Value	Pr > |t|	Adjustment
PolyDose	0	0.3	-3.1111	2.8134	32	-1.11	0.2770	Tukey
PolyDose	0	0.6	-5.1111	2.8134	32	-1.82	0.0786	Tukey
PolyDose	0	1	-6.6667	2.8134	32	-2.37	0.0240	Tukey
PolyDose	0.3	0.6	-2.0000	2.8134	32	-0.71	0.4823	Tukey
PolyDose	0.3	1	-3.5556	2.8134	32	-1.26	0.2154	Tukey
PolyDose	0.6	1	-1.5556	2.8134	32	-0.55	0.5842	Tukey

Differences of Least Squares Means

Effect	Poly Dose	$\overline{\text{Poly}}$ Dose	Adj P
PolyDose	0	0.3	0.6886
PolyDose	0	0.6	0.2843
PolyDose	0	1	0.1037
PolyDose	0.3	0.6	0.8920
PolyDose	0.3	1	0.5920
PolyDose	0.6	1	0.9451

Fig. C-59: Environmental effects on jar test operation, 2:18 pm, output code (1 of 2)

Using REML estimation - TP Data 6

The Mixed Procedure

Type 3 Tests of Fixed Effects

Effect	Num DF	Den DF	F Value	Pr > F
PolyDose2	3	32	5.92	0.0025

Least Squares Means

Effect	Poly Dose2	Estimate	Standard Error	DF	t Value	Pr > |t|
PolyDose2	0	0.5232	0.02717	32	19.26	<.0001
PolyDose2	0.3	0.5828	0.02717	32	21.45	<.0001
PolyDose2	0.6	0.5631	0.02717	32	20.73	<.0001
PolyDose2	1	0.6789	0.02717	32	24.99	<.0001

Differences of Least Squares Means

Effect	Poly Dose2	$\overline{\text{Poly}}$ Dose2	Estimate	Standard Error	DF	t Value	Pr > |t|
PolyDose2	0	0.3	-0.05956	0.03842	32	-1.55	0.1309
PolyDose2	0	0.6	-0.03989	0.03842	32	-1.04	0.3069
PolyDose2	0	1	-0.1557	0.03842	32	-4.05	0.0003
PolyDose2	0.3	0.6	0.01967	0.03842	32	0.51	0.6122
PolyDose2	0.3	1	-0.09611	0.03842	32	-2.50	0.0177
PolyDose2	0.6	1	-0.1158	0.03842	32	-3.01	0.0050

Differences of Least Squares Means

Effect	Poly Dose2	$\overline{\text{Poly}}$ Dose2	Adjustment	Adj P
PolyDose2	0	0.3	Tukey	0.4206
PolyDose2	0	0.6	Tukey	0.7285
PolyDose2	0	1	Tukey	0.0016
PolyDose2	0.3	0.6	Tukey	0.9557
PolyDose2	0.3	1	Tukey	0.0788
PolyDose2	0.6	1	Tukey	0.0246

Fig. C-60: Environmental effects on jar test operation, 2:18 pm, output code (2 of 2)

APPENDIX D: CALCULATIONS FOR ECONOMIC ANALYSIS

Table D-1
Calculations for economic analysis.

	Stock alum solution from Thatcher																
	(per conversation with Jeff Zidek, Thatcher Chemical, March 25, 2011)																
(Multiply		1.33	g/mL	(specific gravity)			57.73765	g Al/L		15000000	gal/day in full size DAF plant						
values		0.082	wt/wt Al_2O_3				6.333333	$Al_2(SO_4)_3$/Al		0.041667	day/hour						
going		0.529411765	Al/Al_2O_3							0.016667	hour/min						
down)		1000	mL/L														
		EQUALS					EQUALS			EQUALS							
		57.73764706	g Al/L				365.6718	g $Al_2(SO_4)_3$/L		10416.67	gal/min in full size DAF plant						
Alum																	
	365.6717647	g alum/kg soln		10417	gal/min	4.058732764	lbs/gal		1182.979	g/min		40.53991	mL/s		925.301662	gal/day	
	1.33	kg/L		3.785412	L/gal	0.45359237	kg/lb		0.002056	L/g		3600	sec/hour		11.09	lbs/gal	
	0.001	kg/g		30	mg alum/L	0.264172053	gal/L		1000	mL/L		24	hours/day		$ 0.1038	cost/lb	
	2.204622622	lbs/kg		0.001	g/mg	1000	g/kg		0.016667	min/sec		0.001	L/mL				
	3.78541178	L/gal										0.264172	gal/L				
	EQUALS			EQUALS		EQUALS			EQUALS						EQUALS		
	4.058732764	lbs alum/gal		1182.979	g/min	486.3434471	g/L		40.53991	mL/s		EQUALS			$ 1,065.15	cost/day	
												925.3017	gal/day				
Polymer																	
	0.3	mg polymer/L process		$ 0.000015	cost/L process												
	1	mL/mg		3.78541178	L/gal												
	0.001	L/mL		15000000	gal/day												
	0.264172053	gal/L															
	8.33	lbs/gal															
	1.07	SG															
	$ 2.15	cost/pound polymer stock		EQUALS													
	0.01	dilution of stock		$ 862.34	cost/day												
	EQUALS																
	$ 0.000015	cost/L process															